ORNL-3061
UC-80 - Reactor Technology

HOMOGENEOUS REACTOR PROGRAM

PROGRESS REPORT FOR

PERIOD FROM

AUGUST 1 TO NOVEMBER 30, 1960

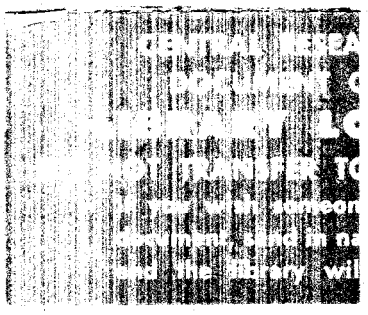

OAK RIDGE NATIONAL LABORATORY
operated by
UNION CARBIDE CORPORATION
for the
U.S. ATOMIC ENERGY COMMISSION

Printed in USA. Price $2.50. Available from the

Office of Technical Services
Department of Commerce
Washington 25, D.C.

ORNL-3061
UC-80 - Reactor Technology
TID-4500 (16th ed.)

Contract No. W-7405-eng-26

HOMOGENEOUS REACTOR PROGRAM PROGRESS REPORT

FOR PERIOD FROM AUGUST 1 TO NOVEMBER 30, 1960

Program Director - R. B. Briggs

Homogeneous Reactor Test - S. E. Beall
Reactor Analysis and Engineering Development - R. N. Lyon
Reactor Materials Research - E. G. Bohlmann
Chemical Engineering Development - D. E. Ferguson
Supporting Chemical Research - H. F. McDuffie
Analytical Chemistry - M. T. Kelley

DATE ISSUED

FEB 27 1961

OAK RIDGE NATIONAL LABORATORY
Oak Ridge, Tennessee
operated by
UNION CARBIDE CORPORATION
for the
U.S. ATOMIC ENERGY COMMISSION

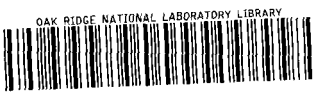

SUMMARY

PART I. HOMOGENEOUS REACTOR TEST

1. HRT Remote Operations, Maintenance, and Testing

Core-Vessel Repair and Inspection

The program of reactor maintenance and major repairs to the core tank was completed.

Both core-vessel holes were patched and leak tested. Leakage through the lower hole was somewhat higher than had been anticipated, but it was within a range to permit the reactor to operate. Leakage through the upper hole, if any, was not measurable.

Using a remote manipulator and ultrasonic measuring equipment, the core-vessel thickness was measured in the cone sections. The greatest corrosion loss (~0.030 in.) was found in the 90° cone.

An optical train was developed and put into operation, using a Questar astronomical telescope, the Omniscope, and an articulated mirror to permit examination and photography of the inner surface of the core vessel at high magnification (4 to 16X). The inner surface of the 90° cone was extensively pitted, the severity decreasing from the junction of the 30 and 90° cones to the junction of the 90° cone and sphere. Small-mound deposits, rather than pits, were the principal visible features in a region centered on the upper hole.

The core system was back-flushed to remove bits of loose debris which resulted from the repair operations. Following this, the temporary equipment that had been installed to permit back-flushing was removed.

Maintenance and System Alterations

Maintenance on other reactor equipment included replacement of a blanket feed-pump diaphragm head, the pressurizer interconnection, and the installation of a heater assembly for the fuel secondary recombiner. A new core circulating pump with inlet and outlet piping revised was installed in order to reverse the direction of flow so that fuel will pass through the core from top to bottom. Also, the new multiple-hydroclone assembly was installed in parallel with the circulating pump. A new dry-maintenance facility was utilized for the first time. It promises to be a time-saving device for small repairs, because work can be done without flooding the shield.

Personnel radiation exposures were below tolerance for the entire period.

2. HRT Operations

Resumption of Nuclear Operations

The HRT resumed nuclear operation after a shutdown period of several months for modification and maintenance. The reactor was brought to criticality on November 7. It is being operated at power levels up to 1.8 Mw in "an initial approach to full power" experiment, which is currently in progress (Nov. 30).

Nearly 12 moles of H_2SO_4 was added to the fuel solution after the start of the new run (No. 22), to reach an acid ratio (0.35 acid-to-sulfate) that will provide a larger margin of safety against fuel instabilities.

Precritical Testing

Before nuclear operations were undertaken, several non-nuclear tests were completed. Among these was a mixing experiment, using chromic acid as a tracer, which established the leakage past the two patched core holes to be much less than that experienced prior to the occurrence of the second hole.

Performance tests indicated that the fuel secondary recombiner operated satisfactorily. The primary unit did not function properly, but it is not needed for normal reactor operation.

Several ventilation and containment improvements were completed.

3. HRT Processing Plant

Solids Removal Systems

In three short runs during this report period, 385 g of corrosion-product solids was collected by the hydroclone systems. Over half (204 g) was removed with the original single hydroclone during the core back-flush operation. The filter in the feed line to the new multiple hydroclone became plugged when first operated during the mixing experiment and was replaced with a new screen element containing larger openings. Bearing failure necessitated replacement of the circulating pump following the mixing-experiment run; the pump had operated 290C hr prior to failure.

Preliminary evaluation, based on solids removal rates during the first run, indicated that the efficiency of the new multiclone is not greater than that of the original unit. The uranium content of the solids removed during the first part of run 22 was only 3.5%, lower than at any time since run 16.

Alternative Fuel Processing Methods

Full-scale testing of the UO_4 fuel processing system was delayed when it was found that, although the precipitate was held quantitatively on a medium glass frit, it could not be retained on the finest available sintered stainless steel filter. Laboratory tests with various filter aids were initiated in an effort to solve this problem.

Basic Studies of Multiple Hydroclones

Basic studies aimed at providing methods for detecting malperformance of multiple hydroclone systems (which might be caused by plugged feed or overflow ports) revealed that the ratio of feed-underflow pressure to feed-overflow

pressure was constant over a wide range of solution densities and viscosities, and independent of flow rate. Departure of this ratio from the normal initial value can be interpreted to indicate the nature of the trouble.

4. HRT Component Design and Development

HRT Remote-Maintenance Development

It was found that sealing of the lower hole of the HRT could be improved if the hole were reamed in a manner similar to that used for the upper hole. A tool to remove the lower patch and to ream the hole was designed and is being fabricated.

Further Studies on Temperature Distribution in HRT Vessel with Reversed Flow

Fluid age measurements in the flow model of the HRT core (reverse flow) were reproducible within approximately 10% following disassembly and reassembly of the model. On the basis of the measurements, the bulk temperature of the HRT core should be about 20% above the outlet temperature relative to the temperature rise across the core. A comparison of HRT core-vessel corrosion, based on ultrasonic measurements, with the in-pile-loop correlation showed the two to be in excellent agreement. A new core corrosion-specimen holder was designed.

HRT Mockup Operation with Dilute, Simulated Fuel Solutions

HRT mockup operation with dilute uranyl sulfate solution confirmed that chemical-phase stability was achieved only above 1 g of uranium per kg of H_2O. No lower limit to the condition of instability was found down to 13 ppm.

HRT Replacement Reactor Vessel

A conceptual design of a cylindrical HRT replacement vessel was made. This vessel would contain a core 21 in. in inside diameter, surrounded partially by a beryllium reflector which would permit achievement of high power densities of 30 to 50 kw/liter at a total reactor power of 5 to 10 Mw. The blanket would contain a 7-in.-thick region of thoria pellets, which could be used to achieve a conversion ratio greater than 1.0 in the Th-U^{233} cycle.

Layouts of the replacement reactor indicate that it is feasible to install the vessel either in an adjacent chemical plant cell or at the location of the present vessel. Flow tests were made of the core proposed for the vessel, indicating that the fluid residence time at all points is adequately low.

5. HRT Reactor Analysis

Calculation of the Pressure Rise in the HRT for Various Ramp Reactivity Additions

Calculations of the pressure rise in the HRT were performed for various reactivity-rate additions and several operating conditions. With a core hole area of 0.1 sq in., a blanket-to-core fuel-concentration ratio of 0.3, and a reactivity-rate addition of 2% Δk_e/sec, the maximum core pressure rise was about 2180 psi with the reactor initially at source-power level. With a rate addition of 1.5% Δk_e/sec the maximum pressure rise was about 1350 psi. Increasing the hole size to 0.5 sq in. decreased the maximum pressure rise by about 200 psi, while removing the hole increased the pressure rise about 70 psi. With no fuel in the blanket, the maximum core pressure rise was about 1200 psi instead of 2180 psi.

Criticality Calculations for the HRT

Calculations were made of HRT critical fuel concentrations for various blanket-to-core fuel-concentration ratios and different core-blanket temperature conditions. With no fuel in the blanket, decreasing the blanket temperature from 280 to 240°C decreased the core critical concentration from 8.8 to 8.1 g of U^{235} per kg of water; if in addition the core temperature were lowered to 260°C, the fuel concentration would be 7.2 g of U^{235} per kg of water. With a blanket-to-core fuel concentration ratio of 0.3, the corresponding core critical concentrations would be 6.1 g of U^{235} per kg of H_2O (280°C core/280°C blanket), 5.6 (280°/240°), and 5.1 (260°/240°).

Criticality Calculations Concerning the HRT Replacement Vessel

Criticality calculations were made concerning an HRT replacement vessel; a spherical reactor was considered with a 27.2-in.-diam core surrounded by a 4-in.-thick beryllium reflector and regions of thoria pellets and D_2O inside a 56.7-in.-diam pressure vessel. The critical U^{233} concentration was 6.1 g/liter, the core wall power density was 5.2 kw/liter per megawatt, and the breeding ratio of the nearly clean reactor was 1.06. The core fuel concentration with U^{235} as the fuel was 9 g of U^{235} per liter.

PART II. ENGINEERING DEVELOPMENT

6. Development of Reactor Components and Systems

Development of Straight-Through Core Vessel

Experimental measurements of fluid age in a cylindrical core model with swirling straight-through flow showed that excessive temperatures are generated near the center. An attempt is being made to improve the axial flow distribution with a vortex generator at the core discharge.

Circulating-Pump Development

Alumina bearings have been operated in high-temperature water in a 200-gpm pump for 6970 hr.

Oxygen Compressor

The drive system of the three-stage oxygen compressor was revised (to contain a water intermediate system) in an attempt to prevent diaphragm failures attributed to dirt particles.

Slurry Engineering

The operation of a number of capillary viscometers ranging in diameter from 11 to 124 mils with a particular pumped thoria slurry at 30°C showed that all pseudoshear diagrams fell on a single curve. It was concluded that no "slip" phenomena were occurring at test conditions. A further conclusion was that the rheology of the suspension at high shear rates could not readily be predicted from measurements at low shear.

Run 22A, in which concentration gradients were observed in a 3.65-μ, 1600°C-fired thoria slurry, was completed. Run 4B, in which heat-transfer measurements were made with a 1600°C-fired slurry, was also completed.

PART III. SOLUTION FUELS

7. Reactions in Aqueous Solutions

Removal of Protactinium and Uranium from Thorium Nitrate - Nitric Acid Solutions

Tracer-level experiments showed that protactinium was coprecipitated with thorium from aqueous, acid, thorium nitrate solutions when hydrogen peroxide was added in an amount sufficient to precipitate no more than 3% of the thorium. The experiments covered ranges of thorium concentration from 1.0 to 3.0 *M* and NO_3:Th ratios from 4:1 to 5:1. Unconfirmed experiments indicate that uranium was not coprecipitated with thorium under similar conditions when the uranium was in the range of 70 to 80 ppm; protactinium, however, was coprecipitated in the presence of this concentration of uranium.

The Solubility of H_2 in H_2O and of D_2 in D_2O

The solubilities of H_2 in H_2O and of D_2 in D_2O were determined from room temperature to 250°C. These data are believed accurate to ±1%. Graphical presentation only is shown. Tabular data up to 300°C will be reported at a later date.

8. Heterogeneous Equilibria in Aqueous Systems

Estimation of Minimum Temperatures of Second-Liquid-Phase Formation in Homogeneous-Reactor Fuel Concentrates: Use of the Acidity Ratio

The temperatures for the appearance of liquid-liquid immiscibility were determined for two homogeneous-reactor fuel solutions and their concentrates. From these and previous data a method which makes use of only the acidity molal ratio, D_2SO_4/total sulfate, for estimation of the minimum two-liquid-phase temperatures is presented.

Liquid-Liquid Equilibria in the Systems UO_3-CuO-SO_3-D_2O and CuO-SO_3-D_2O

Temperature-composition boundaries for liquid-liquid immiscibility and critical phenomena (i.e., the disappearance of the meniscus between liquid and vapor) were determined for the systems UO_3-CuO-SO_3-D_2O, $m_{UO_2}{}^{++}/m_{Cu}{}^{++} = 1$, and CuO-$SO_3$-$D_2O$. These data showed a rising temperature for the appearance of liquid-liquid immiscibility as the molal ratios, metal ions/total sulfate, were decreased and the total sulfate was kept constant. At ratios somewhat below about 0.5, both UO_2SO_4 and $CuSO_4$ became soluble in the supercritical fluid.

Solid-Liquid Equilibria in the System CuO-SO_3-D_2O at 300, 325, and 350°C

Solubilities of $3CuO \cdot SO_3 \cdot 2D_2O$ at 300, 325, and 350°C were determined in solutions of D_2O and D_2SO_4. The results showed an almost undetectable change with temperature in the saturation molal ratio, Cu^{++}/total sulfate, at constant total sulfate. Comparison of saturation molal ratios at 300°C showed higher values in the D_2O than in the analogous H_2O system.

Electrolytic Conductance of Aqueous Solutions and Supercritical Fluids at High Temperature and Pressure

The construction of cells for the measurement of electrolytic conductance at high pressure and high temperature, as well as an assembly for generation of high pressures, were completed. Preliminary measurements on a 0.01 *m* KCl solution were made at 800°C and at pressures up to 4000 atm. This is the first time that reproducible measurements have been made at such a high pressure and temperature.

Three-Dimensional Models for Representation of Solubility Equilibria

Three-dimensional models representing solubility relationships in the system UO_3-CuO-NiO-SO_3-D_2O at 300°C were constructed for solutions having total sulfate concentrations of 0.06, 0.10, 0.20, 0.30, and 0.50 *m*. The results of previously reported solubility studies were used to establish the location of the surfaces of saturation for the several solid and liquid phases which appear at the boundary limits of the region of unsaturated solutions.

9. Solution Corrosion

Chemical Equilibria and Corrosion in High-Temperature Uranyl Sulfate Solutions

An all-titanium pump loop was constructed to study the chemical stability of uranyl sulfate fuel solutions and the corrosion resistance of various materials at temperatures and pressures up to 370°C and 3000 psia. Preliminary runs with water and simulated reactor fuel solutions showed that the loop and control systems functioned properly. In the latter runs, at least a part of the heavy phase that formed at temperatures greater than the two-liquid-phase temperature was separated by the hydroclone. As the temperature of the system was increased beyond the two-liquid-phase temperature, the salt concentration of the light phase decreased and the acid concentration increased. The mole ratios of uranium to sulfate, uranium to copper, and uranium to nickel decreased in the same proportion in the temperature range of 330 to 365°C. Corrosion of titanium and Zircaloy-2 specimens was negligibly small.

10. Radiation Corrosion

Review and Correlation of Zircaloy-2 Radiation Corrosion Data

The results of a review and correlation of many of the past data for Zircaloy-2 radiation corrosion in uranyl sulfate solutions indicate that the following relationship prevails between corrosion rate, R (mpy), fission power density in solution, P (w/ml), and temperature, T (°K), for the conditions tested: values of P up to 110 w/ml, temperatures in the range 225 to 330°C, and a variety of solution compositions and velocities. The relationship is:

$$1/R = \frac{2.3}{P\alpha_{280}} + 2.25 \times 10^{-11} \exp\left(\frac{11{,}500}{T}\right) ,$$

where α is the factor by which the effective power density at the corroding surface is greater than that in the solution, because of uranium sorption on the surface; and α_{280} is the α value determined at 280°C in a given solution. The value of α (thus the effect of sorbed uranium) changes with solution composition and velocity, but it is believed that this is the only way in which these variables affect the corrosion.

Relationship Between Uranium Deposition or Sorption and Copper Concentration in In-Pile Autoclave Experiments of Zircaloy-2 Corrosion

Using these concepts and the equation in a further review of the in-pile autoclave results obtained at 280°C, it has been found that a correlation exists between the initial copper concentration in solution and the amounts of sorbed uranium. The effects of sorbed uranium in systems containing initial copper concentrations less than 0.01 *m* were generally greater than those prevailing in otherwise similar solutions containing more than 0.01 *m* Cu. Changes in the effects of sorbed uranium ranging up to a maximum of about 3.5-fold were correlated with copper concentration changes in four different sets of experiments.

The review of the autoclave data indicated that radiolytic-gas pressures (which are affected by copper concentration) in the range 0 to 650 psi, at least, probably do not affect the uranium sorption. Therefore, it is suggested that these effects may be related to fuel instability effects in the HRT, since reported observations in run 13 indicate a possible relationship between low copper concentration and fuel instability in that run.

General Description of Planned Experiment to Test Zircaloy-2 Corrosion in the HRT Core

Planning and design work for an experiment to test the radiation corrosion of Zircaloy-2 in the HRT is in progress. Design criteria for the experiment include (1) high solution velocities and good mixing near the specimens to minimize the possibility of massive uranium deposition, and (2) the elimination of crevice regions in mounting specimens. As visualized, 27 corrosion coupons, three Zircaloy-2-clad thermocouples and probably some mechanical-property specimens will be welded to a webbed Zircaloy-2 holder which will be aligned vertically in the center of the core vessel.

It is anticipated that at least five days of exposure at 5-Mw core power and 250°C solution entrance temperature will be required to produce, on the most favorably located specimen, weight losses which can be measured within an estimated probable error of ±10%.

Before the design of the experiment can be proved acceptable and the experiment constructed, it will be necessary to test the characteristics of a mockup of the specimen-and-holder array in the HRT core mockup and to establish the feasibility of employing welded specimens.

Sorption of Uranium on Hydrous Zirconia in UO_2SO_4 Solutions

Data from batch autoclave tests of uranium sorption on hydrous zirconia from uranyl sulfate solutions are reported. Most of the work employed a 110°C-air-dried (AF) material of high surface area, but some data using a material of lower surface area autoclaved in water at 300°C (WF) are also reported. In a kinetic study at 280°C, the AF material showed a loss of surface area and marked decreases in uranium and sulfate sorption per gram of ZrO_2 during the first 2 to 4 hr exposure. Little or no time dependence on area or sorption was noted with the WF material.

Sorption isotherms with the AF oxide and uranyl sulfate solutions with 0.02 *M* excess acid and uranium in concentrations to 35 mg-U/ml indicate that uranium sorption on a per-gram-of-ZrO_2 basis was 30 to 40% greater at 280°C than at 250°C. Data at 300 and 325°C at maximum concentrations of 7 and 3 g/liter, respectively, show uranium sorption in about the same amounts as that found at 250°C.

Elution of oxide residues from sorption tests with aqueous reagents indicate that the WF oxide can be readily washed free of uranium, whereas the AF oxide retains significant amounts.

These preliminary data are tentatively interpreted as showing that some of the uranium sorbed on the AF oxide is due to occlusion associated with the surface-area decrease or to compound formation. Sorption on the AF material resembles sorption in Zircaloy-2 films and scales, in that part of the uranium is not removed by washing.

PART IV. SLURRY FUELS

11. Thoria-Pellet Irradiations

A settled bed of 50 thoria pellets in D_2O was irradiated in the LITR for 2900 hr at a thermal-neutron flux of ~2 x 10^{13} and a temperature of 250°C. The pellets were prepared by treating 1400°C-fired Davison Chemical Co. pellets with dibasic aluminum nitrate and then refiring at 1750°C. When the irradiation autoclave was opened, 20 of the pellets were found to have broken into fragments and fines. The remainder had essentially the same bulk density as the original material but showed some damage from the chipping out of surface fragments and the breaking off of spherical segments. All surfaces appeared to be quite porous. A substantial quantity of an unidentified black vitreous substance (density 1.18 g/cc) was found in the upper half of the irradiation autoclave. Pellets removed from a laboratory control experiment showed no apparent damage, and there was no evidence of the black vitreous material.

12. Development of Gas-Recombination Catalyst

Gas-Injection Apparatus

Recalibration of the gas-injection apparatus showed significant gas holdup in the capillary tubing that connects the gas-charging system to the reaction autoclave.

Palladium Catalysis

Re-evaluation of data obtained in the above system with slurries containing the sol-prepared palladium catalyst showed little or no deactivation of the catalyst by excess oxygen partial pressures and showed that reaction of the hydrogen and oxygen was complete. Kinetic data suggest a probable first-order dependence of rate on the hydrogen partial pressure and 0.5-order dependence on the oxygen partial pressure.

13. Slurry Corrosion and Blanket Materials Studies

Thoria-Pellet Test Program

In one phase of an investigation aimed at studying variables which affect the attrition of thoria pellets, a series of laboratory tests were carried out in which the effect of ball-mill charge (pellets and water), mill length, and rotational speed on the wear rate of pellets were studied. Wear rates were proportional to increased rotational speeds and to increased pellet charge at low loadings (10 to 100 pellets). However, the amount of water charged to the

mill (6 to 100% full) or the length of the mill (4 1/2 in. or 2 1/4 in. long, 3 3/4 in. in diameter) had no detectable effect on the wear rate of the pellets.

The fines which resulted from repeated milling of the pellets (prepared from 7-μ powder) had an average particle size of 2 μ.

Thin (~0.3-mil) coatings of zirconium which were applied by an experimental electron vaporization technique were penetrated after 1 hr of exposure in a spouted-bed test, and spalling of the coating was noted after autoclaving the pellets in water at 260°C.

Experimental 0.16-in.-diam ThO_2 pellets obtained from Nuclear Materials and Equipment Corp. displayed high weight-loss rates (1.1×10^{-3} %/hr) in static autoclave tests at 260°C and in ball-mill tests (1.5 %/hr), using 100 pellets, 150 rpm, and in spouted-bed (1.3 to 1.5 %/hr) attrition tests. The high rates were attributed to numerous cracks and pores in the pellets.

In-Pile Autoclave Slurry-Corrosion Tests

An Al_2O_3 filter for application between Zircaloy-2 slurry autoclaves and the attached water-filled capillary lines (previously subject to slurry plugging) leading to pressure instruments has been fabricated as a result of the development by the ORNL Metallurgy Division of Al_2O_3 - Zircaloy-2 brazing procedures.

In-Pile Slurry Loop

The 5-gpm in-pile slurry loop experiment L-2-27S, installed in LITR beam hole HB-2, was terminated after 3115 hr of slurry circulation, of which 2220 hr (July 19 to Oct. 19, 1960) were with continuous operation in-pile, and 1839 hr under irradiation at 3-Mw LITR power. At the time of insertion, the circulating slurry inventory was 1350 g of thorium per kg of D_2O (980 g of thorium per 280°C liter). The slurry contained 0.5 wt % enriched uranium, based on thorium, and 0.019 *m* Pd as a recombination catalyst. The loop was operated at 280°C under oxygen atmosphere. During the course of the irradiation, withdrawal of six samples reduced the circulating inventory concentration to 960 g of thorium per kg of D_2O (735 g of thorium per 280°C liter). Six terminal samples were also withdrawn. Sampling procedures operated entirely without difficulty.

Before removal of the loop from the reactor, essentially all slurry and associated radioactivity were readily drained and flushed from the loop.

Radiolytic-gas levels during in-pile operation remained below 10 psi. Recombination as a result of the absorption of pile gamma radiation was estimated to be sufficient to account for this. As a result, the efficiency of the palladium recombination catalyst was indeterminate.

The flow rate through the filter remained at a level of 0.3 to 0.4 cc/sec, declining to such values from a level of 3 to 4 cc/sec shortly after the beginning of irradiation.

Generalized corrosion during the irradiation period, based on corrosion-product analysis and on oxygen partial-pressure measurement, appeared to be less than 1 mpy, comparable to rates observed during the out-of-pile preirradiation period.

There appeared to be substantial degradation in the size of the slurry particles as irradiation proceeded, with the average diameter decreasing from an original 1.7 μ prior to irradiation to 0.3 μ after 1460 hr of irradiation. Concurrently, the surface area changed from 1.5 m^2/g to 25 m^2/g. In-pile slurry autoclave experiments at comparable doses have not shown similar degradation; consequently, the effect is attributed to the combination of pumping and irradiation. The present loop run has also subjected the slurry to more passes through the pump (a major degradation cause) than any other ORNL slurry run.

PART V. FUEL MANUFACTURE

14. Thorium Oxide Production

Preparation of Thorium Oxide Products

Cracking and poor resistance to attrition of spherical thoria pellets fabricated from ThO_2 powder by automatic pressing and calcination were minimized by increasing the radius of curvature of the punches used in pressing, increasing the firing temperature of powder prior to granulation, increasing the pour density of granulated powder prior to pressing, and providing a 2-hr soaking period at 1200°C during the pellet calcination.

Five per cent thorium-uranium oxide gel fragments of 1/4-in. diameter, imperfectly rounded by ball-milling, gave attrition rates in six successive 1-hr spouting-bed tests of 2.3 to 0.3 %/hr.

Coating of ThO_2 Pellets with Metals and Oxides

Spherical thoria pellets of 1/4-in. diameter were successfully coated in the plasma-jet apparatus with Al_2O_3, Ta_2O_5, ZrO_2, TiO_2, Ni, and Cr. Only nickel-coated pellets, postannealed at 1200°C in hydrogen, showed greater resistance to attrition in spouting-bed tests than did the original thoria pellets.

Development of Oxide Preparation

In a 24-hr flame-calcination run for material-balance study, 40% was recovered as product and 54% as furnace-wall and trap material. Flame calcination of 1 and 2 *M* thoria sols in the 1500 to 1600°C range gave rounded particles of ThO_2 having mean sizes of 2.7 and 4.6 μ, and surface areas of 0.90 and 0.98 m^2/g, respectively. In the flame denitrating of thorium nitrate solutions, some alumina appears to be necessary in order to obtain rounded particles. Nonrounded particles can be recycled to the flame calciner as a slurry to give rounded material. A slurry of 95% ThO_2 - 5% Al_2O_3 (200 g/liter in CH_3OH) was flame calcined at 1600°C to a product of 1.8-μ mean particle size and only 0.84-m^2/g surface area.

PART VI. METALLURGY

15. Metallurgy

Thoria-Pellet Fabrication

A 3.5-kg batch of rounded-end ThO_2 pellets with densities between 9.0 and 9.3 g/cm^3 was successfully produced. The pellets are now being tested both in and out of pile. The addition of up to 2% polyvinyl alcohol was shown to increase both the green and final density of such pellets. A metallographic study of ThO_2 pellets containing Al_2O_3 and fired at various temperatures yielded clues as to the mechanism by which Al_2O_3 increases the abrasion resistance of ThO_2.

Welding of Zircaloy-2

Fabrication studies have been conducted on methods for constructing Zircaloy-2 replacement core vessels. Methods for attaching inlet orifice vanes to the core shell were investigated, and a promising technique was developed. The feasibility of welding misaligned core components was also studied, and it appears that plates misaligned in the range of 0.060 to 0.090 in. can be welded satisfactorily.

PART VII. ANALYTICAL CHEMISTRY

16. Analytical Chemistry

Amperometric Titration of Thorium

An amperometric method is described for the determination of thorium in slurries of ThO_2 and in fuels for the molten-salt reactor. The thorium is titrated with di-sodium ethylenediaminetetraacetate in an acetate-buffered solution (pH 4.5) containing Fe(II) as an indicator. Interferences are discussed and a method is indicated for circumventing the interference of certain commonly encountered contaminants.

Determination of Thorium by an Indirect Polarographic Method

Microgram quantities of thorium in reactor materials can be conveniently determined by an indirect polarographic method, based on thorium displacement of lead from Pb-ethylenediaminetetraacetate and subsequent polarographic determination of the lead. Operating conditions are briefly outlined and interferences are discussed.

Elimination of Interferences in the Flame Photometric Determination of Calcium

The interference of common anionic species with the flame-photometric determination of calcium (and certain other elements) can be largely eliminated by a procedure, briefly discussed, in which an ethylene glycol-water solution is utilized in making the emissivity measurement.

CONTENTS

PART VI. METALLURGY

PART VII. ANALYTICAL CHEMISTRY

PART I. HOMOGENEOUS REACTOR TEST

1. HRT REMOTE OPERATIONS, MAINTENANCE, AND TESTING

S. E. Beall I. Spiewak A. Taboada

P. N. Haubenreich J. W. Hill, Jr.

H. F. Bauman
R. Blumberg
N. C. Bradley
J. R. Buchanan
S. R. Buxton
F. W. Cooke
J. R. Engel
D. F. Frech
R. H. Guymon
P. H. Harley
R. J. Harvey
E. C. Hise
P. P. Holz
J. E. Jones
J. O. Kolb
R. W. McClung
R. E. McDonald
M. L. Picklesimer
H. B. Piper
J. L. Redford
H. C. Roller

The program of maintenance and major repairs to remove the upper five core-vessel diffuser screens, repair the core-vessel holes, reverse the direction of flow through the core, and replace several pieces of equipment was completed. In addition, the core-vessel wall was examined and its thickness measured.

1.1 CORE-VESSEL REPAIR AND INSPECTION

1.1.1 Patching and Leak Testing of Core-Vessel Holes

The patch created from the second plastic impression of the lower core-vessel hole[1] was installed. Leak tests indicated a leak rate somewhat higher than had been anticipated but within a range to permit operation of the reactor. Subsequent examination revealed that the edge of the patch had caught under a screen nubbin and had failed to seat precisely. Figure 1.1 shows the patch in place in the reactor vessel. The nubbin marked by the arrow should have been covered by the patch. Equipment to ream the hole and place a plug in it will be developed while the reactor is being operated with the present patch.

The patch for the taper-reamed upper hole was made with its sealing edge a segment of a sphere, so that it seated like a spherical valve plug in a conical seat. The spherical surface was plated with 0.010 in. of gold to improve sealing contact. The patch was installed and held in place with a 5/16-in. bolt and toggle nut. The patch, as installed in the vessel, is shown in Fig. 1.2. The nickel bolt head visible in Fig. 1.2 is brazed to the Zircaloy-2 bolt. The fuel will dissolve the head, leaving a countersunk bolt and flush patch.

Leakage rates through the patches were determined by pumping water into either the core or blanket vessel and then measuring the rates of level equalization between the vessels. Liquid levels were indicated by bubbler systems. Leakage by the lower patch can be expressed by the equation $L = 5\sqrt{h}$, where L is in lb/min, and h is the pressure difference across the hole in inches of water. Leakage by the upper patch was less than $0.2\sqrt{h}$ -- too small to measure.

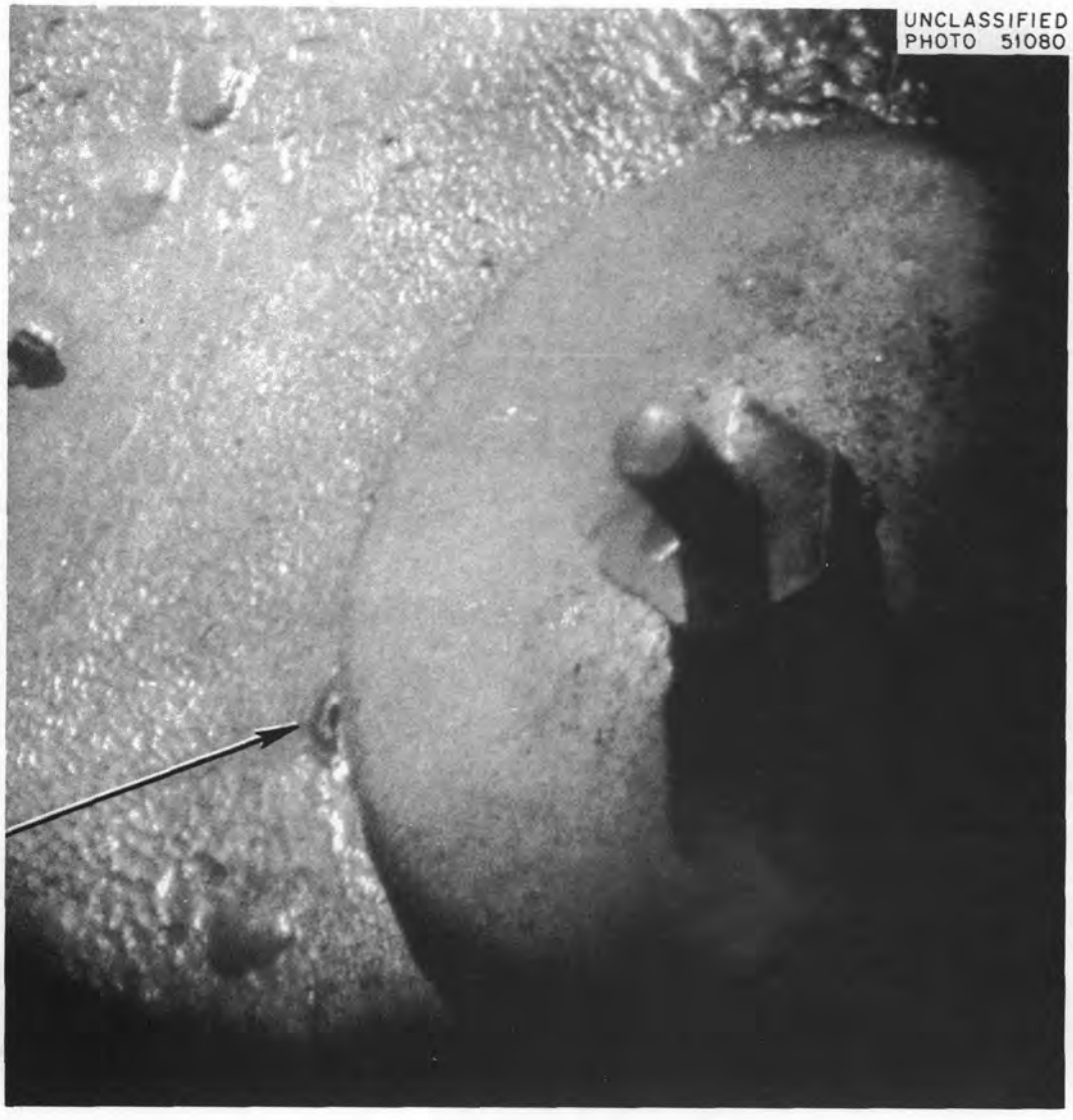

Fig. 1.1. Lower Patch in Place in Reactor Vessel.

1.1.2 Core-Wall Thickness Measurements

Measurements of the HRT core-wall thickness were made in the conical sections of the vessel during the shutdown following run 21. A new manipulator was provided for this purpose by the Remote Maintenance Group, and it allowed accessibility to any point in either cone. However, because of pitting and surface roughness, the area of measurement was limited to a few specific latitudes, all located above screen 6, which had not been removed. Thus these measurements reflect the loss in wall thickness due to generalized corrosion only.

Ultrasonic techniques described previously[2] were used, and the error of the measurements is believed to be less than 4%. Figure 1.3 shows a comparison of the results of these measurements with those made at Newport News[3] prior to installation of the vessel at ORNL.

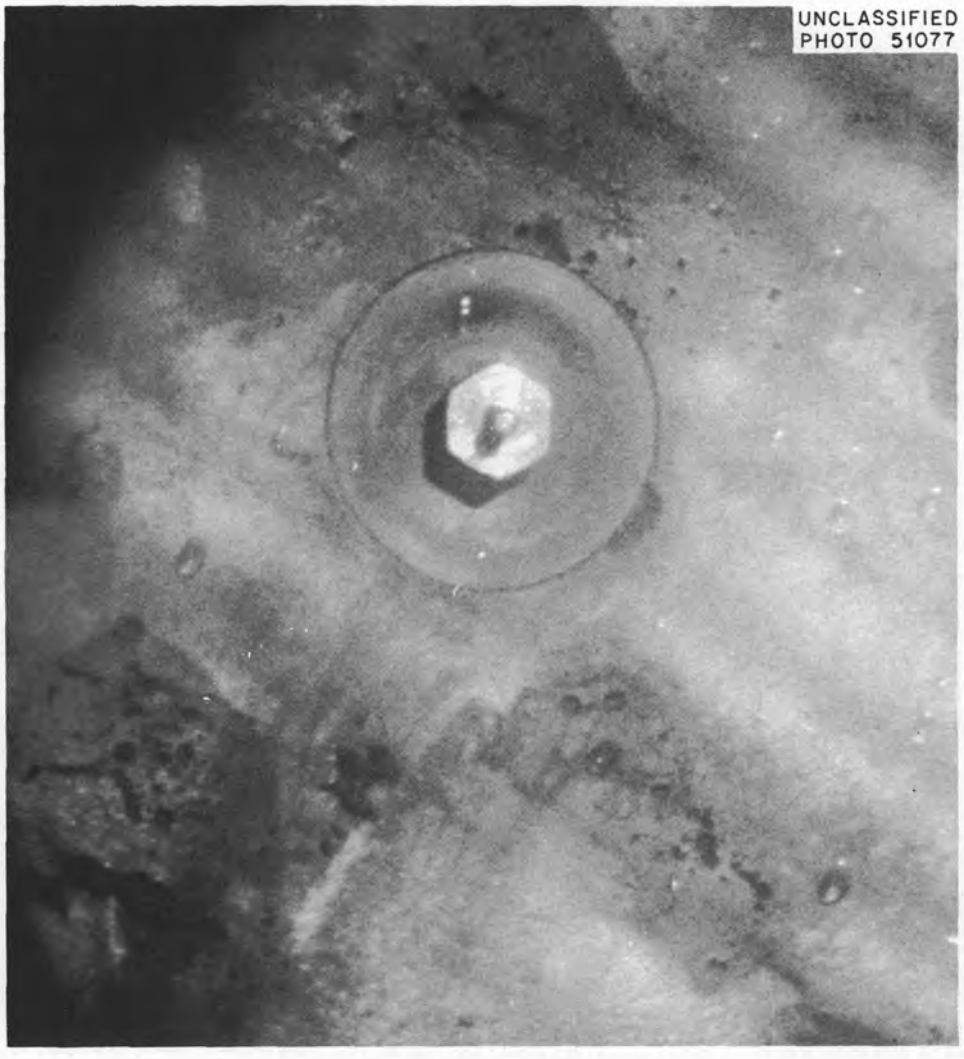

Fig. 1.2. Nickel Bolt Head Brazed to Zircaloy Bolt.

The most significant result is that the greatest corrosion loss (0.030 in.) observed occurred in the upper regions of the 90° cone and that the loss decreased as the fuel velocity increased (e.g., the loss was 0.020 in. in the top of the 30° cone). Measurements could not be obtained in the 90° cone just below the intersection with the sphere, but extrapolation of the data from lower in the cones indicates that the loss here was probably similar to the loss in the sphere just above the intersection. There is good consistency between the several sets of measurements that have been made.

1.1.3 Examination of Inner Surface of Core Tank

A combination of the Questar astronomical telescope, the Omniscope, and a remotely controlled articulated front-surface mirror was used to visually examine and photograph details of several regions of the 90° cone section and the lower portion of the spherical section of the HRT core tank. A schematic diagram of the assembly of the equipment and the resulting optical path is presented in Fig. 1.4. The photographs were made with a 35-mm camera attached to

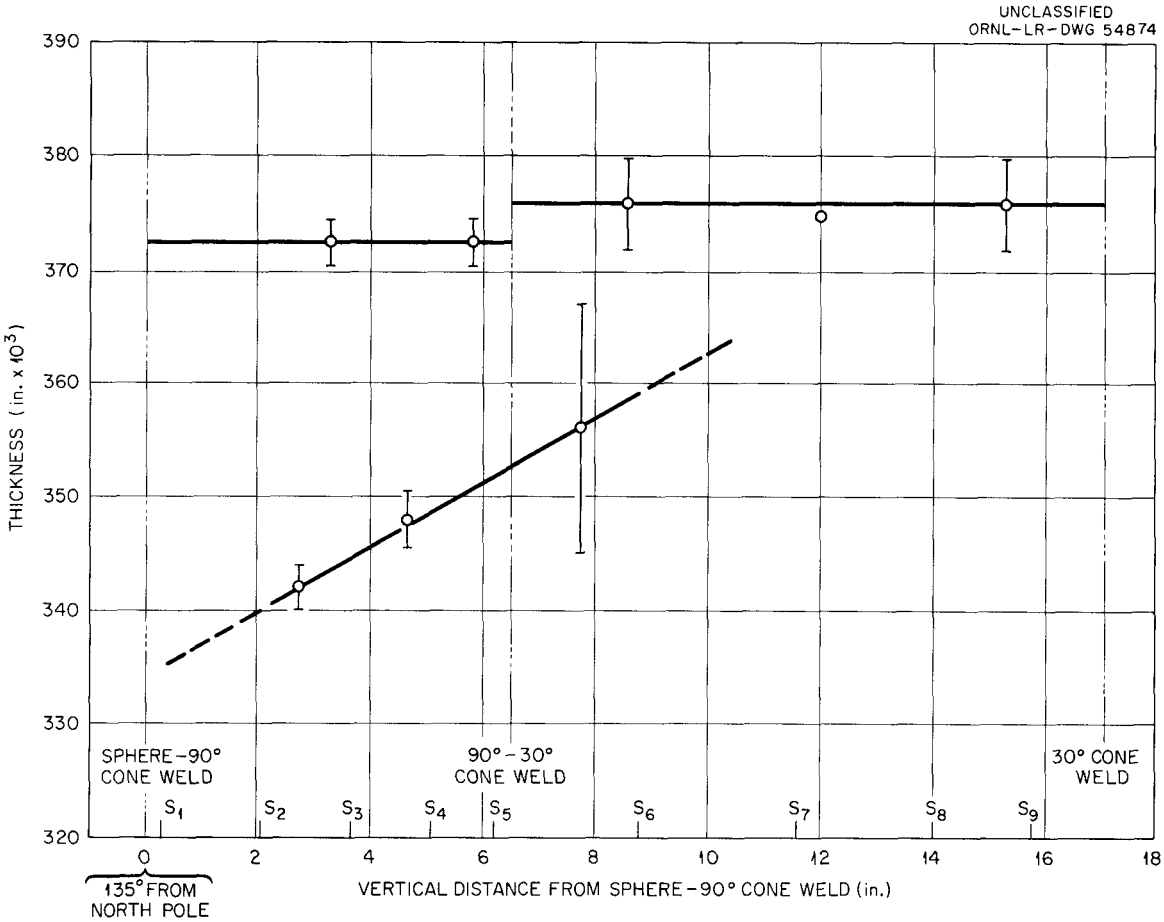

Fig. 1.3. Core-Wall Thickness vs Vertical Position of Measurement.

the Questar telescope, at direct magnifications on the 35-mm film negative of 0.59 and 2.34X. Enlargement of the negatives during printing resulted in magnifications of 4 x 16X on 5- x 7-in. prints. Visual magnifications estimated at 4, 8, 16 and 32X were obtained with the oculars furnished with the telescope.

The visual examination of the junction of the 30° and 90° cones and the surface of the 90° cone showed extensive shallow pitting of the inner wall of the vessel, varying in severity and extent around the wall at each level and decreasing in severity from the junction of the cones to the junction of the 90° cone and the sphere. The surfaces of the pits were bright and smooth on a fine scale, as though formed by highly localized melting of the surface or by attack by the uranium-rich second liquid phase which can be formed in the fuel solution at temperatures of 310 to 340°C.

The band lying between the junction of the 90° cone and the sphere and the equator of the sphere showed attack in a region only about 40° wide and 6 in. high, which was centered on the upper hole. The attack consisted principally of small-mound deposits, definitely projecting above the surface of the vessel. Attack was not extensive and did not appear to be particularly severe. Only three pits could be definitely identified in the region.

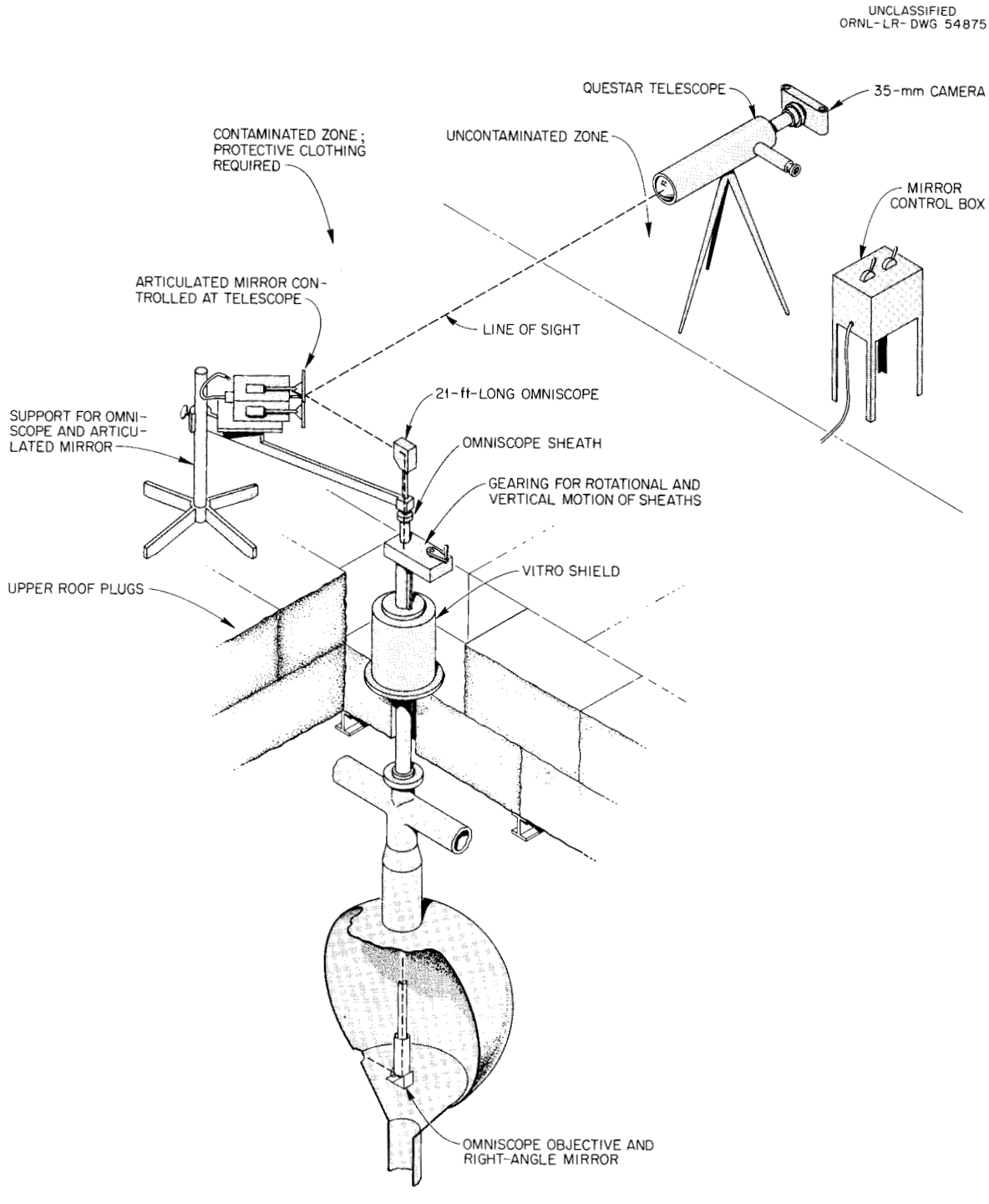

Fig. 1.4. Schematic Drawing of Assembly of Optical Equipment and Optical Path for Examination of Inner Surface of Core Tank at High Magnification.

A band about 4 in. high just above the equator of the vessel was examined. The surface was bright and "etched" on a fine scale, as though a sand-blasted surface had been lightly pickled. No other features were observable in this region. No Questar examinations at higher levels in the core tank were conducted, because of time limitations.

The screen stubs remaining on the wall of the vessel (from the attachment of screen ligaments to the wall by welding) showed degrees of attack ranging from complete removal of the ligament to severe pitting attack, which did not destroy the shape of the ligament, to what appeared to be fresh fracture faces having no attack and possibly resulting from fracture of the ligament during mechanical removal of the screens. The severity of attack varied around the stub line at each screen level and decreased in degree from the middle screen to the upper screen.

Examples of the pitting attack of the wall of the vessel and the attack on the screen stubs are shown in Figs. 1.5 through 1.8. The field of view in Figs. 1.5 and 1.6 is located at the level of the fourth screen from the top and about 5° west of building north. The pitting observable at the base of the screen stub is typical of the moderate-to-severe attack.

The field of view of Figs. 1.7 and 1.8 is on the stub line of the fifth screen from the top (the fifth screen is at the top of the lower patch) and about 10° east of building north, almost diametrically opposite the lower hole. The fracture faces of the screen stub appear to have been molten at some time.

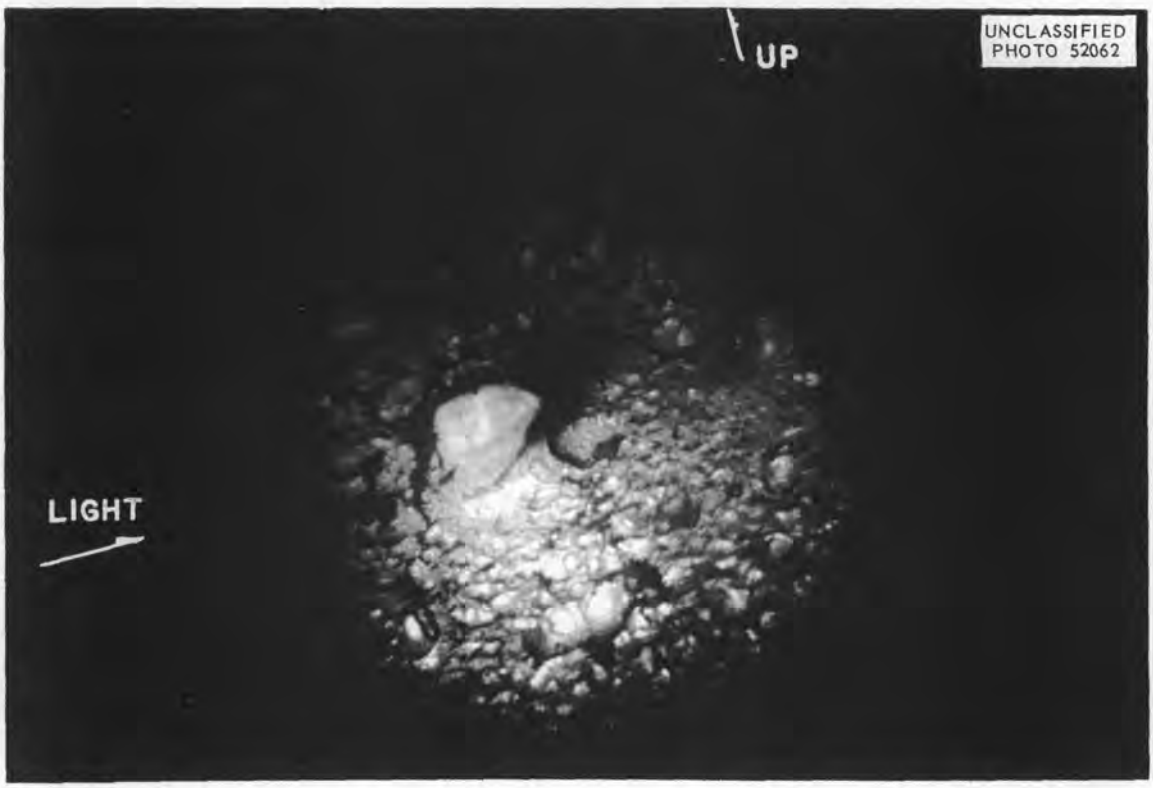

Fig. 1.5. Screen Stub and Pit Region at Screen 4. Location: fourth screen from top and about 5° west of building north. Black deposits are WO_2 from broken light bulb filaments. See Fig. 1.6. 4X. Reduced 8%.

Fig. 1.6. Pit Region at Base of Screen Stub, Screen 4. Point of focus is the pit region just below screen stub. Orientation: about 5° west of building north. See Fig. 1.5. 16X. Reduced 8%.

The black, sooty stringers and deposits observable in Figs. 1.5 through 1.8 are believed to be tungsten oxide formed from a light-bulb filament that burned out in the region shortly before the photographs were taken. (They were not seen during visual examination before the light bulb burned out.)

A typical example of the small-mound deposits found around the upper hole is shown in Fig. 1.9, a field of view located at the top center of the upper patch. The concentration of mounds was, in general, somewhat less than is shown in Fig. 1.9 and occurred as patches of mounds rather than as a general feature of the region.

The scar left on the wall of the vessel at the upper hole (left because a patch sufficiently large to completely cover all the damaged area around the upper hole could not be inserted in the vessel) was carefully examined as to topography and fit with the upper patch. A photograph of the region is shown in Fig. 1.10. The scar appeared to be relatively shallow; that is to say, it did not appear to constitute a major portion of the cross section of the vessel wall at that point. The fit of the upper patch appeared to be good, the inner surface of the patch being practically flush with the inner surface of the vessel. The gap between the wall and the patch, seen in the upper and lower portions of Fig. 1.10, is due to the differences in contour of the mating surfaces, that of the hole being reamed to a straight taper while the mating surface of the patch is curved. The gap is not due to a misfit of the patch.

Fig. 1.7. Y-Fracture Screen Stub, Screen 5. Location: on stub line on top of lower patch, about 10 to 15° east of building north. Point of focus is the fracture face. Black deposit is WO_2. See Fig. 1.8. 4X.

Although visual examination was possible at the higher magnifications, photography was not, because the limited illumination of the surface would not form an image on the film negative, regardless of the time of exposure.

The examination indicated that it is possible to obtain effective magnifications of 30 to 60X if lighting is improved, that stereophotography of various features is feasible (for the determination of depths of pits and heights of projections), and that photographic mapping of the entire inner surface of the

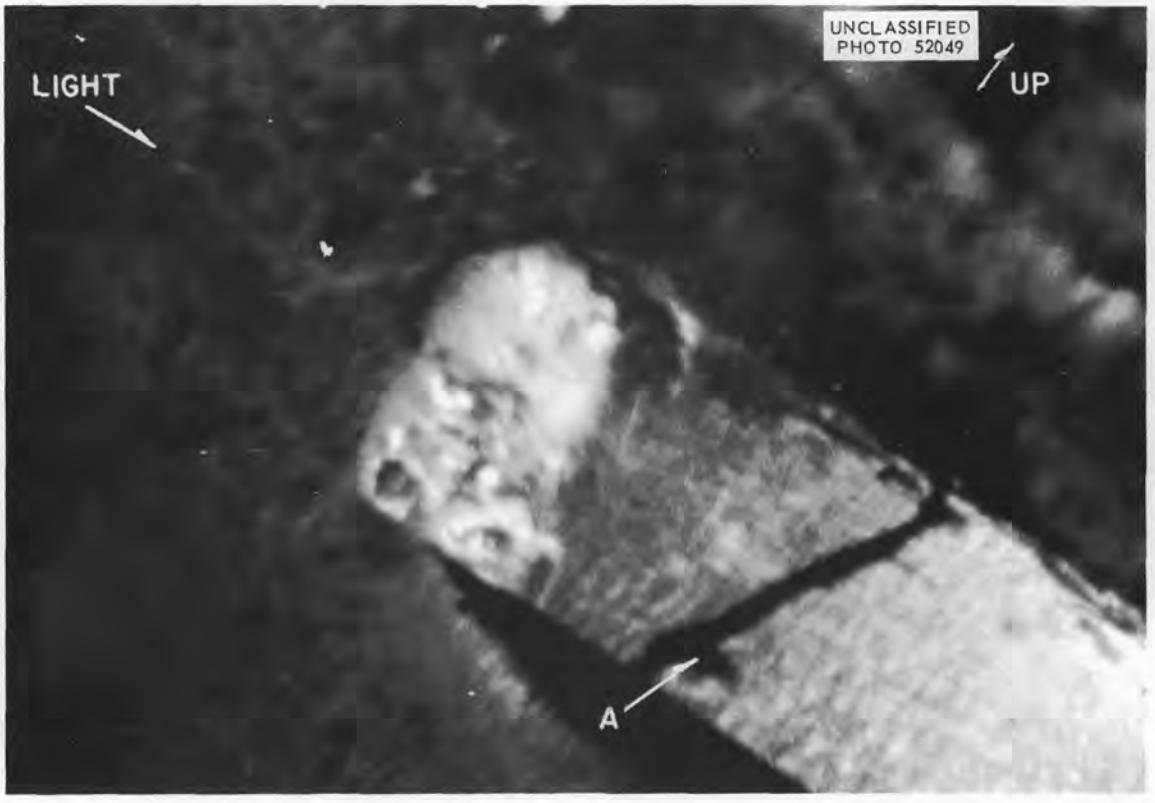

Fig. 1.8. Fracture Surface of Y-Fracture Stub, Screen 5. (A) Black stringer is WO_2 from light bulb filaments. Camera is focused on fracture face. Location: on stub line at top of the lower patch, about 15° east of building north. See Fig. 1.7. 16X. Reduced 8%.

vessel is possible by means of a motion-picture camera attached to the telescope.

1.1.4 Core Back-Flush

As a result of the core-repair operations, bits of debris were left in the core system. The largest contribution was made by the torch-cutting of the diffuser screens; it was estimated that about a half liter of metal droplets was formed. Temporary alterations to the system that would allow this debris to be flushed into a filter had been completed earlier.[4]

After the core holes were patched, the system was closed and the containment shield was emptied of water so that the reactor equipment could be operated. The high-pressure system was hydrostatically tested at 200 psig. A leak was found in some temporary piping on the purge portion of the core circulating pump and was repaired by operating remotely through a lead-shielded work facility. During the hydrostatic test a few pounds of the light-water condensate in the system leaked into the reactor shield. This increased the amount of radioactivity in the water processed at the waste pond (see Sec. 3.3).

After the high-pressure system had been hydrostatically tested, light water was circulated for 10 hr at ambient temperature and 100-psig system pressure. Differential-pressure readings indicated that the core flow was only about 50% of that expected. This suggested the possibility of partial plugging of the

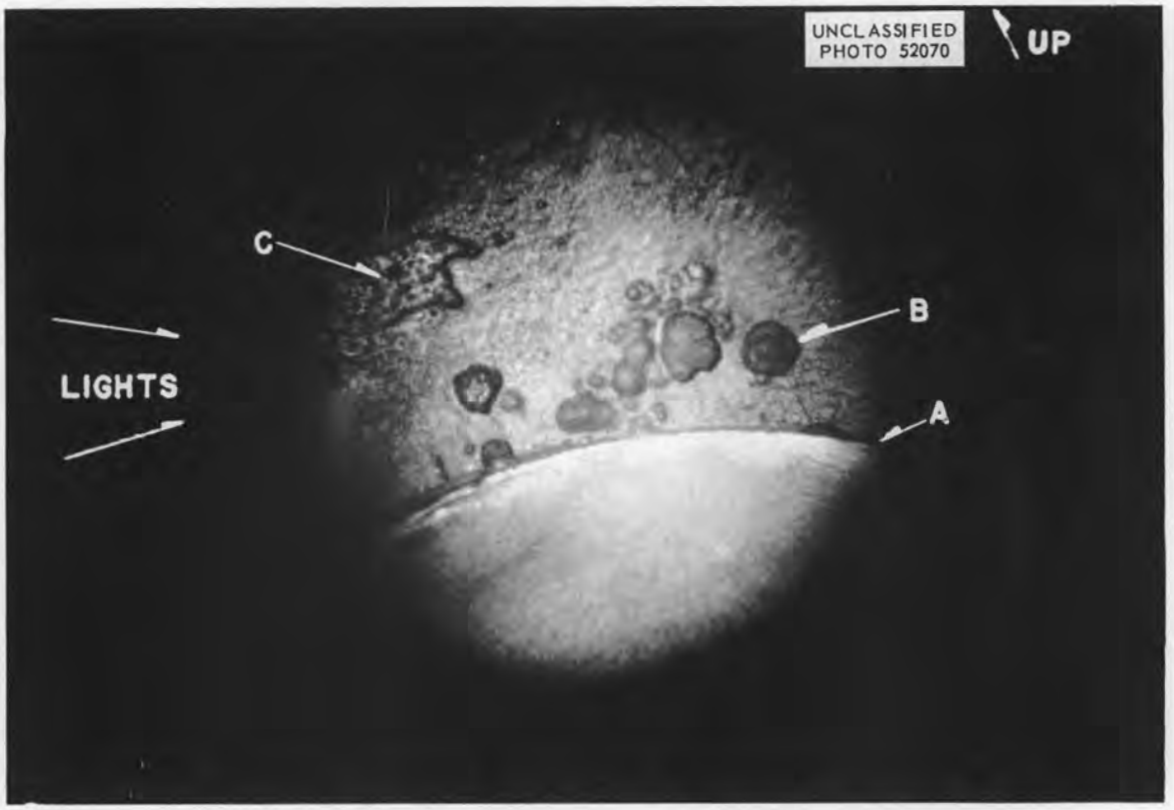

Fig. 1.9. Mound Deposit at Top of Upper Patch. (A) Top edge of upper patch. (B) and (C) Mound deposits. Location: top center of upper patch. 4X. Reduced 6%.

core loop or of the 40-mesh screen of the filter basket. Consequently, preparations were made to inspect the filter and the line (103) between the core and the suction of the circulating pump.

Most of the screen openings were clear when the basket was viewed remotely. It was weighed, showing an increase of approximately 2.5 kg. Radiation levels near the basket ranged up to 27,000 r/hr. Because of the radiation intensity, the basket was remotely canned and stored in the reactor containment shield. A brushing device was passed through the line from the bottom of the reactor vessel to the filter, without meeting any obstructions.

The dry-maintenance facility[5] was utilized for the first time during the filter replacement (see Fig. 1.11). Although unshielded radiation levels were greater than 10 r/hr at floor level, and although the filter activity was approximately 300 r/hr at 1 ft, radiation levels on the platform were less than 5 mr/hr, enabling the replacement to be accomplished without difficulty in a shift and a half. Several days were saved in the over-all schedule, since it was not necessary to flood the reactor shield again.

With a new filter basket installed, the core was back-flushed a second time. Apparently most of the debris had been picked up the first time, since the circulation rate the second time was almost normal. This conclusion was also substantiated by radiation levels, which were less than 1000 r/hr near the second filter.

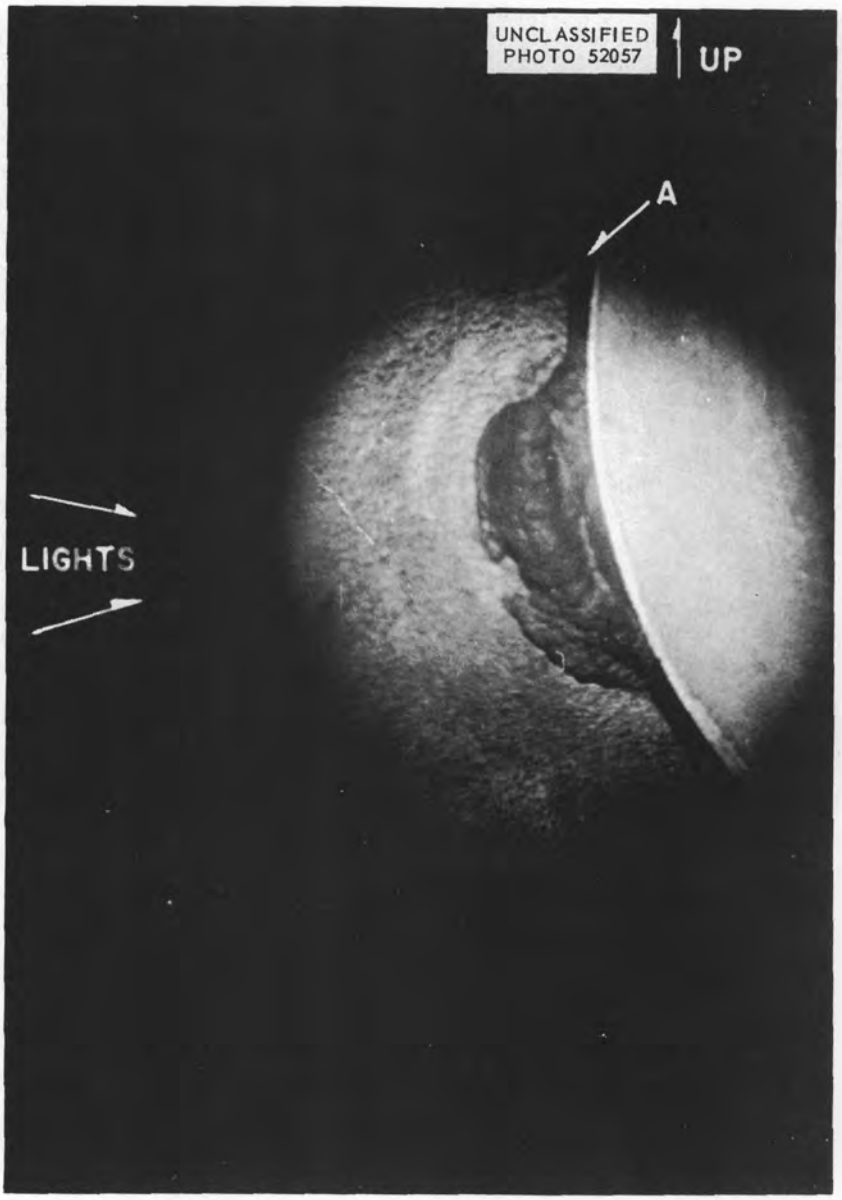

Fig. 1.10. Scar at Upper Patch. Hole scar at left side of upper patch that could not be removed by reaming. Edge of patch is shown. (A) Dark line along edge of patch is due to gap between patch and hole at inner surface, and not a shadow due to lighting. Patch is very nearly flush with inner surface of core tank. 4X.

Each time in an early stage of the back-flush, the dump line was flushed so that any material that might have settled there could be circulated to the filter for capture.

The second filter basket was not stored, but was removed for burial along with the temporary back-flush apparatus (see Sec. 1.2.2).

Fig. 1.11. Dry-Maintenance Facility.

1.2 MAINTENANCE AND SYSTEM ALTERATIONS

Several items of reactor equipment were replaced during the report period while employing both wet- and dry-maintenance practices.

1.2.1 Equipment Replacements

Feed Pumps

The intermediate-system flange (A-657) of the fuel feed diaphragm head, which had been replaced earlier,[6] developed a leak and could not be sealed. With the flange-ring design in use, it was necessary for the stainless steel lens-ring (used to decrease free volume where gas could accumulate) to seal in addition to the O-ring. A stainless steel O-ring, without the passage that interconnects the leak-detector line and lens-ring which the former aluminum ring had, was substituted. With the new ring, no leakage could be detected.

During the mixing experiments (see Sec. 2.2.1), one of the diaphragm heads of the blanket feed pump failed. It had been in use since the reactor was built, three years ago. The head was remotely replaced. Since radiation levels over the pump area were only 600 mr/hr at floor level, and 60 mr/hr 4 ft above the floor, it was not necessary to flood the reactor shield nor to provide special personnel shielding. The head, when removed, was found to have a cracked weld at a plugged hole on the intermediate side. It will be repaired for re-use.

Core Circulating Pump and Multiclone

Following the back-flush, a new core circulating pump with inlet and outlet piping revised was installed in order to reverse the direction of flow so that the fuel will pass through the core from top to bottom. A specially designed tungsten-electrode underwater torch was used to cut a web section from the 3/4-in.-thick pump base, so that the new pump could fit the old base. The pump legs had special connections for a new multiple-hydroclone assembly,[7] which was attached later. Both installations were made with the reactor shield flooded.

Pressurizer Interconnection

During runs 16 through 21, a solid plug was retained in the pressurizer interconnection (flange A-146), so that the blanket pressurizer could be operated liquid-filled. After the core holes were patched, the plug was replaced with a rupture-disk assembly, with a 0.0625-in. orifice,[8] so that both pressurizers could be operated in a normal manner. The rupture disks, although not absolutely necessary, were used to minimize possible differential-pressure fluctuations. After functioning smoothly during the mixing experiments, excessive leakage through the interconnection was indicated during the startup for pretreatment of the high-pressure system (see Sec. 2.4). The disk assembly, which was found to have a ruptured blanket-to-core disk, was replaced with the solid plug, through which a 0.0625-in. orifice was drilled.

Replacement of the interconnection assembly in each case was accomplished with ease, working through the special lead shield designed especially for this task.[9]

Heater Assembly for Secondary Fuel Recombiner

When replaced in the previous quarter,[10] the secondary fuel recombiner was without its electrical heaters, since they were still undergoing fabrication and testing. The heater assembly was installed remotely under water with no difficulty at the same time that the back-flush equipment was removed.

1.2.2 Radiation-Exposure Experience

During the report period, the highest single personnel radiation exposure was approximately 300 mr; no one exceeded his quarterly tolerance. Working backgrounds have usually been less than 50 mr/hr, although on a few occasions they ranged up to a few roentgens per hour for short intervals.

REFERENCES

1. S. E. Beall et al., HRP Quar. Prog. Rep. July 31, 1960, ORNL-3004, p 3.

2. G. M. Adamson et al., HRP Prog. Rep. Oct. 31, 1959, ORNL-2879, p 238.

3. D. E. Tackett, Fabrication History of HRT Core Tank, Appendix E, ORNL CF-58-12-6 (July 1, 1955).

4. S. E. Beall et al., HRP Quar. Prog. Rep. Apr. 30, 1960, ORNL-2947, p 11.

5. P. P. Holz, Dry Maintenance Facility for the HRT, ORNL CF-60-10-85 (Oct. 11, 1960).

6. S. E. Beall et al., HRP Quar. Prog. Rep. Apr. 30, 1960, ORNL-2947, p 11.

7. W. D. Burch et al., HRP Quar. Prog. Rep. Apr. 30, 1960, ORNL-2947, p 15.

8. H. F. Bauman, Specifications of an Orifice for Interconnection of the HRE-2 Pressurizers, HRP-60-103 (Aug. 9, 1960).

9. F. C. Zapp et al., Stepwise Procedures for Remote Handling of Rupture-Disc Assembly and Fuel and Blanket Sample Holders, ORNL CF-57-11-1 (Nov. 15, 1957).

10. S. E. Beall et al., HRP Quar. Prog. Rep. July 31, 1960, ORNL-3004, p 5.

2. HRT OPERATIONS

S. E. Beall P. N. Haubenreich J. W. Hill, Jr.

H. F. Bauman D. F. Frech J. O. Kolb
N. C. Bradley R. H. Guymon H. B. Piper
J. R. Buchanan P. H. Harley J. L. Redford
S. R. Buxton R. J. Harvey D. M. Richardson
J. R. Engel H. C. Roller

Nuclear operation of the HRT was resumed after the maintenance and modification period. The reactor has operated at power levels up to 1.8 Mw in an "initial approach to full power" experiment, which is currently in progress (Nov. 30). Data are being collected and analyzed at each intermediate power level.

2.1 PRELIMINARIES

2.1.1 Shield-Penetration Leak Tests

Leak-testing of the reactor shield and all its penetrations started during the shutdown period and was completed prior to reactor startup. These tests are repeated routinely to ensure that the integrity of the secondary containment is maintained. After the shield was sealed for the last time, a leakage of 2 to 4 liters/min (~0.6% of the cell volume per day) at 0.5 atm was measured. This agrees well with leakages attained in earlier operation.

2.1.2 Reactor Hydrostatic Test

The integrity of the high-pressure system was established by hydrostatically testing the piping and equipment at 2700 psig.

2.1.3 Summary of Operating Changes Since Run 21

Modifications and changes in operating procedures between runs 21 and 22 are summarized as follows:

Core System

The core circulating-pump connections were reversed so that fuel solution now circulates through the core from top to bottom. The upper five diffuser screens were removed from the core; the lower four screens were left in place.

Pressurizers

The pressurizer controls were changed to allow operation of the blanket pressurizer as well as the fuel pressurizer. In order to maintain the blanket level in the range of the sensing instrument, the blanket pressurizer is maintained at a lower pressure than the fuel. The blanket pressurizer heat input is controlled by the blanket liquid level. An orifice (0.0625 in., see Sec. 1.2.3) located in the interconnection between the pressurizers permits a small flow of steam from fuel to blanket and serves to damp out fluctuations in differential pressure.

Blanket Temperature

As an aid in keeping the core-tank wall cool, the blanket average temperature is being maintained at approximately 230°C (core is usually 260°C) by regulating the steam withdrawal rate from the blanket heat exchanger.

Letdown

As in the past, liquid letdown from the high-pressure system is normally to the fuel dump tanks. The blanket letdown valve, however, will open whenever the blanket pressurizer level exceeds its high limit (90%).

Dump Circuit

Both dump valves will now open in case of a dump. The blanket valve, however, will open only after the system pressure reaches the saturation pressure of the blanket system, which is cooler than the fuel.

Condensate Transfer

A new line was installed so that condensate which is transferred from the fuel low-pressure system to the blanket low-pressure system mixes directly into the blanket dump-tank solution instead of being bypassed to the blanket feed pumps. This minimizes the amount of uranium which collects in the blanket dump tanks due to sampling and leakage from the high-pressure system.

Low-Pressure System Pressures

Control mechanisms were alerted so that the pressure in the fuel low-pressure system is controlled (at 18 to 19 psia) by throttling the fuel cold-trap valves. (Initially, in run 22, the differential pressure between fuel dump tank and blanket dump tank was controlled in this manner, but the fuel dump-tank pressure variation apparently caused the fuel feed rate to vary slightly; so the change to constant pressure control was made.) The blanket low-pressure system is operated with a cold-trap valve open at all times. The pressure there is normally below atmospheric, since the off-gas charcoal beds are controlled at about 11 to 12 psia (see Sec. 2.1.4).

2.1.4 Ventilation and Containment Improvements

Secondary Containment of Off-gas Charcoal Beds

To improve containment of the off-gas charcoal beds, a new control system was installed. The major safety improvement is achieved by operating the beds normally below atmospheric pressure, which is accomplished by controlling the downstream pressure at 11 psia with the vacuum pump and automatic air-operated throttling valve. Since upsets can add above-normal quantities of oxygen to the beds and thus raise the pressure upstream of the beds above atmospheric temporarily, additional protection was gained by ventilating the space above the water which covers the beds to the stack via the regular waste-tank vent system. Activity releases of significant magnitude from the entire waste vent system, including this pit and the sample cubicles, are prevented by automatic diversion of ventilation gas flow to the reactor shield upon detection of activity in the line in the east valve pit. In the first 500 hr of run 22, this diversion system was not required to function.

Improved Stack Fan and Filter System

A higher-capacity dual-unit stack fan and improved particulate filter and iodine trap were installed to further minimize the possibility of significant activity releases. The filter includes an absolute filter, a 4-in.-thick silver-plated copper-mesh-and-charcoal canister system as iodine traps, followed by a second absolute filter. The spare fan will come on automatically if the operating unit fails. This system replaced a single fan and absolute filter. In addition to the normal particulate-activity monitor, the Operations Division has provided a sampler to monitor for iodine releases on a daily basis.

Other Ventilation Improvements

Other areas which are potential sources of activity release following equipment failure are being provided with ventilation systems which include absolute filters and charcoal-bed iodine traps. The reactor control-room levels are ventilated directly to the main stack. The steam pit and chemical-plant operating levels will have separate systems which discharge air above the building through small stacks.

2.2 PRECRITICAL TESTING

2.2.1 Mixing Experiments

Before the light water was removed, the reactor was operated at temperature (core, 260°C; blanket, 230°C) and pressure (1400 psig) for approximately seven days to study the core-blanket mixing rate,[1] to check equipment performance, and to evaluate the reliability of the new control loops. Equilibrium blanket-to-core concentration ratios, determined by using chromic acid (see Sec. 2.4) as a tracer, were 0.07 and 0.23, with the blanket purge rates of 6 and 3 lb/min. Leakage past the two patched holes was much less than that experienced prior to the occurrence of the second hole.

Most reactor components operated satisfactorily during the experiments. An exception was a blanket feed-pump diaphragm head which failed (see Sec. 1.2.3). Two chemical-plant elements also malfunctioned: the multiclone filter (see Sec. 3.1.2) and the circulating pump (see Sec. 3.2).

2.2.2 Recombiner Performance Tests

Both the primary and secondary recombiners in the fuel low-pressure system were replaced with redesigned units.[2] Tests to evaluate the performance of both recombiners were carried out with H_2 and O_2 from cylinders.[3]

Simulated radiolytic-gas mixtures of the concentrations expected during reactor operation were recombined satisfactorily by the secondary unit. The efficiency of the primary recombiner, however, appeared to be near zero at these low concentrations. It did function on richer gas mixtures. Since it appeared that the secondary recombiner would efficiently recombine reactor radiolytic gases, making the primary unit unnecessary for normal reactor operations, no further alterations were made.

2.3 LIGHT-WATER REMOVAL

During equipment replacement operations in the past several months, sufficient light-water condensate was kept in the system to establish freeze plugs and to prevent gross entry of water when the shield was flooded. Fuel and D_2O were kept in isolation in the storage tanks to prevent contamination by the light water.

During repair and maintenance operations, light water was used in all reactor tests (back-flush, hydrostatic, mixing, etc.) until all in-shield activities had been completed. After replacement of components following the mixing experiments, all possible light water was transferred from the reactor to the waste system (for concentration to a rich heel), and rinsing with heavy water was begun. Approximately 230 kg of D_2O was used in three rinses to satisfactorily remove the light water. An assay of the water in the reactor, after operation with fuel solution was resumed, revealed that it was 97.0% D_2O, a decline of only 3% after three years of use.

2.4 PRETREATMENT OF HIGH-PRESSURE SYSTEM

In order to form protective (corrosion) films on the walls of the high-pressure equipment and piping, the reactor was pretreated at 280°C and 1400 psig with oxygenated D_2O for 50 hr and then with dilute fuel solution (subcritical) for 50 hr.

During the initial startup for the pretreatment operation, excessive leakage through the pressurizer interconnection prevented operation of the circulating pumps. The interconnection assembly was replaced (see Sec. 1.2.3) and operation resumed.

2.5 APPROACH TO FULL POWER

The HRT resumed nuclear operations after being brought to criticality on November 7. The initial approach to full power in the modified core, now in progress, will require several weeks, because many data are being collected at a number of intermediate power steps.

After the start of the new run (No. 22) nearly 12 moles of H_2SO_4 was added to the fuel solution to increase the acid-to-sulfate ratio to 0.35. The higher acid level provides a larger margin of safety against fuel instabilities. Although the total power level has not yet exceeded 1.8 Mw, there have been no indications of instabilities such as those seen in the operation which preceded the core modifications. Corrosion data so far in the run indicate a generalized high-pressure system rate of <0.5 mpy.

So far, equipment problems have been minor. The diaphragm pump that supplies a condensate purge to the core circulating pump stopped pumping. The difficulty, which appeared to be due to check-valve leakage, was overcome by installing a faster-acting pump drive unit without interrupting reactor operation. Some difficulty was also encountered with a leak in the intermediate system of one of the fuel feed pumps. The leak was repaired by replacing the oil-to-water pulsator housing and the intermediate-system phasing valve. Since these items are in an accessible area, reactor operation was unaffected.

At the current total power level of 1.8 Mw (Nov. 30), studies are being made of chemical, inventory, and other operating data and power fluctuations. In the 653 hr of power operation accumulated since November 7, it appeared that the performance of the reactor with reversed flow was satisfactory. Although power oscillations are larger (up to 350 kw at 1800 kw) than had been experienced in earlier runs, the flow patterns observed in mockup studies suggest that the power variations should be larger than with upward flow.

In order to study the oscillations more thoroughly, provision was made to digitize continuously the power signal; the digitizer tape is then fed to one of the laboratory computers for analysis. Insufficient information has been accumulated to permit conclusions on the exact nature of the oscillations.

REFERENCES

1. H. B. Piper, Results of Mixing Experiment, HRP-60-133 (Oct. 26, 1960).

2. S. E. Beall et al., HRP Quar. Prog. Rep. July 31, 1960, ORNL-3004, p 5.

3. J. R. Engel, Performance Tests of Newly Installed Primary and Secondary Fuel Low-Pressure Recombiners, HRP-60-134 (Oct. 25, 1960).

3. HRT PROCESSING PLANT

W. D. Burch P. A. Haas
O. O. Yarbro J. M. Chilton

Tests of the solids removal system were resumed, with essentially continuous operation of the new multiple-hydroclone unit following startup of the reactor. Preliminary results did not indicate significant improvement with this unit as compared with performance of the first multiclone.

3.1 SOLIDS REMOVAL SYSTEMS

3.1.1 Back-Flush Run

During the core back-flush operation, the processing plant was on stream with only the original single hydroclone in operation. The first multiclone had been removed earlier, and the revised unit was not installed prior to the back-flush operation. Flow was maintained in the normal direction through the hydroclone, even though reactor flow was reversed, by operating the chemical-plant pump at high frequencies (70 cps), and thus high heads, to overcome the reversed pressure drop across the take-off lines. As expected, collection rates were very high, indicating high concentrations of solids in circulation (>0.1 g/liter). Solids compositions for this run and the other two operating periods are listed in Table 3.1. The solids composition for this run was very similar to that from other runs; the solids removed by the hydroclone were predominantly small particles of corrosion-product scale and not the large particles of zirconium and ZrO_2 formed in the screen-cutting operation.

3.1.2 Mixing Experiment

The revised multiple-hydroclone unit was operated initially during the core-to-blanket mixing experiments. Early in this period low underflow-pot temperatures pointed to the possibility of a low flow rate through the multiclone. No flowmeter is provided in the circuit, but pressure changes in the underflow pot, observed when the reactor circulating pump was stopped and restarted, could be related to pressure drops in the multiclone circuit, and clearly showed that the flow was only a small fraction of the normal 12 gpm. Since the measurements indicated that the restriction was on the upstream side of the multiclone, the plug was assumed to be at the filter, which was provided to prevent large pieces of scale from plugging the hydroclone ports. Subsequently, the filter screen, which contained two thousand 1/32-in. holes, was replaced with a similar one in which the holes were enlarged to 1/16 in., and tests showed that flow was restored to normal. It is not possible to determine at what period the screen plugged, since investigation of the low underflow-pot temperatures revealed that these were normal and resulted from the longer underflow pot, the induced-underflow method of operation, and normal heat losses from the cell C loop rather than from low flow through the unit. The only net heat input to the hydroclone system from the reactor is by conduction and very limited turbulent mixing down the 18-in.-long underflow pot.

Table 3.1. Hydroclone-System Removal Rates and Solids Composition

Run No.	HRT-CP-21-24	HRT-CP-22-25	HRT-CP-22-26
Operation	Back-flushing	Mixing Expts.	Run 22 Startup
Time on stream, hr	9	47	60
Removal rate, g/hr	23	1.9	1.5
Solids composition, %			
Fe	12	12	10
Cr	4	5	7
Zr	56	52	53
Ti	1.2	1.4	1.5
U	4.1	3.7	3.3
Cu		0.4	0.5
Ni	0.4	0.8	0.8

In a low-pressure experiment, it was found that temperatures at the bottom of a multiclone underflow pot (initially at room temperature) approached the feed-stream temperature with a time constant of several hours when the feed stream was below 100°C. It is presumed that at higher temperatures the time constant would be even longer.

Heat losses from the collection hydroclone loop, including 5 kw removed by the circulating-pump cooling water, cannot be completely made up by the existing heaters. Therefore the system runs at only 200°C with maximum heat input when the reactor core temperature is 260°C.

3.1.3 Initial Operation in Run 22

The solids removal system was started up with the reactor at the beginning of run 22. After 60 hr, just prior to pump-up of the fuel, the initial batch of solids was isolated and subsequently dissolved. While solids removal rates as high as 5 g/hr are expected at the beginning of a run, the rate observed for this period was only 1.5 g/hr. Whether this was due to a lower-than-normal circulating-solids concentration or an inherent lower efficiency of the multiple hydroclone with induced underflow[1] cannot be determined until data have been acquired from several runs.

The uranium content of the solids removed was significantly lower than in past runs. Solids from runs 20 and 21 averaged greater than 5% uranium, compared with 3.3% for this period.

The system was placed back on stream and operated for 550 hr before isolation of the second solids batch.

3.1.4 Basic Studies of Multiple Hydroclones

Flow rate vs pressure-drop measurements for multiple hydroclones in parallel on a single induced-underflow receiver indicate that the ratio of pressure drops, (feed to underflow)/(feed to overflow), is a sensitive indicator of plugging of individual hydroclone ports. For a given multiclone configuration, this ratio appears to be independent of flow ratio and should be independent of density changes such as might be caused by temperature or solution concentration changes.

This is shown from flow vs pressure-drop curves for a test multiclone, using twenty 0.4-in.-diam Bakelite hydroclones in a Dorr TM stage. These pressure ratios were determined for various plugged ports, using two sets of hydroclones (Table 3.2).

The changes in the pressure-drop ratios agree qualitatively with the flow changes that would be expected. Hydroclones with plugged feed ports should act as channels for flow from the underflow receiver to the overflow, thus increasing the feed-to-underflow pressure drop. Hydroclones with plugged overflow ports would act as flow channels from the feed to the underflow receiver, thus reducing the feed-to-underflow pressure drop. Plugged underflow ports for one or several units of a multiclone would not affect these ratios.

These pressure ratios appear to be practical indicators of multiclone malperformance. Density effects due to temperature or composition changes cancel out. Measurements of relative pressure drops should be more accurate than flow-rate measurements at reactor operating temperatures and pressures.

The change in pressure-drop ratio for the first HRT multiclone following reactor service (see Table 3.2) agrees with the previous interpretation that several feed ports had become plugged.[2] The pressure ratios for this unit are different from the others tested, because the hydroclone diameters were larger (0.6 in. as compared with 0.4 in.). The values for the second HRT multiclone should be usable for testing its condition when it is removed from the reactor cell. The pressure-drop ratios for this unit appeared to vary with flow rate, probably because of poor calibration curves.

3.2 MAINTENANCE: REPLACEMENT OF CIRCULATING PUMP

While the underflow pot was being rinsed following the mixing experiments (HRT-CP runs 22-25), the 1-gpm circulating pump became noisy and current drawn was very erratic, indicating incipient bearing failure. The pump was replaced with a spare, using the normal underwater techniques. Total time required for the replacement was less than three full 8-hr shifts, including several hours required to salvage the microphones and thermocouples from the failed pump and reinstall them on the replacement.

The pump had operated 2900 hr before failure, approximately 95% of which was at high temperatures and pressures, with the remaining time at low pressure during the rinsing operations.

3.3 WASTE-POND TREATMENT

Normal scavenging treatments removed 99.6% of the 160 curies of activity added to the waste pond in 660,000 gal of water in this period. Most of this activity resulted from leakage into the cell during the back-flushing operation (see Sec. 1.1.4). The major activities in the 0.7 curie released were Sr^{89}, 30%; Sr^{90}, 20%, and Cs^{137}, 35%.

Table 3.2. Effects of Individual Hydroclone Variations or Plugs on Multiclone Pressure Drops vs Flow rates

Multiclone: Modified Dorr TM stage with twenty 0.4-in.-diam hydroclone units on outer circle; inner circle for twelve units plugged off

Conditions: Water at room temperature; atmospheric pressure discharge; data calculated from curves plotted from experimental data

Basic Unit				$\frac{P_F-P_u}{P_F-P_o}$ at Three Flow Rates (gpm/clone)		
L (in.)	D_u (in.)	No. Used	Variation	0.3	0.5	0.6
2.64	0.132	20		0.630	0.639	0.638
		18	Two feed ports plugged	0.688	0.689	0.686
		18	Two overflow ports plugged	0.428	0.455	0.463
		18	Two 3.14-in. L, 0.090-in. D_u clones replacing original ones	0.610	0.629	0.631
3.14	0.090	20		0.622	0.627	0.629
		18	Two feed ports plugged	0.754	0.754	0.762
		18	Two overflow ports plugged	0.429	0.434	0.438
		18	Two 2.64-in. L, 0.132-in. D_u clones replacing original ones	0.600	0.614	0.630
2.40[a]	0.104	18			0.59	0.63
3.60[b]	0.120	13		0.420[b]	0.459[b]	0.477[b]
3.60[b]	0.120	13	Not known[c]	0.542[b]	0.536[b]	0.554[b]

[a]Second HRT multiclone as fabricated from Dwg. D-34004 with 0.4-in.-diam hydroclone.

[b]First HRT multiclone as fabricated from Dwg. D-33741 with 0.6-in.-diam hydroclones; pressure drops for flows of 8, 10, and 12 gpm to multiclone.

[c]First HRT multiclone after removal--reported earlier to have two plugged feed ports.[2]

3.4 ALTERNATIVE FUEL-PROCESSING METHODS

Further laboratory studies were carried out to optimize the conditions for the processing of the 8 kg of uranium contained in the present fuel batch by peroxide precipitation. In order to process the entire fuel batch at one time, it is necessary to concentrate to 150 g of uranium per liter. It was found that the peroxide filtered easier if the precipitation was carried out from 75-g/liter uranium solution and that under these conditions more than 96% of the uranium could be recovered with only about 1% of the copper and nickel being carried with the uranium.

In full-scale tests with nonradioactive solutions at the HRT, difficulty was encountered in retaining the uranium peroxide precipitate on a stainless steel filter of the G pore size. No difficulty had been encountered in the laboratory in retaining this precipitate on a sintered glass filter of even larger pore size. Laboratory studies demonstrated that the use of paper pulp and diatomaceous-earth filter aids at 10-g/liter concentrations improved filtration by the sintered stainless steel filter. Approximately 3.5% of the precipitate passed through the filter under these conditions; however, even with filter aids, the precipitate was not contained at pressure differences greater than about 15 psi across the filter.

The possibility of separating the uranium contained in the decay-tank solution at a concentration of 5 g of uranium per liter from the 4 *M* H_2SO_4, containing zirconium (4 g/liter) and stainless steel corrosion products at lower concentrations, was investigated. Of the methods studied, anion exchange, using Dowex 1, appears to be the most promising. When a synthetic solution of the composition in the decay tanks was diluted by a factor of 15 and partially neutralized with ammonium hydroxide, a resin loading of 30 g/liter could be obtained with only a 0.03% loss. The uranium can be eluted with 1 N HNO_3, and precipitated as a peroxide from this solution.

REFERENCES

1. P. A. Haas et al., HRP Quar. Prog. Rep. July 31, 1960, ORNL-3004, p 21.

2. O. O. Yarbro, Test of HRT-CP Multiclone No. 1 Following Removal From the Reactor Cell, ORNL CF-60-6-105 (June 28, 1960).

4. HRT COMPONENT DESIGN AND DEVELOPMENT

I. Spiewak

R. Blumberg
R. H. Chapman
P. H. Harley
E. C. Hise
J. E. Jones
C. G. Lawson
W. R. Mixon
W. Terry

4.1 HRT REMOTE-MAINTENANCE DEVELOPMENT

When the leak rate through the patched lower hole of the HRT was found to be greater than 8 lb/min of water, a program was initiated to develop a tighter patch which could be installed at a later shutdown. A replica of the area around the hole was fashioned and was reproduced in aluminum castings for study and practice in the mockup. One casting was bored in a lathe with a 2-in.-diam 60°-tapered reamer, demonstrating that reaming will provide an uninterrupted seating surface for the same type of plug used previously in the upper hole. A contoured plug was designed and fabricated. It is shown installed on the hole replica in Fig. 4.1.

Concurrently, a tool was designed with two working attachments, one for removing the existing patch and one for reaming the lower hole. Fabrication of this tool, shown in Fig. 4.2, is about 75% complete.

4.2 HRT FEED-PUMP-DESIGN MODIFICATIONS

Design modifications were made to the feed-pump diaphragm heads to permit fabrication in a more economical manner and yet retain the same degree of assurance that chips and dirt can be kept out of the finished assembly. Jigs and fixtures were designed to permit testing of component parts of the check valves at various stages of fabrication in order to increase the probability of obtaining leak-tight check-valve assemblies upon completion.

4.3 HRT SPARE CIRCULATING PUMP

Stainless steel parts were machined to replace the titanium parts in the hydraulic end of the spare circulating pump. Materials were changed because titanium parts ignited in two circulating pumps while in HRT service.[1]

4.4 HRT CORE

4.4.1 Further Studies on Temperature Distribution in HRT Vessel with Reversed Flow

Several additional sets of measurements[2] of local residence time were made in the equatorial plane of the HRT flow model by means of conductivity probes which follow changes in salt concentration. Between sets of measurements, the flow model was disassembled and reassembled to determine the reproducibility

UNCLASSIFIED
PHOTO 36345

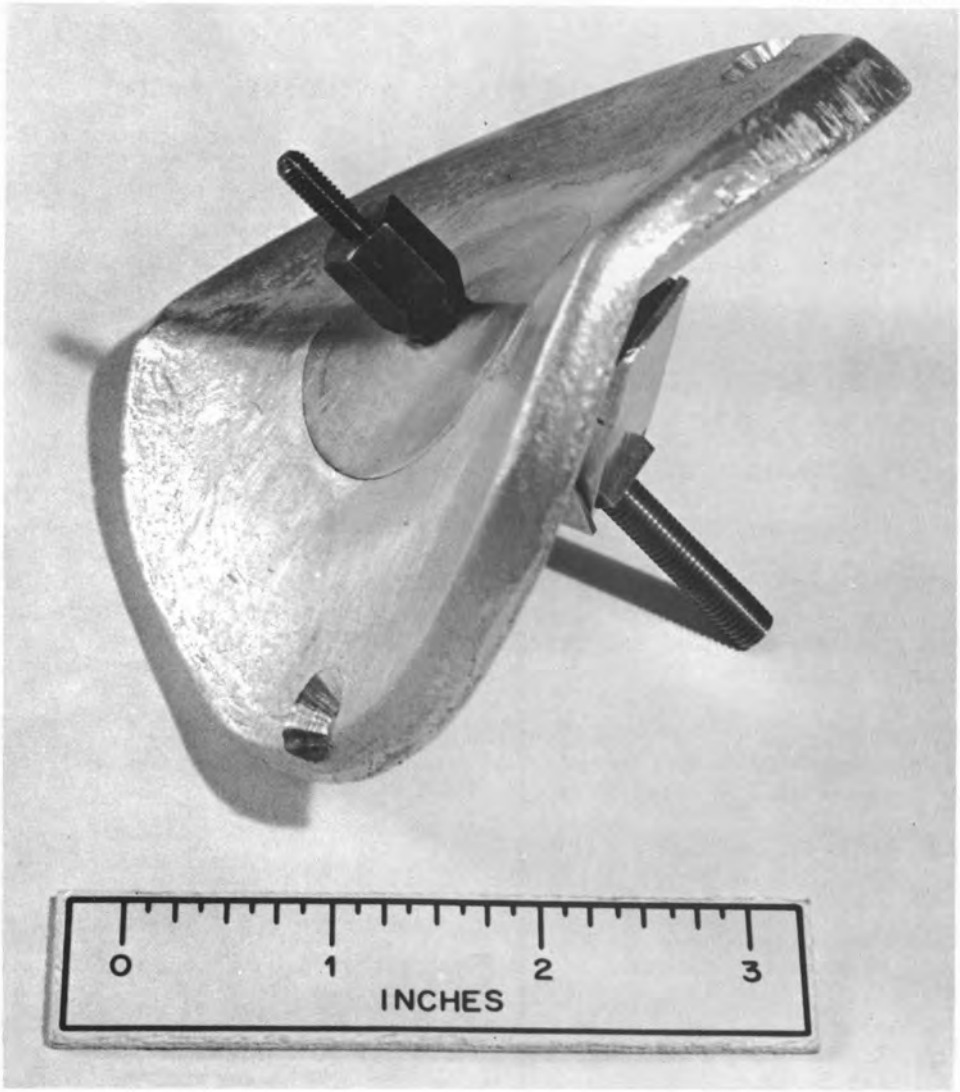

Fig. 4.1. Contoured Plug in Lower Hole.

of the measurements as a result of small changes in the fit of the assembly. The ages so obtained, when plotted against distance from the wall, suggest that the bulk average temperature in the core will be

$$T_B \cong T_1 + [(1.2 \pm 0.1)(T_2 - T_1)],$$

where

T_B = bulk core temperature,

T_1 = core inlet temperature,

T_2 = core outlet temperature.

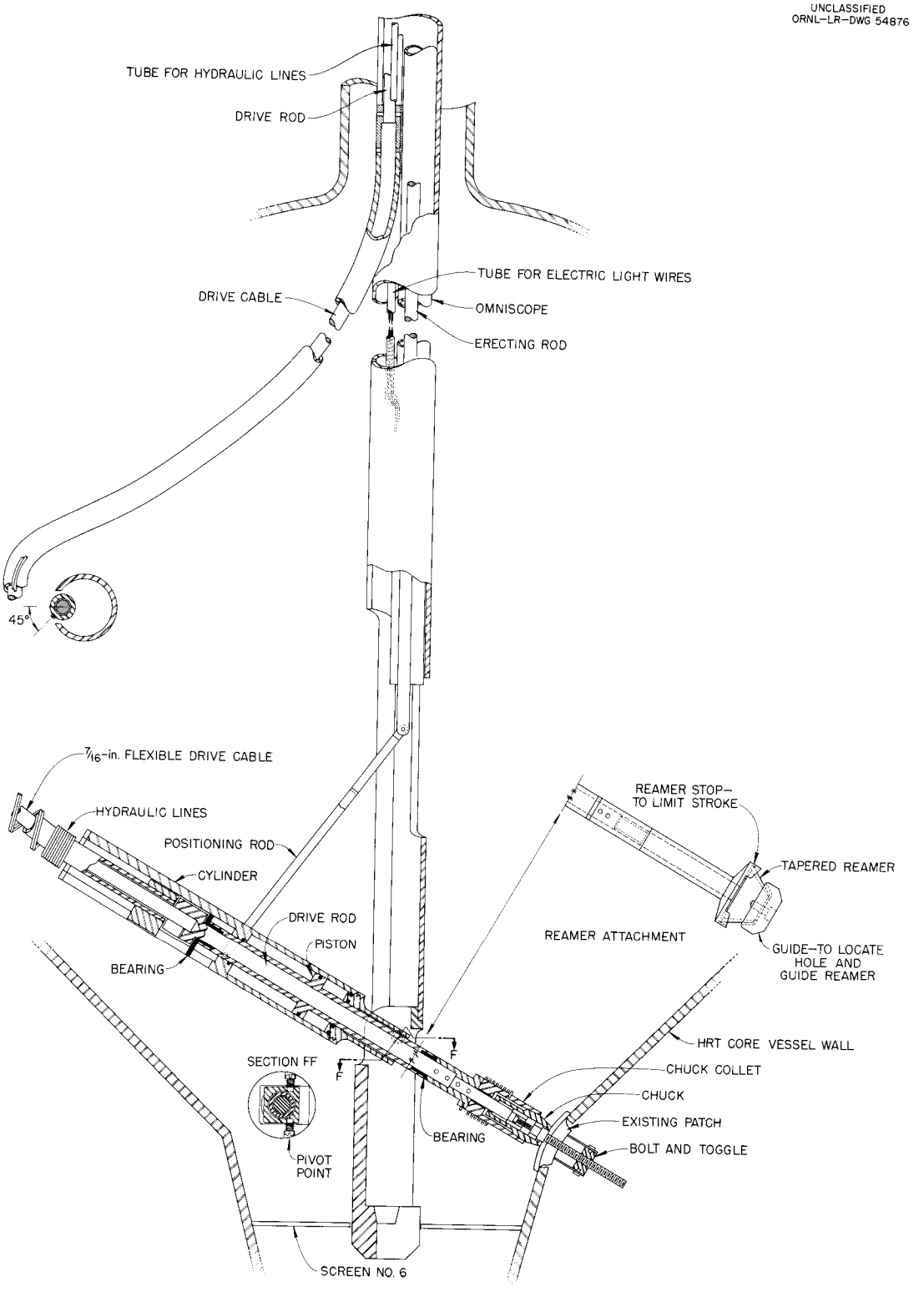

Fig. 4.2. Wrench for Removal of Lower Patch in HRT Core Tank.

Reproducibility of the conductivity-probe age measurements is ±5% when measurements are made in identical situations. It is believed that the variation in age distribution is caused by variation in the mechanical assembly of the system. Furthermore, the prediction of average temperature of the HRT core is possible to within only 10%.

4.4.2 Comparison of Calculated Corrosion with Measured Decrease in Core-Tank Thickness

A comparison was made between the ultrasonically measured decrease in core wall thickness of the HRT vessel[3] and the corrosion that would be predicted from the correlations obtained from the in-pile-loop data. For an HRT solution containing 5 g of U per liter and a fluid velocity of 0.3 fps, the estimated corrosion rates as a function of wall temperature and power density are shown in Fig. 4.3. The corrosion on the blanket side is estimated to be half the corrosion on the core side. For the upper hemisphere, the wall temperature is estimated to be close to the outlet temperature when there is no gross deposition of scale.

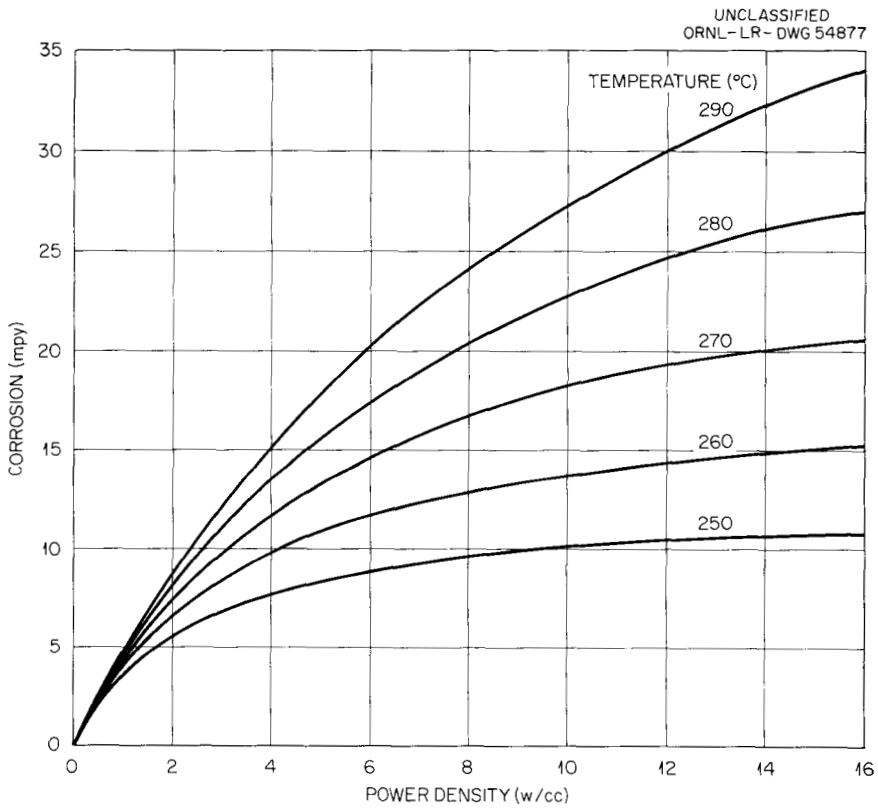

Fig. 4.3. Corrosion Rate for Zircaloy-2 in HRT Solution (5 g of U per kg of D_2O) at 0.3 fps.

The power-time-temperature history of the HRT was integrated over its operating life to estimate the corrosion that would be obtained on the basis of in-pile-loop tests. The corrosion calculated is compared in Fig. 4.4 with that measured ultrasonically. The calculated corrosion through run 20 was 6 mils, and the calculated corrosion during run 21 was 4 mils, giving a total of 10 mils. Total measured corrosion was 8 to 14 mils.

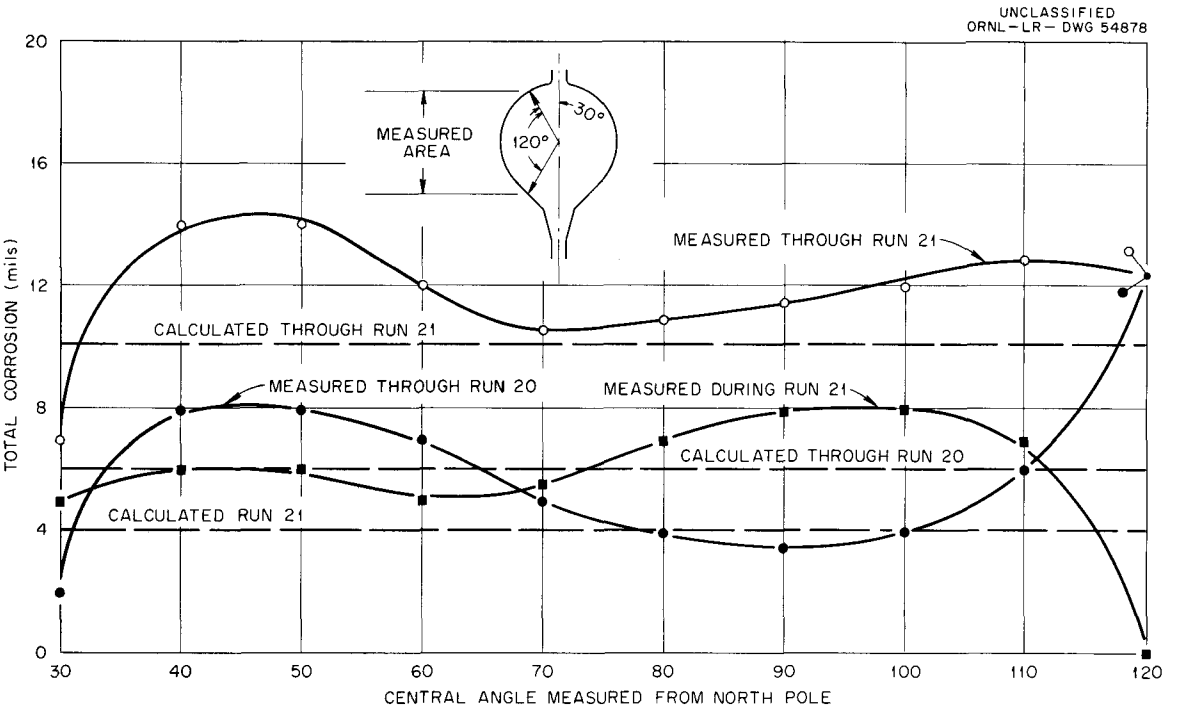

Fig. 4.4. Comparison of Calculated and Measured Corrosion in HRT.

It is concluded from the above comparison that it is reasonable to predict core-wall life on the basis of in-pile-loop measurements.

4.4.3 HRT Core Corrosion-Specimen Holder

A new corrosion-specimen holder was designed for insertion into the core of the HRT. The design, shown in Fig. 4.5, is a more streamlined assembly than the one previously exposed[4] in the HRT. All parts in contact with fuel solution are constructed of Zircaloy-2. The specimens, shaped as shown in the figure, are welded to the central structural member and can be disassembled by shearing next to the weld at the support member. Tests have indicated that the uncertainty in the measurement of the weight loss of the specimen can be controlled by shearing at a cross section having a small area.

Three thermocouples, sheathed in stainless steel clad with Zircaloy-2, are used to indicate temperatures at different levels in the core. Extending below each thermocouple is a simple rod-type metallurgical specimen of Zircaloy-2 for physical-property measurements following irradiation.

4.5 HRT MOCKUP OPERATION WITH DILUTE SOLUTIONS

The HRT mockup loop was operated during the report period to investigate further the chemical stability of diluted simulated HRT fuel solutions. The basic fuel solution, 0.04 $\underline{m}$ UO_2SO_4, 0.02 $\underline{m}$ $CuSO_4$, 0.035 $\underline{m}$ H_2SO_4, and 0.014 $\underline{m}$ $NiSO_4$, was diluted various amounts and circulated through the system at constant temperature and pressure. The range of uranium concentration investigated was from 1700 ppm to 13 ppm.

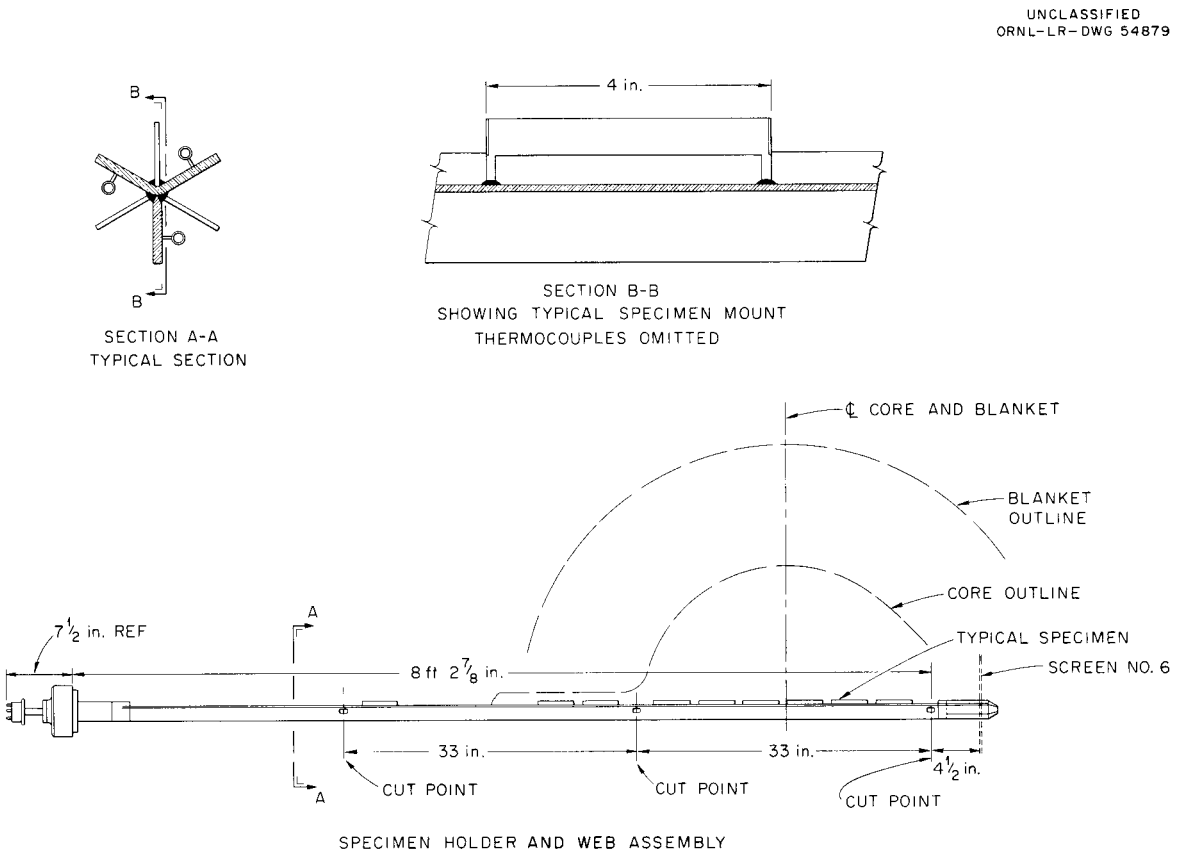

Fig. 4.5. Replacement HRT Corrosion Specimen Holder.

No hydrolysis was noted at a uranium concentration of 0.8 g/liter or above. This confirmed earlier work with a similar solution.[5] At concentrations of 13 to 500 ppm uranium instability was noted at temperatures above 250°C, while the solutions appeared to be stable at 150 to 225°C.

It was concluded that the HRT blanket fuel concentration should be maintained above 1 g of U per kg of D_2O. Attempts to define a lower concentration limit in this series of tests were not successful, since loss of uranium was noted in solutions of the lowest concentration tested, 13 ppm.

4.6 HRT REPLACEMENT REACTOR VESSEL

Conceptual designs were made of reactor vessel assemblies suitable for replacement of the present HRT vessel assembly. Preliminary nuclear calculations (see Sec. 5.3) indicate that it may be possible to achieve Th-U^{233} conversion ratios greater than unity in small reactor sizes such as those under consideration. In order to obtain core-wall power densities in the range of economic interest, that is, 30 to 50 kw/liter for a reactor operating at 5 to 10 Mw, a partial beryllium reflector is employed. The core requires a concentration of 9 g of U^{235} per kg of D_2O for criticality. Fuel solution and blanket D_2O inventories must be held to a minimum so that the existing HRT low-pressure systems will be adequate.

The best concept developed to date is shown in Fig. 4.6, where the core tank is a cylinder, 21 in. in inside diameter by 42.25 in. in inside over-all length (volume = 200 liters). A 4-in.-thick beryllium region is located about 3/4 in. away from the core wall. Two regions of thoria pellets, each about 3.5 in. thick, are located outside the reflector region. There are coolant passages between each of the regions, as indicated in the figure. The pressure vessel is about 52 in. in inside diameter by 88 in. inside over-all height.

The flow pattern recommended for the core is that induced by the "slotted side entry" concept, where two headers are attached to the side of the cylindrical portion of the core tank. Flow enters the tank through tangential slots, thus inducing rotational flow within the core, with the main outlet vertical at the top. A small bypass flow is taken off the bottom to remove solids and to provide a gravity-drain connection.

Access to the core proper is through a single 5.5-in.-ID flanged opening. Access to the blanket region is possible through four 5.5-in.-ID flanged openings. However, one of these openings is not readily available as it also serves as the blanket pressurizer and circulating-line connection. The small flange on the core bypass line can be manipulated through one of the blanket access ports.

4.6.1 Layouts for HRT Replacement Reactor Vessel

Conceptual layouts were made in order to show how a replacement reactor vessel might be installed in the present HRT. Investigations were made with respect to locating the replacement vessel in the adjacent chemical-plant cell B or in the location now occupied by the HRT reactor vessel. The use of one or two circulating pumps and heat exchangers was considered.

In the currently favored layout, the new vessel is in the same position as the present one, and it utilizes both of the existing 5-Mw steam generators as fuel heat exchangers, with two 450-gpm canned-motor pumps circulating fuel through the core and the exchangers. A new heat-removal system, including another heat exchanger and canned-motor pump, would be installed to remove the heat generated within the blanket region.

4.6.2 Flow Tests of the HRT Replacement Core

Fluid age measurements, using salt conductivity probes, were completed in a 5-in.-diam cylindrical plastic model. A vaned annular entrance and an axial outlet, both at the top of the vessel, were employed. The ratio of mean fluid age at any point to mean residence time in the vessel, which is equivalent to the ratio of fluid temperature rise at that point to the temperature rise from core inlet to outlet when constant and uniform heat generation rate within the fluid in the core is assumed, ranged down the length of the core from 0.2 to 1.04 at the wall and from 1.9 to 2.2 in the center. There was no appreciable change in the relative age when the water flow rate was decreased from 36 gpm (mean residence time of 2.45 sec) to 13 gpm (mean residence time of 6.78 sec).

In other tests, a 5-in.-diameter plastic model, 15 in. long, was fabricated with two slot inlets, 180° apart and 0.060 in. wide, extending axially down the side of the model. The slots directed incoming fluid tangentially along the cylindrical wall. Fluid exit was through a pipe in the center of the top of the model, and the top and bottom heads were flat. The ratio of mean fluid age at a point to the vessel mean residence time ranged down the length of the vessel from 1.05 to 0.48 at the wall and from 1.35 to 1.16 in the center. Fluid ages

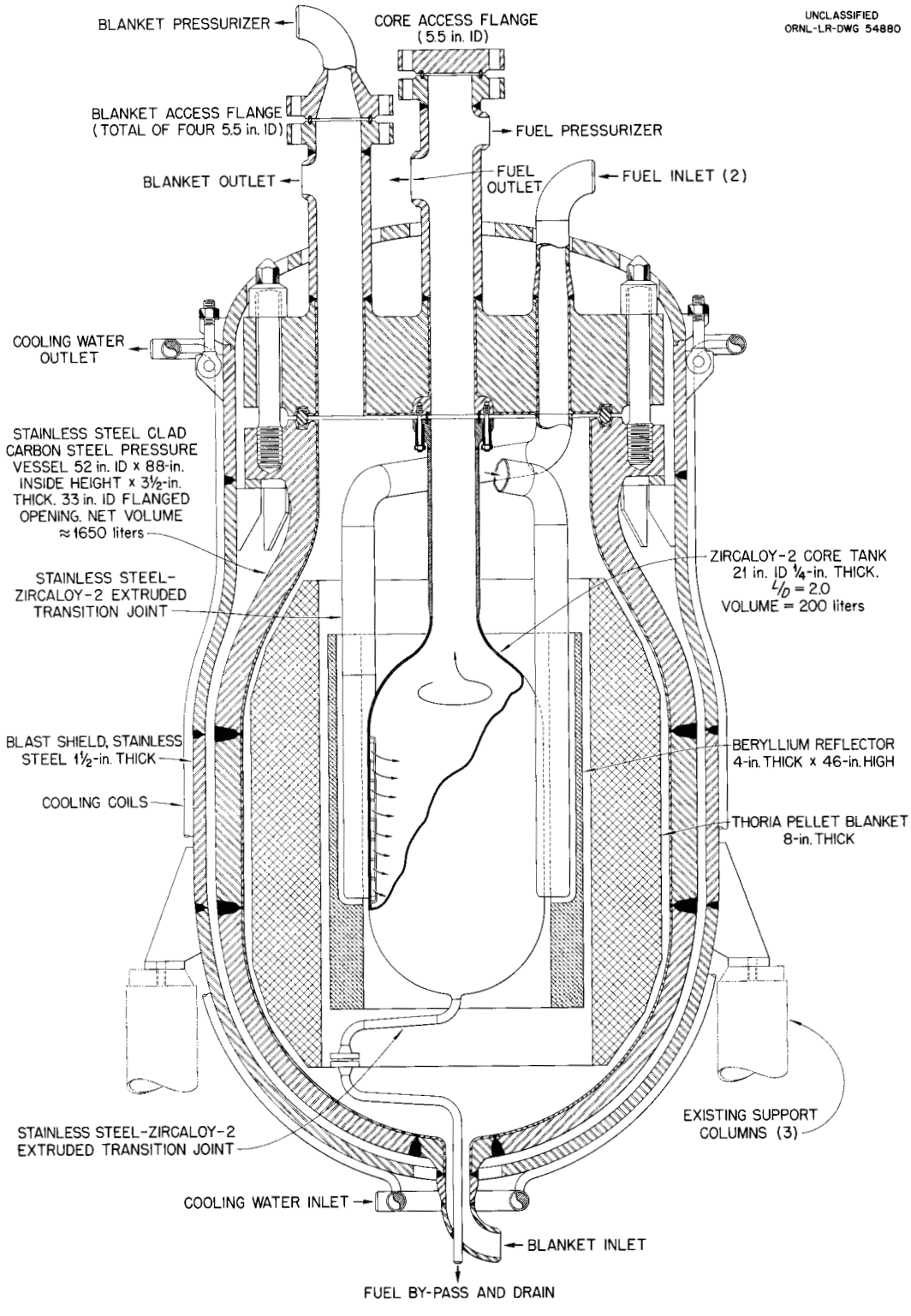

Fig. 4.6. Concept of HRT Replacement Reactor Vessel.

were relatively less at the lower part of the model, due to more fluid entering at the bottom of the slot than at the top. If this design were used in a core operating between 250 and 290°C, maximum hot-spot temperature would be 304°C.

The slot-entry model was modified to have 1.104-in. slots, hemispherical heads, an over-all length of 10 in., and two jets in each head to direct incoming fluid along the walls of the head. Fluid age measurements with conductivity probes, dye-injection studies, and velocity-probe traverses will be completed for this model which corresponds to the preferred concept for the replacement vessel. Preliminary flow tests showed that solids would be removed readily from the vessel, and dye tests suggested that the maximum wall temperature would be below the outlet temperature.

REFERENCES

1. S. E. Beall et al., HRP Quar. Prog. Rep. Oct. 31, 1959, ORNL-2879, p 13.

2. I. Spiewak et al., HRP Quar. Prog. Rep. July 31, 1960, ORNL-3004, p 29-31.

3. S. E. Beall et al., HRP Quar. Prog. Rep. July 31, 1960, ORNL-3004, p 18.

4. R. M. Warner et al., HRT Corrosion Specimens and Holder: Core Region of Pressure Vessel (Loading No. 1), ORNL CF-58-7-68 (July 1958).

5. J. C. Griess and H. C. Savage, HRP Quar. Prog. Rep. July 31, 1960, ORNL-3004, p 56-60.

5. HRT REACTOR ANALYSIS

P. R. Kasten

M. L. Tobias D. R. Vondy

5.1 CALCULATION OF THE PRESSURE RISE IN THE HRT FOR VARIOUS RAMP REACTIVITY ADDITIONS

The pressure rise in the HRT as a result of ramp reactivity additions was studied for the case of operation with the blanket pressurizer filled with liquid. The necessary calculations were done using an IBM-704 code based upon frequently used relationships[1] which were modified to account for the presence of a hole in the core vessel. Pressure rises in the core and blanket regions were calculated as functions of the cross-sectional area of the core-tank-hole, blanket-to-core fuel concentration ratio, and rate of reactivity addition. The ranges of these parameters are indicated in Table 5.1. Emphasis was placed on the results for a hole area of 0.1 sq in., a blanket-to-core fuel concentration ratio of 0.3, and a ramp rate of 2% per second. This ramp rate was suggested as an extreme incident by the work of Bennett and Jaye.[2] Figure 5.1 shows the maximum pressure rises obtained as a function of blanket-to-core fuel ratio for a 0.1 sq in. hole and a ramp reactivity addition of 2% Δk_e per second. Table 5.2 shows results obtained for other conditions. Note that the maximum difference between core and blanket pressures is not the same as the difference between the maximum pressures in each region.

Table 5.1. Values of Parameters Considered in Pressure-Rise Calculations

Parameter	
Blanket-to-core fuel ratio	0, 0.3, 0.5, 1.0
Rate of reactivity addition, % Δk_e/sec	1, 1.5, 2
Core-tank hole area, sq in.	0, 0.1, 0.25, 0.5

5.2 CRITICALITY STUDIES FOR THE HRT

Calculation of HRT critical concentrations for various conditions were made using the GNU multigroup code. The blanket-to-core fuel concentration ratio was varied between 0 and 0.3, the core temperature was taken between 240 and 280°C, and blanket temperatures were between 150 and 280°C. Table 5.3 lists the results obtained for a poison cross section of about 0.9% of the absorption cross section of U^{235} (corresponding to operating conditions).

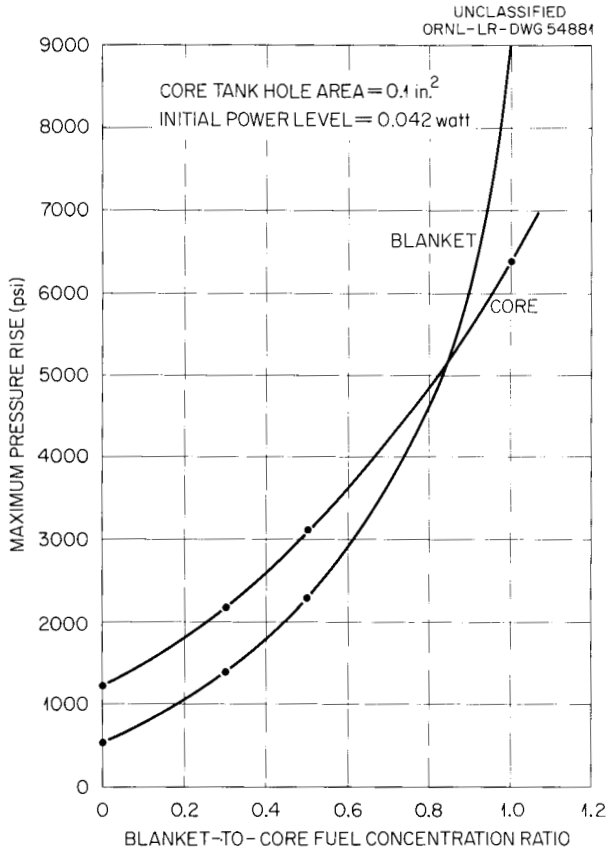

Fig. 5.1. Pressure Rise Associated with a 2%/sec Ramp Reactivity Addition in the HRT with the Blanket Pressurizer Filled with Liquid.

Table 5.2. Pressure Rises Due to Ramp Reactivity Additions to the HRT with the Blanket Pressurizer Filled with Liquid

Ratio of Blanket-to-Core Fuel Concentration = 0.3

Core-Tank Hole Area, sq in.	Reactivity Addition (%/sec)	Max. Core Press. Rise (psi)	Max. Blanket Press. Rise (psi)	Max. Difference Between Core and Blanket Pressure (psi)
0	2	2249	1374	1237
0.1	1	739	805	180
0.1	1.5	1341	1085	588
0.25	2	2104	1406	1052
0.5	2	1978	1431	1127

Table 5.3. Fuel Concentrations Calculated for Various Conditions in the HRT Using the GNU Multigroup Code

Fuel enrichment, 84% U^{235}; moderator, 97.5% D_2O; poison level, 0.9%

Core Temp. (°C)	Blanket Temp. (°C)	Core Fuel Conc. (g of U^{235} per kg of moderator)	Blanket Fuel Conc. (g of U^{235} per kg of moderator)
		A. No Fuel in Blanket	
280	280	8.8	
	240	8.1	
260	260	7.5	
	240	7.2	
	200	6.7	
		B. 0.15 g of U^{235} per Liter in Blanket per g of U^{235} per Liter in Core	
280	280	7.18	1.08
	260	6.85	0.98
	240	6.59	0.91
	200	6.12	0.79
260	280	6.46	1.01
	260	6.17	0.92
	240	5.94	0.86
	200	5.55	0.75
	150	5.20	0.66
240	260	5.69	0.88
	240	5.49	0.82
	200	5.14	0.72
		C. 0.30 g of U^{235} per Liter in Blanket per g of U^{235} per Liter in Core	
280	280	6.05	1.82
	240	5.55	1.54
	200	5.15	1.34
260	260	5.25	1.58
	240	5.08	1.47
	200	4.72	1.28
240	240	4.74	1.42
	200	4.42	1.24

The fuel enrichment was 84% U^{235}, and the moderator was 97.5% D_2O. Figure 5.2 shows some results for a blanket temperature of 230°C. The calculations showed that a linear correlation resulted when the inverse of core fuel concentration was plotted against the blanket-to-core fuel concentration ratio, as shown in Fig. 5.3. The results in Fig. 5.3 are for a variety of core-and-blanket temperature combinations.

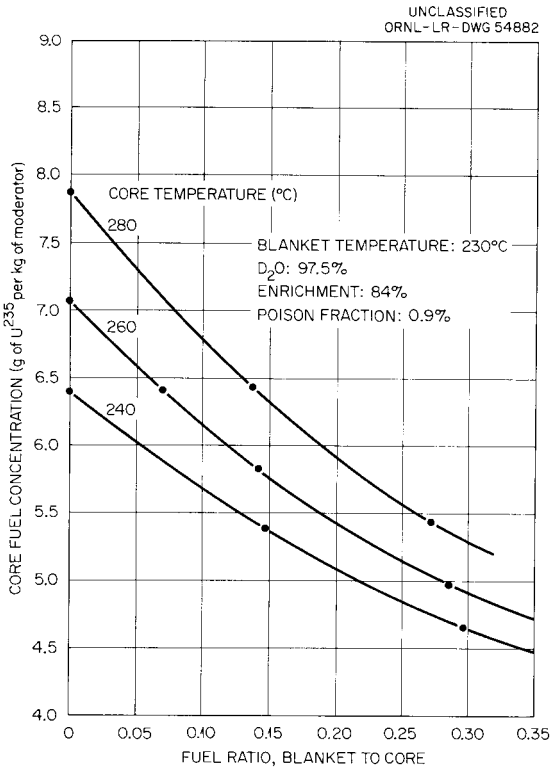

Fig. 5.2. HRT Critical Fuel Requirements as a Function of Blanket Fuel Concentration and Core Temperature.

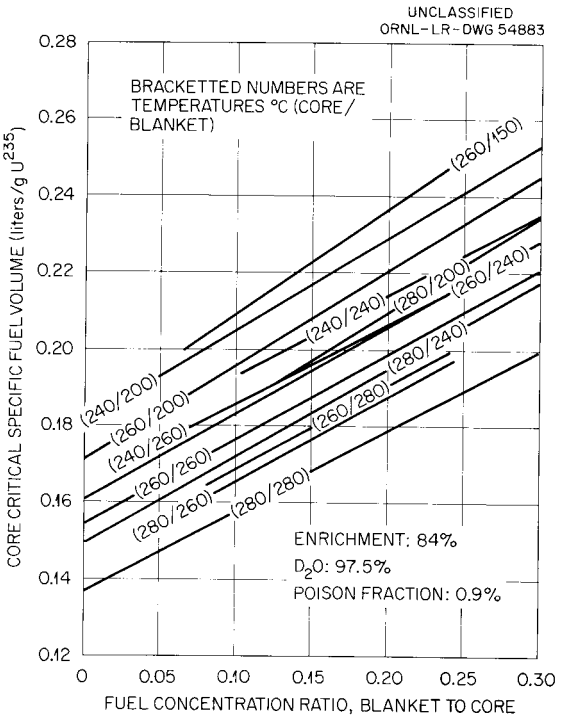

Fig. 5.3. Effects of Fuel in Blanket and Blanket-Core Temperatures on HRT Fuel Requirements.

The few comparisons which were made between calculated and observed critical conditions in current HRT operations show experimental concentrations about 6% higher than calculated values.

5.3 CRITICALITY CALCULATIONS CONCERNING THE HRT REPLACEMENT VESSEL

The objective of nuclear calculations concerning the HRT replacement vessel was to find a small reactor which had a core-wall power density of about 30 kw/liter at a total power of 5 Mw, and a fuel concentration less than 10 g of U^{235} per liter. It was further hoped that a high breeding ratio would be possible if the reactor were fueled with U^{233} and if the blanket contained baskets of thoria pellets. A large number of concepts were studied in an effort to meet these objectives; the most successful concept appears to be a core surrounded by a reflector of beryllium or beryllium oxide and regions of thoria-D_2O mixtures. An example of such a reactor is indicated in Fig. 5.4, which displays schematically the radial distribution of materials in a spherical reactor. With U^{235} fuel, the concentration in the core was 9 g/liter as calculated by the GNU multigroup code for a temperature of 280°C. If U^{233} were used, the concentration would be 6.1 g/liter. The poison level used in these calculations was associated with present HRT operating conditions and a power level of 10 Mw. The core wall power density was 5.2 kw/liter per megawatt of reactor power. The core volume was 172 liters, and the pressure vessel was 56.66 in. in inside diameter. Table 5.4 gives a neutron balance for this case.

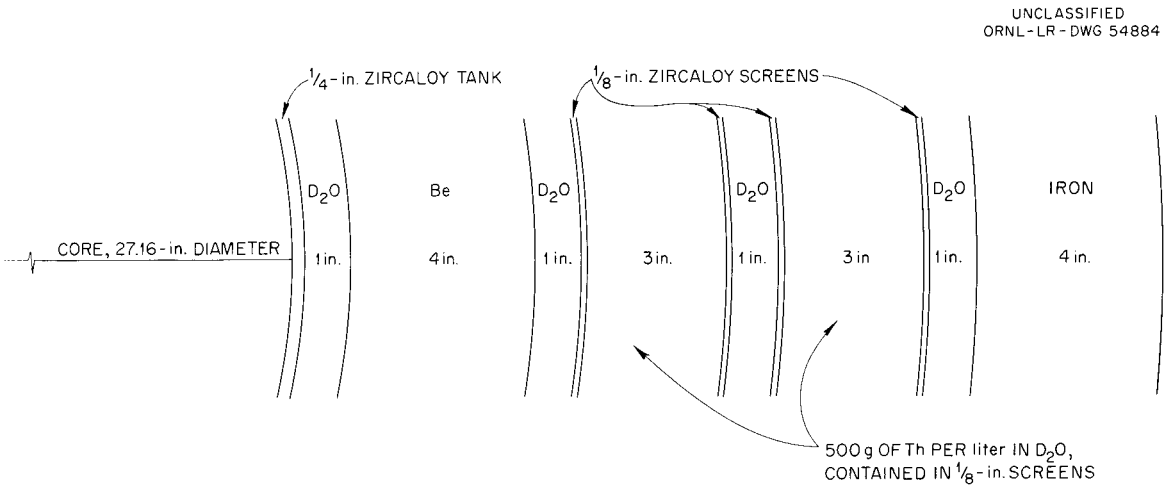

Fig. 5.4. Schematic Diagram of Radial Distribution of Materials in HRT Replacement-Vessel Concept (Pressure-Vessel ID, 56.66 in.).

Table 5.4. Neutron Balance for Spherical Version of HRT Replacement Reactor

	Material	Absorptions per Neutron Produced
Core:	Water (99.6% D_2O)	0.004
	S	0.001
	Ni	0.001
	Cu	0.001
	Xe	0.004
	Sm	0.002
	Other fission products	0.004
	U^{233}	0.435
Core tank		0.020
Blanket regions		
	Water	0.001
	Be	0.048
	Zircaloy	0.005
	Thorium (of which 87% is in first region)	0.462
Pressure vessel		0.009
Leakage		0.001
Breeding ratio (neglecting Pa losses)		1.062

The results cited here are probably optimistic since an actual reactor configuration is not so well reflected as the spherical idealization just described. There is little doubt, however, that use of a beryllium reflector permits the use of cores small enough so that high core wall power densities can be attained at low total power. Calculations have also shown beryllium oxide to be almost as satisfactory as beryllium.

REFERENCES

1. P. R. Kasten, Dynamics of the Homogeneous Reactor Test, ORNL-2072 (June 7, 1956).

2. L. L. Bennett and S. Jaye, Pressure Rise in the Reversed Flow HRT Following a Cold Fluid Accident During Startup, ORNL CF-60-7-61 (July 20, 1960).

PART II. ENGINEERING DEVELOPMENT

6. DEVELOPMENT OF REACTOR COMPONENTS AND SYSTEMS

I. Spiewak

R. H. Chapman
D. M. Eissenberg
P. H. Harley
J. E. Jones
C. G. Lawson
J. C. Moyers

6.1 DEVELOPMENT OF STRAIGHT-THROUGH CORE VESSEL

Experimental measurements of velocity and age distributions are being made for a cylindrical core model with swirling straight-through flow. Preliminary data have shown that the age in the center of the core is approximately 130% greater than the mean age of fluid leaving the core and that the age in the vicinity of the wall is about 6% less than the mean age.

A vortex generator has been installed in the exit of the core in an attempt to reduce the age (and thereby the temperature) in the center and also to recover the dynamic pressure of the swirling component.

6.2 CIRCULATING-PUMP DEVELOPMENT

The 200Z canned-motor pump, which has a motor similar to those used in the HRT circulating pumps but which contains parts more suitable for use in circulating thoria slurries, continued to operate in high-temperature water in a test of its alumina radial bearings. The pump has operated satisfactorily for 6970 hr to date.

6.3 OXYGEN COMPRESSOR

Operation of the three-stage diaphragm compressor was resumed, and another third-stage-diaphragm failure occurred (a total of six to date) after 705 hr of operation. The first- and second-stage diaphragms have operated a total of 1950 hr each without a failure. Foreign matter entering the system seems to be the major factor in each of the third-stage-diaphragm failures.

The system is being modified to replace the packed-piston drive unit with an oil-driven triplex unit. This unit will actuate an intermediate water system through Neoprene pulsator units. These modifications should prevent inleakage of air at the packing gland and improve the cleanness of the intermediate water system, thereby lessening two troublesome problems.

6.4 SLURRY ENGINEERING

6.4.1 Viscometry

In order to design and develop slurry components, reliable physical-property measurements of the slurry are needed. Due to the fast-settling nature of most thoria slurries, capillary-tube viscometers have been used to obtain the rheological properties. However, it has been observed[1] that a wall-slip phenomenon may be responsible for erroneously low coefficients of rigidity if the capillary tube has a diameter less than approximately 120 mils.

Experiments were carried out with capillary-tube viscometers in order to determine the magnitude of the slip phenomenon and, if possible, to define the importance of slip phenomena to heat transfer and turbulent friction-factor measurements. A total of nine new and old capillary tubes were calibrated with water, and those tubes that did not exhibit the expected pressure drop in laminar flow up to the calculated critical Reynolds number were presumed to have internal dimensional irregularities and were discarded. This resulted in five acceptable tubes with inside diameters of 11, 18, 35, 57, and 124 mils, respectively. All the tubes except one had an L/D ratio greater than 1000, and one (57 mil) had an L/D ratio of 880.

These five tubes were then used to obtain pseudoshear diagrams (plots of $8V/g_cD$ vs $D\Delta P/4L$) of a pumped, 1600°C-fired, 1.5-micron thoria slurry (200B-4B) at four concentrations -- 550, 700, 800, and 1000 g of ThO_2 per liter. The tubes were operated in a vertical position.

In the laminar range, all the viscometer tubes gave data which fell on the same line, generally within $\pm 2\%$, except at the very low shear rates, where the data scattered somewhat more. This leads to the conclusion that for vertical-tube viscometers there is no observable diameter dependence (slip phenomenon) at room temperature for the thoria slurry tested.

One of the pseudoshear diagrams is shown in Fig. 6.1. The 11-mil tube tended to plug, and although it was possible to get some data, they are not plotted.

A further result of this study is the discovery that the slurry tested can be well represented by the Bingham-plastic model at shear rates greater than 300 $(lb_f \text{ sec})/(lb_m \text{ ft})$, provided that the Bingham constants are obtained at these high shear rates. A deviation from the Bingham-plastic model occurs at shear rates less than approximately 300 $(lb_f \text{ sec})/(lb_m \text{ ft})$. In fact, at shear rates below 100 $(lb_f \text{ sec})/(lb_m \text{ ft})$, the slurry appears to follow the power-law model.

6.4.2 200A Loop

Run 22A was completed this quarter. Concentration-gradient data were obtained by means of vertical scans across a 3-in. horizontal pipe sufficient to compare the dropout behavior of the slurry (3.65-μ diam, 1600°C-fired) with that used in run 21A (1.7-μ diam, 800°C-fired). The data have not been processed, although gradients qualitatively similar to those observed earlier[2] were again obtained.

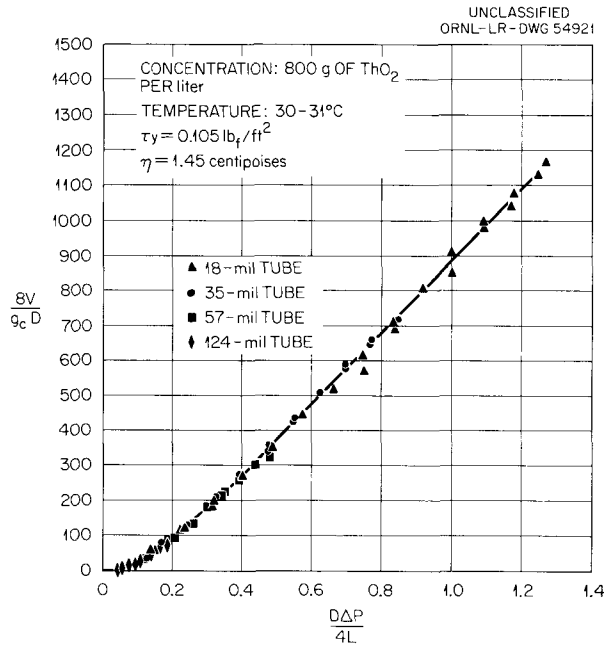

Fig. 6.1. Pseudoshear Diagram of Pumped Thoria Slurry in Several Viscometer Tubes.

6.4.3 200B Loop

A new heat meter was fabricated and installed in the 200B loop to permit continuation of run 4B. Heat transfer coefficients at several pump frequencies were obtained at ThO_2 concentrations of 800 and 1000 g/liter and at temperatures of 200, 250, and 280°C. The run will be concluded after heat transfer coefficients are obtained for water at these temperatures.

REFERENCES

1. C. H. Gibson, Rheology of Several ThO_2 Slurries at High Temperature, ORNL CF-58-9-98 (Sept. 10, 1958).

2. I. Spiewak, F. N. Peebles, et al., HRP Quar. Prog. Rep. Jan. 31, 1960, ORNL-2920, p 37-38; I. Spiewak, F. N. Peebles, et al., HRP Quar. Prog. Rep. Apr. 30, 1960, ORNL-2947, p 39-40.

PART III. SOLUTION FUELS

7. REACTIONS IN AQUEOUS SOLUTIONS

M. J. Kelly

D. R. Cuneo
L. O. Gilpatrick
G. L. Johnson[1]
H. H. Stone

7.1 REMOVAL OF PROTACTINIUM AND URANIUM FROM THORIUM NITRATE-NITRIC ACID SOLUTIONS

7.1.1 Introduction

Consideration of thorium nitrate as a breeder blanket component is dependent in part on the removal of protactinium as it is formed, in order to maintain a low steady-state value in the blanket solution. This prevents excess neutron loss by capture and allows decay of the Pa^{233} to U^{233}, a fissionable product.

This preliminary study was made to determine if Pa^{233} and its daughter U^{233} could be removed from acid thorium nitrate solutions to an arbitrarily low level by a chemical technique which would not be deleterious to the blanket solution.

A recent chemical engineering survey[2] shows that it is desirable that 90% of the protactinium and uranium be removed from a solution containing protactinium (83 mg/liter, initially) and uranium (2 mg/liter, initially). If the uranium were not removed, the steady-state value of protactinium could not be permitted to exceed 51 mg/liter.

Previous work on the removal of protactinium from molten salts[3] by precipitation on thorium oxide suggested the investigation of the adsorption of protactinium on thoria. At low (<0.5 *M*) concentrations of thorium nitrate, adsorption did occur. Increasing the thorium concentration or the addition of nitric acid caused this effect to disappear.

The most promising alternative seemed to be the coprecipitation of protactinium and uranium with a thorium compound. Precipitation with peroxide provides so many advantages that it was the second system investigated.

7.1.2 Experimental Procedure

As this was a preliminary survey, standard laboratory techniques were used. Polyethylene bottles were used to obviate the problem of protactinium adsorption on the container walls. Experiments were performed in a temperature-controlled bath over a range of 55 to 75°C. Thorium concentrations were 2 and 3 *M*, and added nitric acid concentration varied from 0 to 3.5 *M*. Hydrogen peroxide additions ranged over calculated values of 0.1 to 0.45 *M*.

All chemicals were standard laboratory materials, and no special purification was attempted. The thorium nitrate was ignited and found to be the pentahydrate; solution-concentration calculations were performed on this weight basis. The protactinium tracer solution was obtained by irradiating $Th(NO_3)_4 \cdot 5H_2O$ in the ORNL Graphite Reactor and then dissolving in acid solution.

In a typical experiment, 20 ml of a particular thorium nitrate and acid solution was placed in a 1-oz polyethylene bottle; from 100 to 500 λ of protactinium tracer solution was added; and a plastic-coated magnetic stirring rod was put in the bottle. The bottle was then placed on a magnetic stirrer immersed in the water bath and allowed to come to thermal equilibrium while stirring, after which the gamma activity of a 100-λ sample was determined. Sufficient peroxide was then added to provide a chosen zero-time concentration.

At predetermined intervals the reaction mixture was centrifuged in an insulated centrifuge cup, and samples were withdrawn and analyzed for soluble peroxide and protactinium tracer activity.

In the experiments involving uranium, the tracer used was U^{237}. In all other cases the tracer was Pa^{233}.

7.1.3 Results and Discussion

A clear-cut example of the success of the technique in removing protactinium from solution is shown in Fig. 7.1. The protactinium did not precipitate instantly but gradually disappeared from solution over a period of 25 min; the rate of its disappearance was probably related to a slow growth of the peroxide particles. The shaded area in the figure represents that fraction of the total peroxide which was in the form of thorium peroxide precipitate (which also included the protactinium precipitate) and had been removed from the supernatant by centrifugation. Based on the assumption of a one-to-one correspondence

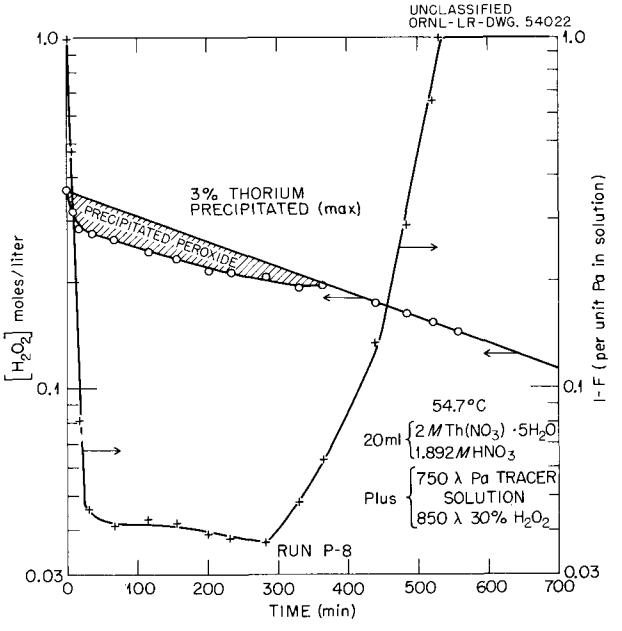

Fig. 7.1. Coprecipitation of Pa^{233} Tracer with Thorium Peroxide.

between hydrogen peroxide and thorium peroxide, it was calculated that about 3% of the total thorium had been precipitated. At the same time, nevertheless, 96% of the tracer protactinium had been removed.

When the soluble-peroxide level fell below 0.2 *M* (at ~275 min), the protactinium began to return to solution. Therefore it appears likely that enforcement of a steady-state level of 0.225 *M* soluble peroxide would also have effectively precipitated the protactinium and that the use of the larger initial quantity of H_2O_2 would not have been unnecessary.

The effect of temperature on the rate of peroxide decomposition is shown in Fig. 7.2. The energy of activation calculated from these data corresponds to (22 ± 2) kcal/mole, a value which is very close to those for the catalyzed decomposition of peroxide in uranium solution systems.

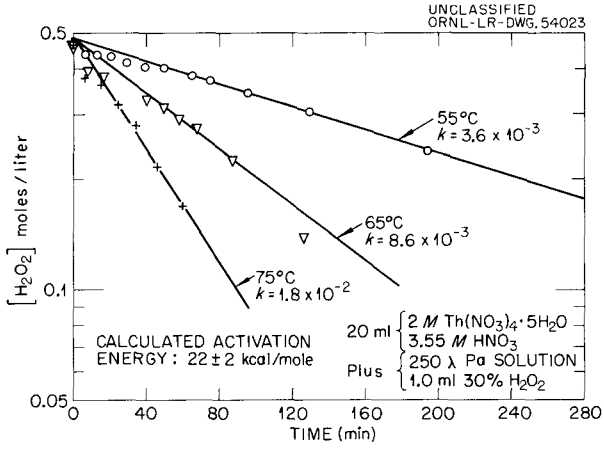

Fig. 7.2. Effect of Temperature on Peroxide Decomposition.

It was noted that increasing the acidity, with all other conditions constant, caused an increase in the rate of reaction. This result was contrary to the usual experience in uranium systems.

Figure 7.3 shows the combined results of two runs with 3 *M* thorium and roughly 2 *M* acid. The protactinium and thorium were still effectively precipitated even at the higher temperature and thorium concentration. The concentration of peroxide required at steady state was less than that required in Fig. 7.1. However, the concentration of peroxide necessary for precipitation apparently varies with the ratio of thorium to acid. For 2 *M* thorium solutions at 55°C, the threshold level of peroxide for precipitation was a function of the stoichiometric acid concentration, as follows:

Acid Concentration (*M*)	Peroxide Concentration for Precipitation (*M*)
0.00	0.085 ± 0.01
0.922	0.105 ± 0.01
1.892	0.20 ± 0.01
3.544	0.40 ± 0.02

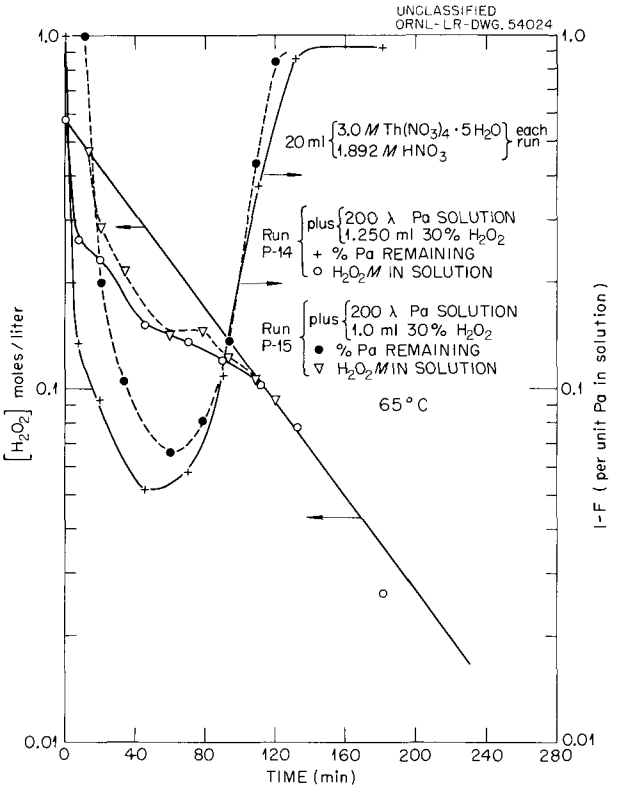

Fig. 7.3. Coprecipitation of Protactinium Tracer with Thorium Peroxide.

The small change between the 0.922 *M* value and the stoichiometric value may be rationalized by the comment that the measured pH of 2.0 *M* thorium nitrate solution was approximately zero.

In every case where sufficient peroxide was added to exceed the concentration required for precipitation and when the particulate material reached a size where it could be satisfactorily centrifuged from the solution, the protactinium was removed with the precipitate. The protactinium did not reappear so long as any observable precipitate was present. It is reasonable to assume at this point that the protactinium peroxide is more insoluble than the thorium peroxide and that quantities greater than 5 ppm could be removed by precipitating a very small quantity of the thorium. Protactinium-231 has been requested for experiments to test this assumption.

A single experiment was run at 48.9°C with 2 *M* thorium nitrate, 2 *M* nitric acid, and ~75 ppm of uranium, using the technique described above. Uranium was not removed from the solution when a portion of the thorium was precipitated. Another experiment, identical to this experiment except for the initial addition of protactinium tracer, showed that the protactinium was removed as successfully in the presence of uranium as in the experiments with no uranium present.

7.1.4 Conclusions

The results reported here seem to indicate that protactinium could be held at an arbitrarily low steady-state concentration in a thorium nitrate - nitric

acid breeder blanket solution. This could be accomplished by coprecipitating the protactinium together with a small percentage of the thorium by means of peroxide addition in a side-stream operation. Methods for removal of the solid peroxides would have to be determined, but a continuous method such as hydroclone extraction would seem desirable. The peroxide remaining in solution will decompose, leaving no undesirable contaminants in the blanket solution.

This technique did not remove small amounts of uranium from the blanket solution. It has been shown that (1) allowing the uranium to attain steady-state conditions in the blanket will require that the protactinium be held below 51 ppm for acceptable reactor operating conditions, and (2) the removal of Pa^{233} at tracer levels in the present experiments suggests that a steady-state concentration of less than 51 ppm could be achieved.

7.2 SOLUBILITY OF H_2 IN H_2O AND OF D_2 IN D_2O

7.2.1 Introduction

Precise data on gas solubilities in homogeneous reactor fuel solutions are required so that recombination rates can be calculated and operating conditions can be specified such that the gas will remain in solution in the reactor. Some data are available,[4] but not of sufficient scope to supply information for a wide range of reactor operating conditions or for the precise calculations required to delineate the mechanism of the recombination reaction.

This study was undertaken to supply the data desired. The solubility of gases of interest over a wide range of chemical systems and temperatures is being determined. The data reported here were obtained to test the feasibility and precision of the technique but are of sufficient interest to warrant reporting at this time.

7.2.2 Experimental Procedure

The solvent is placed in a small (25-ml) titanium bomb with a core pressure fitting on one end, connected to a 20-mil-ID gas-feed line. The other end of the bomb is connected by a swage closure to a 6-mil-ID sampling tube. Several hundred psi of the saturating gas is applied to the solvent. The bomb is shaken to speed saturation, and the gas is vented to atmosphere. This is repeated three times to remove any air from the system. The bomb is placed in the furnace and brought to the test temperature. A suitable pressure of the saturating gas is applied, and the bomb is rocked until the liquid is saturated with gas.

After saturation, the rocking furnace is stopped at an angle such that the 6-mil sample line is at the lowest point, and any entrained gas is allowed to separate.

The sampling line is connected to a valving arrangement so that the line may be flushed with gas-saturated sample, and the line is then opened at another point to an evacuated sample container. There is no dead volume, and while segregation of the gas and liquid undoubtedly occurs in the sample line, the sweep velocity is so high that a homogeneous sample is taken.

The amount of sample drawn is determined by weighing the sample container before and after sampling. The sample container is attached to a gas-extraction

apparatus, and the dissolved gas is put into a known volume by standard techniques and measured. The measured amount of gas is corrected to standard conditions and reported as the amount dissolved converted to standard conditions per gram of sample per atmosphere of pressure.

7.2.3 Results and Discussion

The results obtained to date are shown on Fig. 7.4. The H_2-H_2O data are in essential agreement with those of Wiebe and Gaddy[5] below 100°C and with the data of Pray et al.[6] above 100°C. The D_2-D_2O data vary by several per cent from those reported by Stephan et al.[4]

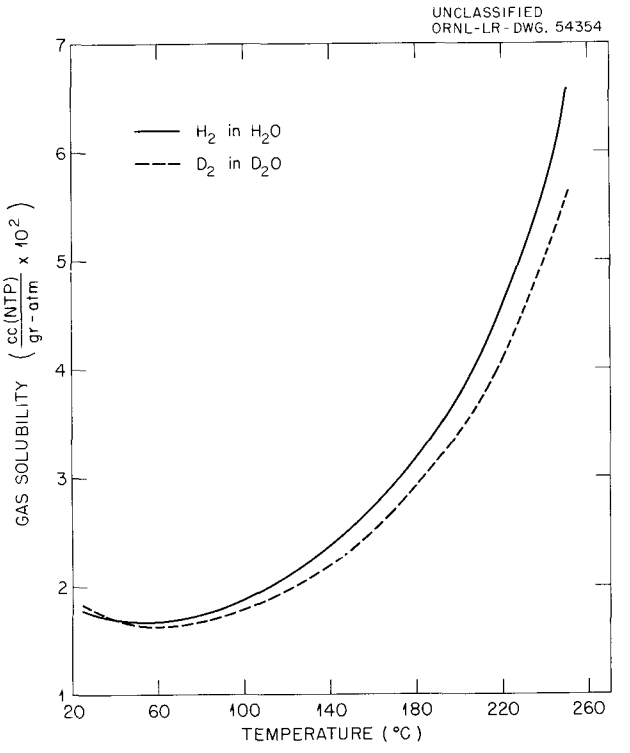

Fig. 7.4. Solubility of H_2 in H_2O and of D_2 in D_2O.

Graphical results are shown since a complete tabulation of data will be reported later up to 300°C. Data were taken at 10°C intervals and plotted as the average of several independent determinations. Internal agreement of data at a single temperature was usually better than ±0.5%. Errors in pressure and temperature measurement probably contribute sufficient indeterminate error that the precision may be considered to be no better than ±1%.

REFERENCES

1. Research participant from Duke University, Durham, North Carolina.

2. E. E. Lindsey, Thorium Nitrate as a Breeder Blanket, ORNL CF-60-9-150 (Sept. 1960).

3. J. H. Shaffer et al., "The Recovery of Uranium and Protactinium from Molten Fluoride Systems by Precipitation as Oxides," Paper No. 37 in First Conference on Nuclear Reactor Chemistry, Oct. 14, 1960.

4. E. F. Stephan et al., The Solubility of Gases in Water and in Aqueous Uranyl Salt Solutions at Elevated Temperatures and Pressures, BMI-1067 (Jan. 23, 1956).

5. R. Wiebe and V. L. Gaddy, J. Am. Chem. Soc. 56, 76 (1934).

6. O. F. Pray et al., Ind. Eng. Chem. 44, 1146-51 (1952).

8. HETEROGENEOUS EQUILIBRIA IN AQUEOUS SYSTEMS

W. L. Marshall

E. U. Franck[1] E. V. Jones R. Slusher
J. S. Gill J. E. Savolainen F. J. Smith[2]

8.1 ESTIMATION OF MINIMUM TEMPERATURES OF SECOND-LIQUID-PHASE FORMATION IN HOMOGENEOUS-REACTOR FUEL CONCENTRATES: USE OF THE ACIDITY RATIO

8.1.1 Introduction

The temperatures for the appearance of a second liquid phase were determined for two aqueous homogeneous-reactor fuel compositions and their concentrates. The data supplement those given previously.[3-5] Mole ratios, UO_3/SO_3, CuO/SO_3, and NiO/SO_3, for the two compositions studied are near those for the fuel used in the current homogeneous-reactor operation.

Comparison of the results herein with those previously presented suggests a more general criterion for estimation of the minimum liquid-liquid immiscibility temperature for homogeneous-reactor fuel concentrates.

The experimental details are given in an HRP report.[6] Temperatures for the appearance of liquid-liquid immiscibility were determined by visual observations in the conventional manner.[7] Concentrations of the stock solutions used for preparing dilutions are given below:

	Solution A		Solution B	
	Molarity	Molality	Molarity	Molality
UO_2SO_4	0.415	0.385	0.2653	0.2432
$CuSO_4$	0.2100	0.1948	0.1377	0.1262
$NiSO_4$	0.1370	0.1271	0.0906	0.0831
Total sulfate	1.159	1.075	0.851	0.780

8.1.2 Discussion

The experimental results are plotted in Fig. 8.1. The concentration factor x is a number which, when multiplied by the concentration of a component at x = 1, gives the concentration of that component in the concentrate. Both molal and molar concentration factors are given in the above table; these have been converted to unity at 0.0258 *M* or the equivalent 0.0218 *m* UO_2^{++} for comparison with results presented previously.[3-5] A solution of series A at x = 1 corresponds closely to the expected homogeneous-reactor fuel composition in the core, whereas in series B the relative free acid is somewhat higher.

In Fig. 8.2 the lowest temperature for appearance of liquid-liquid immiscibility upon concentration of a fuel composition is plotted against the molal ratio, D_2SO_4/total sulfate. Figure 8.3 shows the variation in the molar

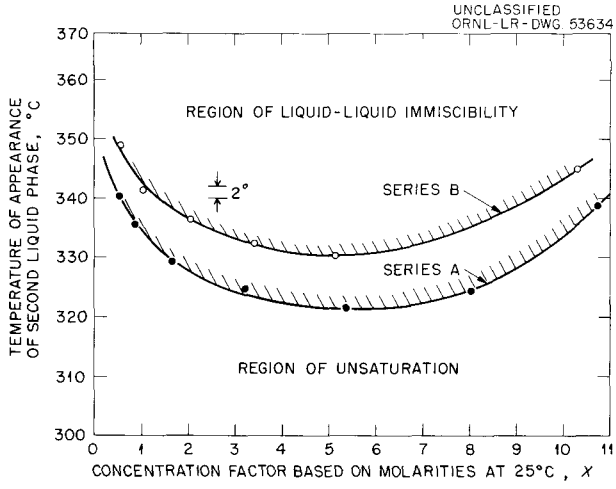

Fig. 8.1. The Temperature of Appearance of Second Liquid Phase as a Function of Dilution and Concentration of Two HR Fuel Compositions (x = 1 at 0.0258 M UO_2SO_4; D_2O Solutions).

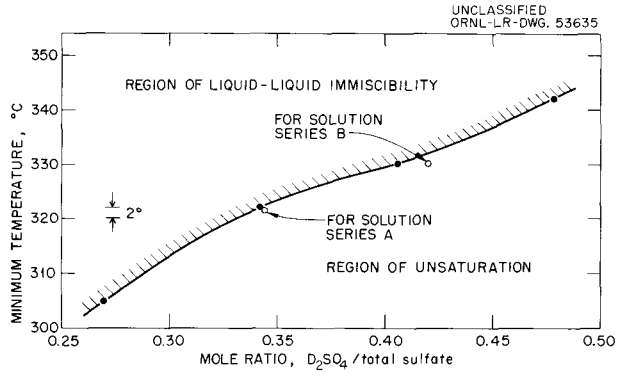

Fig. 8.2. Minimum Temperature for Appearance of Second Liquid Phase in Aqueous Homogeneous Reactor Fuel Concentrates (D_2O Solutions). Derived from data in refs 3 and 4.

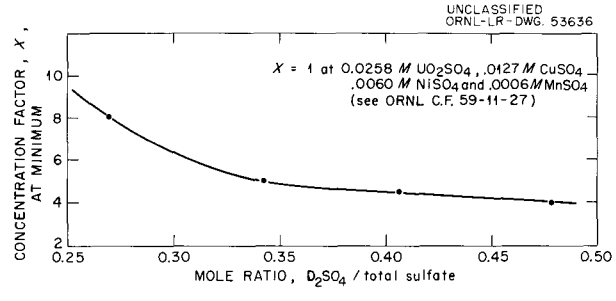

Fig. 8.3. Concentration Factor at Minimum Temperature for Appearance of Second Liquid Phase in Aqueous Homogeneous Reactor Fuel Concentrates (D_2O Solutions). Derived from data in refs 3 and 4.

concentration factor at the minimum temperature as a function of this same relative acidity ratio. For these curves, prepared from data in refs 3 and 4, the molal ratio, $UO_2^{++}/Cu^{++}/Ni^{++}$, is 1:0.492:0.232, compared with 1:0.506:0.330 and 1:0.519:0.340 for the present two series of solutions. The two-liquid-phase minimum temperatures obtained from the curves in Fig. 8.1 are 1°C lower for series A and 2°C lower for series B than the curve in Fig. 8.2 would indicate at the corresponding mole ratios, D_2SO_4/total sulfate, of 0.343 and 0.420. Doubling the relative concentration of Cu^{++} and eliminating Ni^{++} to give a mole ratio, $UO_2^{++}/Cu^{++}/Ni^{++}$, of 1:1:0 (ref 5) raised the temperature at the minimum by only 8, 6, and 4°C at acidity mole ratios, D_2SO_4/total sulfate, of 0.33, 0.43, and 0.50, respectively. These changes in temperature are small, considering that the relative Cu^{++} concentration was increased by 100% and that Ni^{++} was eliminated.

Large differences in temperature for small changes in the mole ratio, D_2SO_4/total sulfate, and small differences in temperature for moderately large changes in mole ratios, Cu^{++}/UO_2^{++} and Ni^{++}/UO_2^{++}, substantiate the belief that relative acidity is the most important variable in the range of current homogeneous-reactor fuel compositions. As secondary effects, an increase in the mole ratio, Ni^{++}/UO_2^{++}, appears to lower somewhat the temperature for occurrence of immiscibility, whereas an increase in the mole ratio, Cu^{++}/UO_2^{++}, is known to raise this temperature.[3-5]

As a first approximation, the curve in Fig. 8.2 may be used to estimate two-liquid-phase minimum temperatures within 2 or 3°C for solution concentrates of current homogeneous-reactor fuel compositions showing moderate variations in mole ratios, Cu^{++}/UO_2^{++} and Ni^{++}/UO_2^{++}, and large variations in D_2SO_4/total sulfate.

8.2 LIQUID-LIQUID EQUILIBRIA IN THE SYSTEMS UO_3-CuO-SO_3-D_2O AND CuO-SO_3-D_2O

The investigation of liquid-liquid immiscibility boundaries in the systems UO_3-CuO-SO_3-D_2O and CuO-SO_3-D_2O forms a part of the over-all study of the five-component system UO_3-CuO-NiO-SO_3-D_2O at temperatures above 300°C. Previous studies have defined two-liquid-phase temperature boundaries in the system UO_3-SO_3-D_2O[8] and have presented information concerning solid-liquid equilibria in the system NiO-SO_3-H_2O[9,10] and its D_2O analog.[11] These past investigations also have indicated the temperatures at which supercritical fluids are formed (that is to say, the meniscus between the vapor and liquid phases disappears) and have presented evidence of the solubility of the components in the supercritical fluid. Other studies have shown the nature and composition of the heavy-liquid phases in equilibrium with the light-liquid phases for both H_2O and D_2O systems at 285, 300, 325, and 350°C.[12] A desirable goal of this work is the development of an equation to express the two-liquid-phase and critical-temperature boundaries as a function of the concentrations of the various solution components.

In this investigation, using a synthetic method previously described,[7] the temperatures of formation of a second liquid phase and the critical temperatures were determined for a set of solution compositions containing $CuSO_4$, UO_2SO_4, D_2SO_4, and D_2O in which the molal ratio, Cu^{++}/UO_2^{++}, was kept at unity. The set of solutions was divided into several series; the molal concentration of total sulfate was held constant for each series, and the molal ratio, $(Cu^{++} + UO_2^{++})$/total sulfate, R, was varied from 0 to 1. This procedure was used, since in previous work R values for the formation of a second liquid phase for

any series appeared to be nearly linear with temperature. The results are displayed in Fig. 8.4 and show the approximate linear relationships.

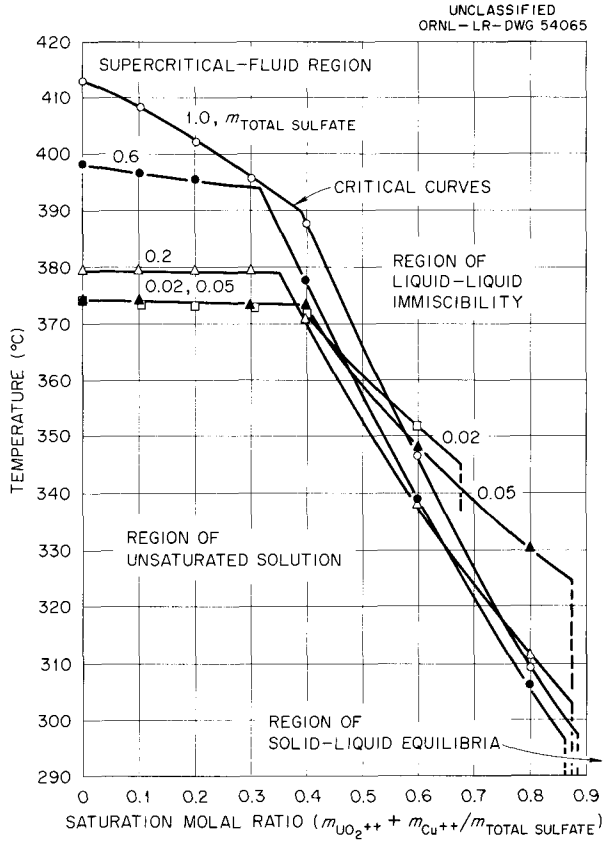

Fig. 8.4. Liquid-Liquid Immiscibility and Critical Phenomena in the System UO_3-CuO-SO_3-D_2O; $m_{Cu^{++}}/m_{UO_2^{++}} = 1$.

The two-liquid-phase region in the system CuO-SO_3-D_2O was investigated, using the same experimental methods and techniques. These data are presented in Fig. 8.5.

The results shown in Fig. 8.4 show considerable solubility for both UO_2^{++} and Cu^{++} ions in the supercritical fluid region, as might have been expected from previous observations in the system UO_3-SO_3-D_2O. Figure 8.5, for the system containing Cu^{++} but no UO_2^{++}, also shows that there was a large solubility of Cu^{++} in the supercritical D_2SO_4-D_2O fluid.

If hydrodynamic pressures greater than the critical pressures of liquid phases are maintained on fuel systems at lower temperature, and if the temperature is raised, the solution phases may be phase stable to temperatures somewhat above 400°C. Critical phenomena (i.e., disappearance of the meniscus) are not observed in these cases because a pressure greater than the critical pressure never allows the existence of a vapor phase. On a long-range basis, this means that a sulfate-based reactor fuel might be available for aqueous homogeneous reactors operating at temperatures above 400°C.

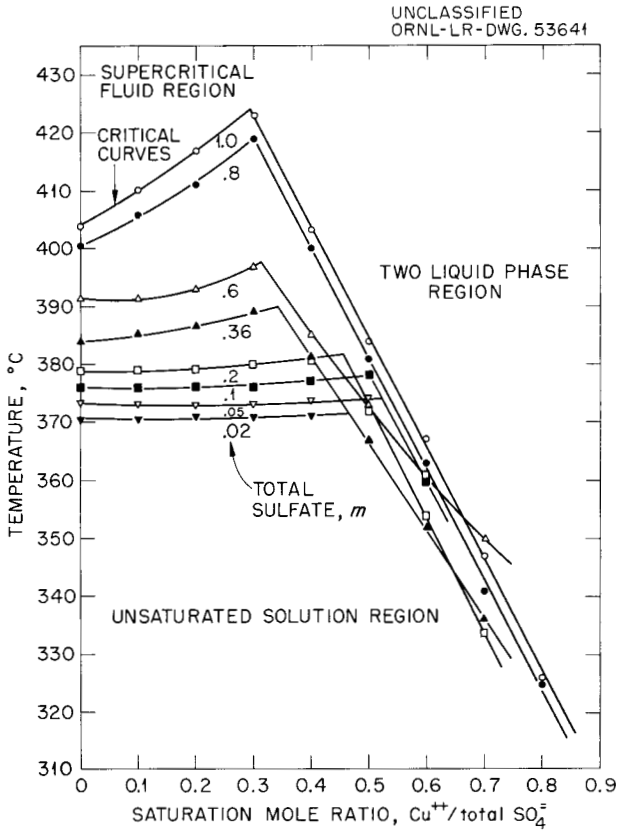

Fig. 8.5. System $CuSO_4$-D_2SO_4-D_2O Above 300°C.

8.3 SOLID-LIQUID EQUILIBRIA IN THE SYSTEM CuO-SO_3-D_2O AT 300, 325, AND 350°C

The solubility of $3CuO \cdot SO_3 \cdot 2H_2O$ (antlerite) was determined previously at 300°C in solutions varying from 0.0025 to 2.0 *m* in total sulfate.[13] The purpose of this present investigation was to extend the study to the analogous D_2O system at 300, 325, and 350°C and to attempt to locate the points of intersection between the solid-liquid region and the region of liquid-liquid immiscibility. The solubilities were determined by the method of direct sampling and subsequent analysis used previously.[13]

In Fig. 8.6 the results at 300°C for the solubility of deuterated antlerite, $3CuO \cdot SO_3 \cdot 2D_2O$, in D_2SO_4 solution are compared with the results obtained previously in the H_2O system.[13] The saturation molal ratio, Cu^{++}/total sulfate, is plotted against the logarithm of the total sulfate to show its variation over a wide range of concentration. The compound $3CuO \cdot SO_3 \cdot 2D_2O$ in the D_2O system showed a greater solubility than in the corresponding H_2O system, analogous to the behavior of $NiSO_4 \cdot D_2O$ at 300°C in the D_2SO_4-D_2O and H_2SO_4-H_2O system.[9]

Saturation molal ratios of Cu^{++}/total sulfate and concentrations of total sulfate were found at 0.34 ± 0.02 and 0.0014 ± 0.0001, respectively, although the initial solution compositions contained varying concentrations of D_2SO_4, all greater than 0.0014 *m*. This point is believed to constitute an invariant at which solution, $3CuO \cdot SO_3 \cdot 2D_2O$ (solid), and an unidentified solid are stable

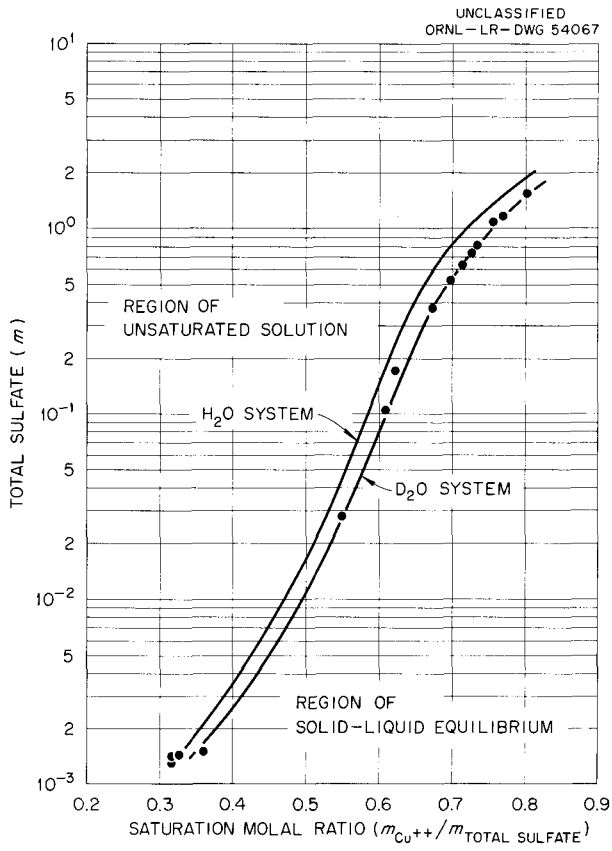

Fig. 8.6. The Solubility of $3CuO \cdot SO_3 \cdot 2D_2O$ in D_2SO_4-D_2O Solutions at 300°C; Comparison with Analogous H_2O System.

phases. Going to lower concentrations than 0.0014 *m* total sulfate, that is, moving from the invariant point, would be expected to eliminate antlerite as a stable solid.

The absence of change, within experimental error in saturation molal ratio, as the temperature is raised to 325 and 350°C is shown in Fig. 8.7. These solubility data are compared with the previously determined values at 300°C. At 350°C the second liquid phase is believed to exist at high concentrations of solutes, which accounts for a discontinuity in the saturation molal ratio at 0.1 *m* total sulfate. The invariant point for the simultaneous existence of the unidentified solid and $3CuO \cdot SO_3 \cdot 2D_2O$ appear to be nearly the same at 300 and 325°C.

The change of saturation molal ratio, CuO/SO_3, at constant molality of total sulfate over the concentration range in which $3CuO \cdot SO_3 \cdot 2D_2O$ is a stable solid shows very little decrease as the temperature is raised from 300 to 350°C. As the second liquid phase appears, the decrease in the molal ratio with temperature is considerably greater.

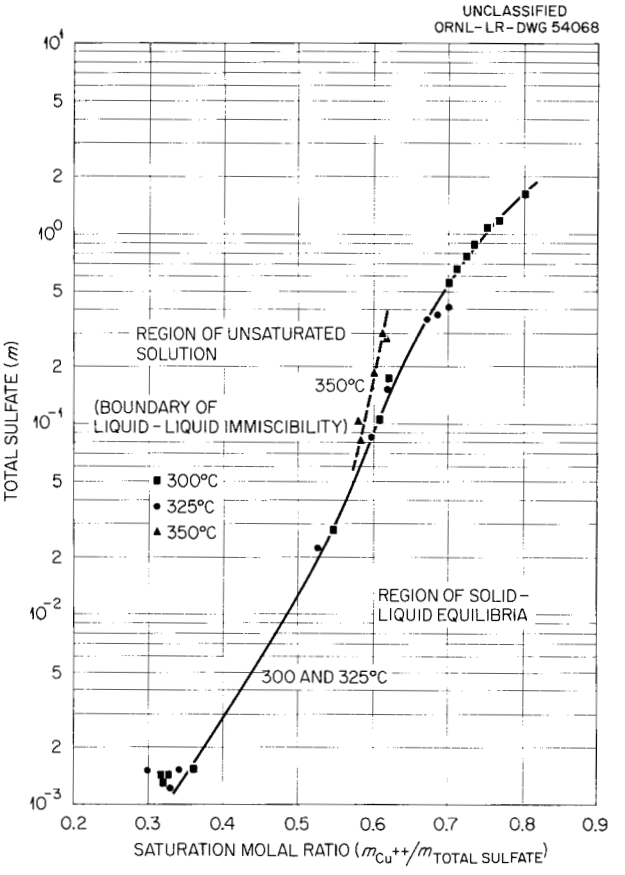

Fig. 8.7. The Solubility of $3CuO \cdot SO_3 \cdot 2D_2O$ in D_2SO_4-D_2O Solutions at 300, 325, and 350°C.

8.4 ELECTROLYTIC CONDUCTANCE OF AQUEOUS SOLUTIONS AND SUPERCRITICAL FLUIDS AT HIGH TEMPERATURE AND PRESSURE

The construction of cells for the measurement of electrolytic conductance of aqueous solutions and supercritical fluids at high temperature and pressure and associated equipment for generating high pressure was completed. The electrolytic conductivities for a 0.01 *m* KCl solution were determined at pressures up to 4000 atm at 800°C as well as at lower temperatures. Some preliminary results at 800°C are shown in Fig. 8.8, plotted as conductance, 1/R, against the pressure. The cell constant was estimated as 0.32 (±4%), according to conductance measurements of the 0.01 *M* KCl solution at the ambient temperature, (27 ± 2)°C. A constant-temperature bath, which was not available for the preliminary work, will be used later for the accurate determination of the cell constant. The conductivity values are to be converted to equivalent conductivities by making use of estimated densities of the supercritical KCl-H_2O fluid and a precisely measured cell constant.

The construction of the apparatus and preliminary measurements were carried out under the direction of E. U. Franck. These measurements are the first made at 800°C and 4000 atm. Previously conductance measurements had been made at 700°C and 2500 atm, by Frank in Gottingen.

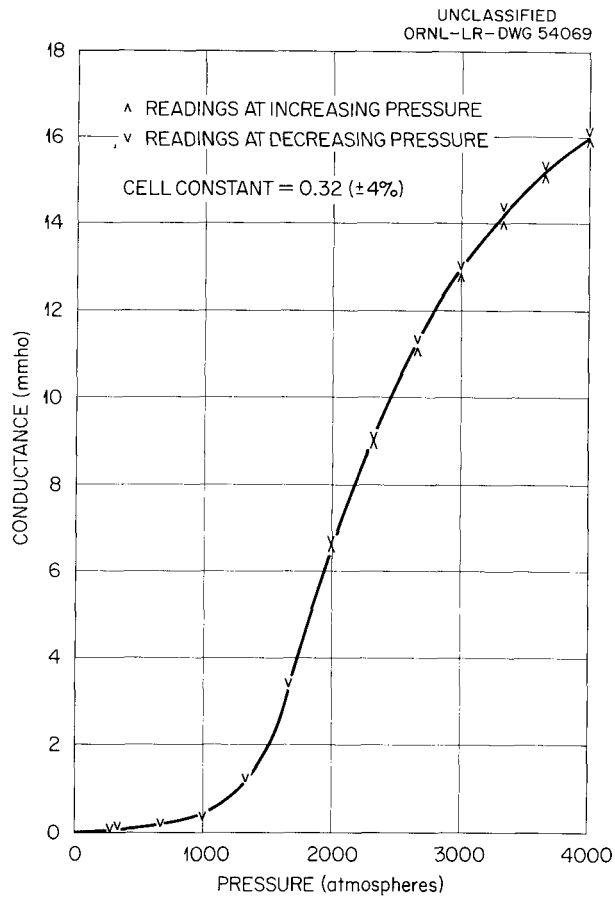

Fig. 8.8. Conductance Readings of 0.01-*m* KCl Solution at 800°C.

8.5 THREE-DIMENSIONAL MODELS FOR REPRESENTATION OF SOLUBILITY EQUILIBRIA

Three-dimensional models representing the solubility relationships in the system UO_3-CuO-NiO-SO_3-D_2O at 300°C were constructed for solutions having total sulfate concentrations of 0.06, 0.10, 0.20, 0.30, and 0.50 *m*. The results of previously reported solubility studies[13] were used to establish the location of the surfaces of saturation for the several solid and liquid phases which appear at the boundary limits of the region of unsaturated solutions. The saturating phases shown in these models are the solids $3CuO \cdot SO_3 \cdot 2D_2O$, $NiSO_4 \cdot D_2O$, $UO_3 \cdot UO_2SO_4 \cdot 5D_2O$, $CuO \cdot 2UO_2SO_4 \cdot 7D_2O$, $CuO \cdot 3UO_3$, $NiO \cdot 3UO_3$, and a second-liquid phase of variable composition.

A model showing the solubility relationships at 0.10 *m* total sulfate, represented as mSO_3 on the model, is shown in Fig. 8.9. All five models are shown in Fig. 8.10, for comparison. The unit of length, $m_{\text{metal oxide}}/m_{\text{total sulfate}}$, on all axes is the same for all models; therefore dimensional changes as a function of sulfate concentration are directly comparable. A series of these models shows the change in surface area for saturating solid phases as the total sulfate concentration is varied. In general, there appear to be several concentration

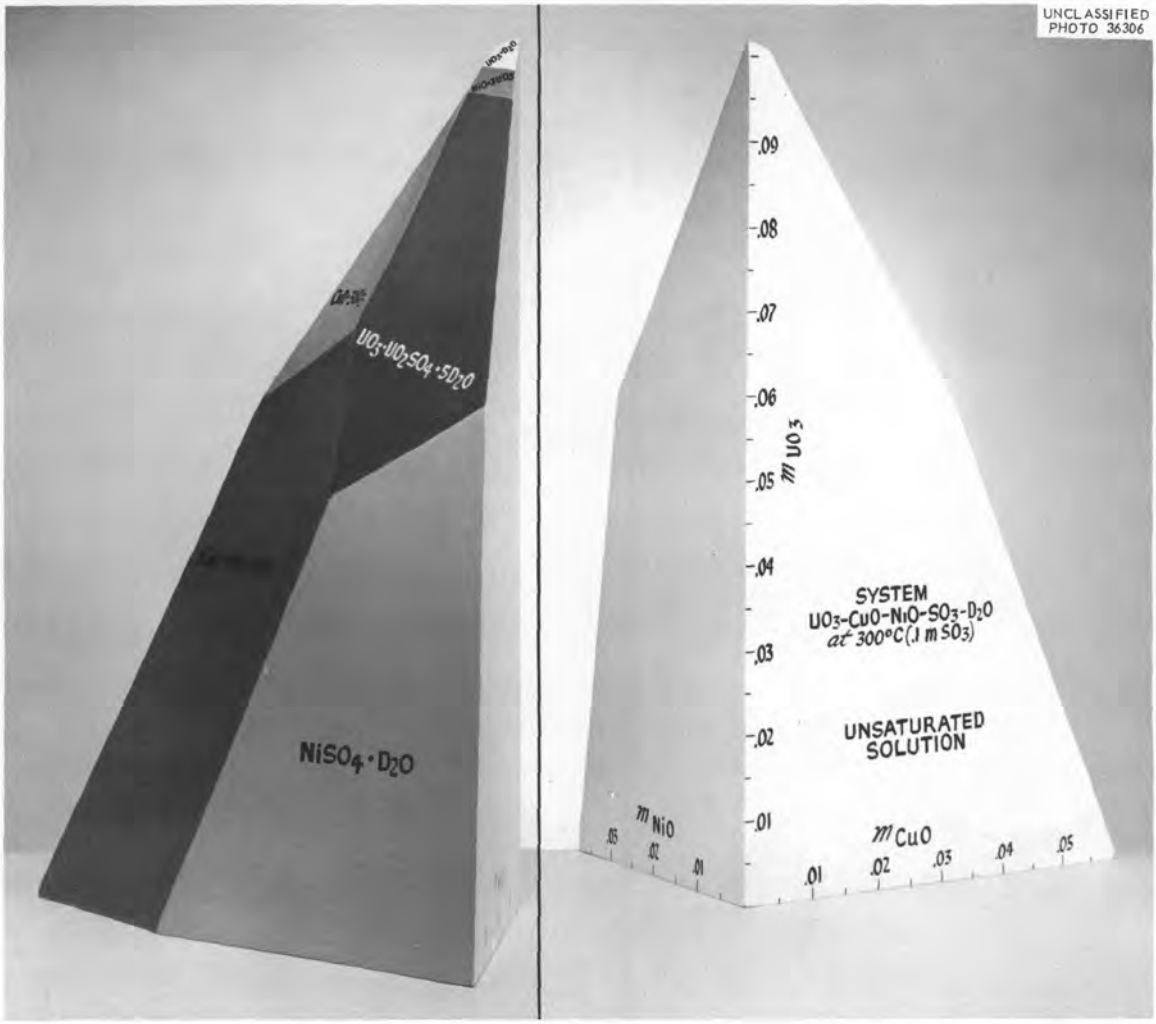

Fig. 8.9. Three-Dimensional Model Representing System UO_3-CuO-NiO-SO_3-D_2O at 300°C; 0.1-*m* in Total Sulfate.

ranges over which different types of solids are stable. At very low sulfate concentrations, hydroxides and oxides are stable--the areas of saturation may become independent of anionic solvating species and should appear the same in a nitrate as well as in a sulfate system. At moderately low concentrations of total sulfate, oxysulfates appear, for example, $Ni(OH)_2 \cdot NiSO_4$, $3CuO \cdot SO_3 \cdot 2D_2O$, and $UO_3 \cdot UO_2SO_4 \cdot 5D_2O$, whereas at higher concentrations the stoichiometric salts, such as the solid $NiSO_4 \cdot D_2O$ or the liquid pseudosalt $UO_2SO_4 \cdot H_2O$, engulf the oxysulfate surfaces. At the highest concentrations the acid salts will appear.

These models are useful for selecting fuel compositions for homogeneous reactors and for anticipating solid phases which may precipitate from solution if boundaries of saturation are exceeded. Each three-dimensional model shows much solubility information, and it is easier to visualize the solubility relationships by means of such a representation than by means of two-dimensional figures. The models form a background of information from which to make further studies.

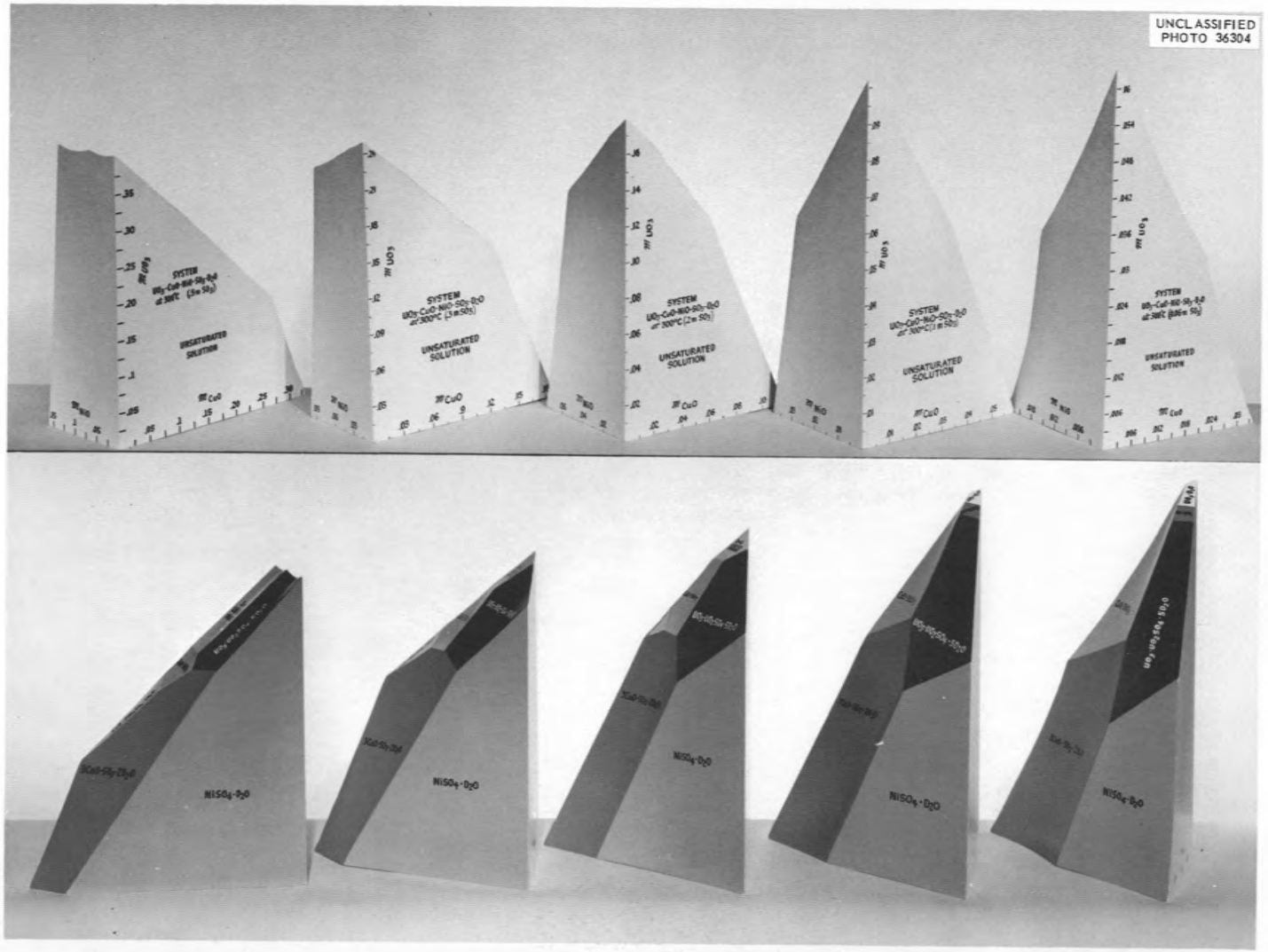

Fig. 8.10. Three-Dimensional Models Representing System UO_3-CuO-NiO-SO_3-D_2O at 300°C; 0.06, 0.1, 0.2, 0.3, and 0.5-*m* in Total Sulfate.

REFERENCES

1. On leave from the University of Gottingen, Germany, March to November, 1960.

2. Summer employee, 1960, now at Louisiana State University, Baton Rouge.

3. W. L. Marshall, J. S. Gill, and R. E. Moore, Two Liquid Phase Temperature Limits for the Homogeneous Reactor Fuel Solution and its Concentrates; Comments on Solid-Liquid Equilibria, ORNL CF-59-8-41 (Aug. 11, 1959).

4. R. E. Moore and W. L. Marshall, Effect of Excess Acid on Two Liquid Phase Temperature Limits for the Homogeneous Reactor Fuel Solution and its Concentrates, ORNL CF-59-11-27 (Nov. 9, 1959).

5. W. L. Marshall and J. E. Savolainen, HRP Quar. Prog. Rep. Jan. 31, 1960, ORNL-2920, p 62.

6. W. L. Marshall and E. V. Jones, Temperature of Second Liquid Phase Formation for Two Aqueous Homogeneous Reactor Fuel Compositions and Their Concentrates; Estimation of Temperatures for Liquid-Liquid Immiscibility, HRP 60-142 (Nov. 9, 1960).

7. C. J. Barton, G. M. Hebert, and W. L. Marshall, Liquid-Liquid Immiscibility Above 300°C in the System UO_3-SO_3-N_2O_5-H_2O, ORNL CF-59-11-64 (Nov. 17, 1959).

8. E. V. Jones and W. L. Marshall, HRP Quar. Prog. Rep. July 31, 1960, ORNL-3004, p 49-51.

9. W. L. Marshall and F. J. Smith, HRP Quar. Prog. Rep. July 31, 1960, ORNL-3004, p 49-51.

10. W. L. Marshall, R. Slusher, and J. S. Gill, HRP Prog. Rep. Apr. 30-July 31, 1958, ORNL-2561, p 308-11.

11. W. L. Marshall, R. Slusher, and J. S. Gill, HRP Quar. Prog. Rep. Apr. 30, 1959, ORNL-2743, p 235-38.

12. E. V. Jones and W. L. Marshall, HRP Quar. Prog. Rep. Apr. 30, 1960, ORNL-2947, p 55-58.

13. W. L. Marshall and J. S. Gill, Investigation of the System UO_3-CuO-NiO-H_2O at 300°C, ORNL CF-59-12-60, Rev. 1 (Jan. 27, 1960).

9. SOLUTION CORROSION

J. C. Griess H. C. Savage
J. M. Baker
S. E. Bolt

9.1 CHEMICAL EQUILIBRIA AND CORROSION IN HIGH-TEMPERATURE URANYL SULFATE SOLUTIONS

In the Aqueous Homogeneous Reactor Program at ORNL the chemical stability of uranyl sulfate fuel solutions at elevated temperatures has been the subject of a large number of investigations.[1,2] These studies have been carried out in static autoclaves and in dynamic pump loops. In the pump loops, reactor conditions of fluid flow, temperatures, and dissolved-gas concentrations (i.e., oxygen) can be more nearly duplicated than in autoclaves. Samples of fuel solution can be routinely removed for chemical analyses, and corrosion-test specimens can be exposed to the circulating solution for evaluation of the corrosion resistance of many materials. In addition, the effect of the heated and cooled metal surface of the loop on solution stability and corrosion can be investigated.

The design of the pump loops operated in the past has limited their operation to temperatures and pressures up to ~330°C and 2000 psia. In order to extend the studies of the chemical stability of uranyl sulfate fuel solutions and corrosion resistance of various materials to temperatures near the critical temperature of water (372°C), a pump loop was constructed to withstand temperatures and pressures up to 370°C and 3000 psia.

9.1.1 Description of Loop

The loop is similar in design to the HRP in-pile loops.[3] Titanium was chosen as the material of construction since it is extremely corrosion resistant to acid-containing uranyl sulfate solutions, and in this respect it is far superior to type 347 stainless steel. Titanium also eliminates the introduction of soluble stainless steel corrosion products into the test solution. A 5-gpm canned-rotor pump circulates the solution through the 1/4-in. main-loop piping, which contains a combination heater-cooler unit to control the main-stream temperature. Corrosion-test specimens are placed in the main-loop stream, and a horizontally mounted pressurizer is used to provide steam pressurization and expansion volume when heating the solution to elevated temperatures. For continuous removal of solids or heavy-phase material which might be formed during operation at elevated temperatures, part of the circulating solution is passed through a hydroclone[4] located in a bypass line. Also included are provisions for removing samples of the fuel solution from the main-loop stream and the hydroclone underflow pipe (where solids and heavy-phase material are collected) while the loop is operating at temperature and pressure. A schematic diagram of the loop is shown in Fig. 9.1.

After final assembly, the internal surfaces of the loop were cleaned by circulating a 3% trisodium phosphate solution at 100°C, and, after rinsing, this was followed by a similar run with a 5% nitric acid solution at 100°C for 25 hr.

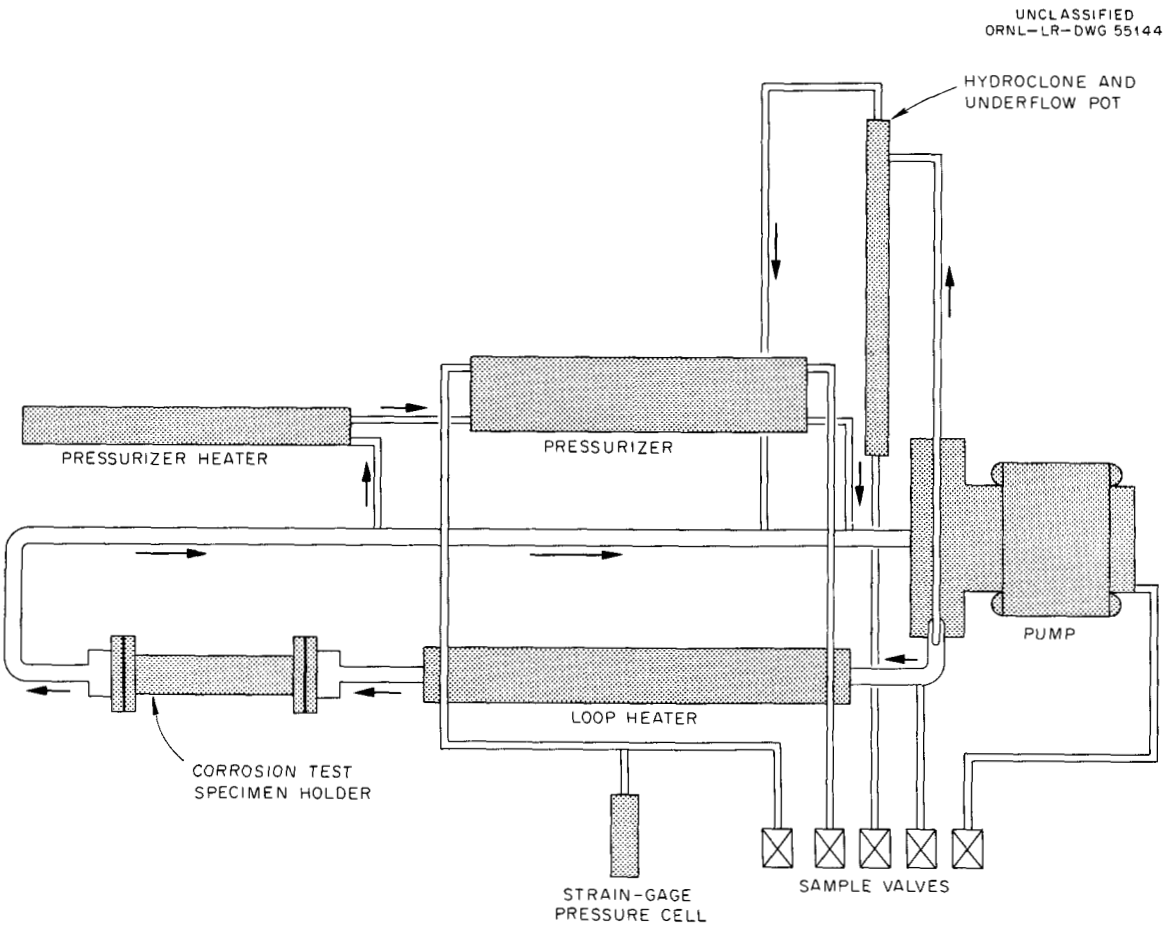

Fig. 9.1. High-Pressure Titanium Loop.

Subsequent tests were made in which the loop was operated with water at temperatures up to 365°C, and these tests demonstrated that the loop is satisfactory for operation at temperatures and pressures up to at least 365°C and 3000 psia.

9.1.2 Preliminary Test Results

After cleaning and calibrating the loop, three relatively short runs (30, 48, and 75 hr) were made to determine the stability and corrosiveness of a heavy-water solution containing 0.044 *M* (0.040 *m*) UO_2SO_4, 0.022 *M* (0.020 *m*) $CuSO_4$, 0.0149 *M* (0.0135 *m*) $NiSO_4$, and 0.038 *M* (0.035 *m*) D_2SO_4 at temperatures up to 360 to 365°C. The temperature of the main circulating stream was maintained about 5°C below that in the pressurizer and was increased in steps. After increasing the temperature and allowing the system to reach equilibrium, a solution sample was withdrawn from the circulating stream and occasionally from the underflow pot of the hydroclone. It was presumed that the solution withdrawn from the circulating stream at temperatures above which an extra liquid phase formed contained only the light phase and that the solution taken from the underflow pot contained a mixture of light and heavy phases. The temperature of phase separation in the solution tested is 327°C.[5]

Assuming that the samples removed from the circulating stream contained only the light phase, the following results were obtained:

1. As the temperature of the system was increased beyond 327°C, all constituents of the light phase except free acid decreased in concentration. With a pressurizer temperature of 365°C and the circulating stream at 360°C, the room-temperature concentration of uranium, copper, nickel, and sulfate in the light phase was 0.01, 0.014, 0.005, and 0.071 *M*, respectively.

2. As the temperature of the loop was increased beyond 327°C, the mole ratios of uranium to sulfate, uranium to copper, and uranium to nickel decreased in approximately the same proportion. On the other hand, the mole ratios of copper to nickel, nickel to sulfate, and copper to sulfate were essentially constant from room temperature to the highest temperature investigated.

3. Solution samples removed from the underflow pot of the hydroclone at temperatures greater than 327°C contained more salts than did samples removed from the line. However, the concentrations of salts indicated that not all the heavy-phase material collected at that location. It is highly probable that a substantial amount of the heavy phase collected in the pressurizer, where temperatures were slightly higher.

4. Corrosion specimens made from Ti-75A and from a Zircaloy-2 weldment showed negligible attack during the 153 hr of the run. The titanium specimens developed a dark blue-gray color and exhibited weight gains of about 0.03 mg/cm^2. The Zircaloy-2 specimens were covered with a black film which appeared to be transforming to a white film at a few isolated areas; weight gains of about 0.1 mg/cm^2 were observed.

5. The performance of the loop was very satisfactory, indicating that it should be a useful tool for studying solution stability and corrosion at temperatures nearly as high as the critical temperature of water.

REFERENCES

1. J. A. Lane, H. G. MacPherson, and F. Maslin (eds.), Fluid Fuel Reactors, chap. 3, "Properties of Aqueous Fuel Solutions," p 85-120, Addison-Wesley, Reading, Mass., 1958.

2. W. L. Marshall et al., HRP Quar. Prog. Rep. July 31, 1960, ORNL-3004, p 49-60.

3. H. C. Savage, G. H. Jenks, and E. G. Bohlmann, In-Pile Corrosion Test Loops for Aqueous Homogeneous Reactor Solutions, ORNL-2977 (Nov. 10, 1960).

4. P. A. Haas, Hydraulic Cyclones for Application to Homogeneous Reactor Chemical Processing, ORNL-2301 (Nov. 18, 1957).

5. W. L. Marshall, private communication.

10. RADIATION CORROSION

G. H. Jenks H. C. Savage

J. E. Baker R. J. Davis
J. M. Baker S. H. Wheeler

10.1 REVIEW AND CORRELATION OF ZIRCALOY-2 RADIATION CORROSION DATA

Many of the data obtained at ORNL for the in-pile corrosion of Zircaloy-2 in uranyl sulfate solution have been reviewed and correlated, and a report of the work has been prepared.[1] The correlations are based on the following equation for the relationship between corrosion rate (R) and fission power density in solution (P).

$$1/R = \frac{K_1}{KP\alpha} + 1/K \ , \qquad (1)$$

where α is a factor by which the effective power density at the corroding surface is greater than that in the solution, because of uranium sorption on the surface; and K_1 and K are constants which are evaluated from the experimental data. A model for the radiation effects on Zircaloy-2 corrosion which leads to this equation is also described and discussed in this report.

The work had the purpose of evaluating the applicability of the general equation as well as the data review and correlation.

The basic postulates for the model are described by Eqs. (2) through (5), as follows: (1) The corrosion rate is assumed to be directly proportional to the concentration of radiation defects N in the metal or protective oxide. (2) The defects are formed at a rate proportional to $P\alpha$ and are removed by radiation annealing at a rate proportional to $P\alpha N$ and by thermal or corrosion annealing at a rate proportional to N. (3) A steady-state concentration of defects is reached. (4) Substitution of the expression for N_s in Eq. (2) gives an expression similar to that of Eq. (1).

$$R = aN \ , \qquad (2)$$

$$dN/dt = K''P\alpha - K^\circ P\alpha N - K'N \ , \qquad (3)$$

$$N_s = \frac{K''P\alpha}{K^\circ P\alpha + K'} \ , \qquad (4)$$

$$\frac{1}{R_s} = \frac{K'/K^\circ}{a(K''/K^\circ)P\alpha} + \frac{1}{aK''/K^\circ} \ . \qquad (5)$$

The results of the correlations of the experimental data obtained at 280°C show that a relationship of the general form of Eq. (1) is obeyed within the power-density range tested (up to 110 w/ml) and that the values of K are essentially independent of solution composition. They also indicate that the value of the ratio of K'/K° is independent of solution composition. The experimental information for temperatures other than 280°C is not sufficient to establish the validity of the general relationship at other temperatures. However, if the reasonable assumption is made that the relationship is obeyed and that α does not change or changes slowly with temperature, the data are sufficient to establish a range of K values at 250 and 300°C and also to establish that over the temperature range investigated, 225 to 330°C, the data are reasonably well expressed by Eq. (6):

$$1/R = \frac{2.3}{P\alpha_{280}} + 2.25 \times 10^{-11} \exp\left(\frac{11,500}{T}\right), \qquad (6)$$

where α_{280} is the α value prevailing in a given solution at 280°C, and T is the temperature in °K. As expressed by the equation, maximum corrosion rates of 12, 40, and 84 mpy are expected at 250, 280, and 300°C, respectively.

The value for α prevailing during exposure depends upon the solution composition and the velocity of solution flow past a surface. Some values for α in solutions of several different compositions and at several different velocities are shown below (these values are considered applicable to convergent and to straight-channel type flow).

1. Solution: 0.04 *m* UO_2SO_4, 0.005 to 0.0075 *m* $CuSO_4$, and 0.02 to 0.03 *m* H_2SO_4, in H_2O (tests at 280 and 300°C). Best estimates of α at a velocity of about 0.8 fps are between 6 and 7. At 10 and 18 fps, the estimates are between 2 and 3, and 1 and 1.7, respectively.

2. Solution: 0.17 *m* UO_2SO_4, 0.02 to 0.03 *m* H_2SO_4, in H_2O (tests at 280°C). Values of α are 2.5 to 3.5 at velocities of about 0.8 fps, and values of unity at 10 fps and above (to ~45 fps).

3. Solution: 0.17 *m* UO_2SO_4 with 0.15 *m* $CuSO_4$ and 0.4 *m* H_2SO_4 or with 0.02 *m* $CuSO_4$, 0.1 *m* H_2SO_4, and 0.2 *m* Li_2SO_4, in H_2O (tests at 280°C). At all velocities to about 45 fps, the α values were unity.

10.2 RELATIONSHIP BETWEEN URANIUM DEPOSITION OR SORPTION AND COPPER CONCENTRATION IN IN-PILE AUTOCLAVE EXPERIMENTS OF ZIRCALOY-2 CORROSION

In the correlation[1] of the data described in Sec. 10.1, it was shown that the relationship between Zircaloy-2 corrosion rate in uranyl sulfate solutions and fission power density in solution can be expressed by an equation of the general form of Eq. (1) and the specific form of Eq. (6). Changes in corrosion rate with solution composition are believed to result from changes in the amounts or relative importance of sorbed uranium, as given by the value of α. Using these concepts and equations in a further review of the in-pile autoclave results, it has been found that a correlation exists between the initial copper concentration in solution and the amounts of uranium sorption prevailing during exposure. The radiolytic-gas pressure normally varies inversely with copper concentration, and the autoclave data have also been examined for a possible correlation between the radiolytic-gas pressures and uranium sorption. The results of these considerations of the data are reported elsewhere in detail and are summarized here.[2]

They are considered of importance in the evaluations of the in-pile corrosion of Zircaloy-2. They may also bear some relationship to the question of the stability of uranyl sulfate solutions under irradiation, since reported observations in HRT run 13 indicate a possible relationship between low copper concentration and fuel instability in that run.[3]

Most of the experiments employing low copper concentrations were made at 280°C, and experiments at this temperature only were considered. A few low-copper experiments had been made at 250°C, but these were not considered in detail because the accuracy of the calculated α values at 250°C is poor. However, the trends of the 250°C results appear to be in agreement with those at 280°C. Some 250°C results obtained in experiments in which the reactor operated at two different power levels, and other 250°C results obtained at high radiolytic-gas pressures, were used in evaluation of the effects of high radiolytic-gas pressures on the effects of sorbed uranium.

The results of the data correlations show that, in general, the uranium sorption in solutions that contained initial copper concentrations of less than 0.01 *m* was greater than that prevailing when the solutions contained more than 0.01 *m* copper. The effects on the sorption of increasing copper in the range 0.01 to 0.04 *m* appear negligible in some sets of experiments, but there is some evidence for a difference between 0.01 and 0.04 *m* in another set. Changes in the effects of sorbed uranium ranging up to a maximum of about 3.5-fold were correlated with copper concentration changes in four different sets of experiments at 280°C.

For many of the experimental results it was not possible to directly distinguish whether the effects of low concentrations of copper were associated with the higher-than-usual radiolytic-gas pressures which resulted from the low copper concentrations. However, several types of data indicate that pressures in the range 0 to 650 psi, at least, probably do not affect the uranium sorption.

10.3 GENERAL DESCRIPTION OF PLANNED EXPERIMENT TO TEST ZIRCALOY-2 CORROSION IN THE HRT CORE

An experiment is planned to test the radiation corrosion of Zircaloy-2 and possibly other zirconium-alloy specimens in the HRT core. Design work for this experiment has been under way for several months, with most of the work being done in the Engineering Development Section of the Reactor Division. A memorandum has been prepared which summarizes the conceptual design and plans and the general status of the work.[4] These are summarized briefly here.

Criteria for the conceptual design of the experiment include (1) high velocities and good solution mixing near the specimens to minimize the possibility of massive uranium deposition and (2) the elimination of crevice regions in mounting specimens. Results obtained in in-pile-loop experiments have shown that surfaces in crevice regions corrode at higher rates than surfaces exposed to flowing solution and that this crevice corrosion leads to difficulties in determining the exposed-surface corrosion from weight results. Also, the penetration expected for crevice surfaces in this experiment would be, under some conditions, such that specimens might become loose in the clamp and thus suffer fretting attack.

The experiment provides for the simultaneous exposure of 27 corrosion specimens in the HRT core and core-inlet positions. The specimens are to be 1/2- x 4-in. coupons, 1/16 in. thick. Each coupon will also have two integral

"ears," 1/16 x 1/8 x 3/8 in., by which the coupon will be welded to a specimen holder. The specimen holder (see Fig. 4.5) will be a three-leafed web of 1/8-in. Zircaloy-2 of sufficient length to extend from the core flange to the vicinity of screen No. 7. Each specimen will in effect comprise an additional web for the length of the specimen. Three Zircaloy-2-clad thermocouples will also be welded to the web at various elevations to provide a means of sensing the temperature during the experiment. Some mechanical-property specimens may also be included, for the HRP Metallurgy Section, in the form of long rectangular pieces which would be welded to the web at locations below the thermocouples.

The corrosion specimens are to be welded to the holder at nine different positions (stations) in such a manner that when the array is aligned vertically in the center of the core, three of the stations will be located in the core neck and six in the core body. In these positions, the three core-entrance stations (three specimens to a station) will be exposed to an estimated solution velocity of 16 fps, while the velocities at the six core stations will vary from about 15 to 6 fps, as shown in Table 10.1. Assuming an entrance solution temperature of 250°C and 5-Mw core power, the estimated temperatures at the three core-entrance stations will be about 250°C, and those for the core stations, from 254 to 283°C. Also at 5 Mw, the estimated values for the solution fission-power densities to which the core specimens will be exposed range from about 17 to 24 w/ml. Specimens in the core entrance will be exposed to a maximum power density of about 15 w/ml. The temperature and velocity values were estimated by Lawson[5] from the results of HRT core-mockup measurements. The power-density values were estimated from values computed by Vondy[6] for power densities at 1-Mw core power, a uranium concentration of 6.4 g/liter, no fuel in the blanket, and a temperature of 260°C.

The corrosive attack of the specimens will be determined from weight measurements after the specimens are removed by cutting through the ears. The accuracy of the corrosion determinations will then depend on the accuracy with which the weight of those portions of the ears cut from the specimens can be estimated. Estimates of the probable errors which will be encountered from this source have been made and are listed in Table 10.1 in terms of the exposure times required to achieve probable errors of ±10% at 5-Mw core power and the expected solution temperatures and velocities. Two sets of values are given: one based on the maximum uncertainty expected and the other on a more optimistic but probably achievable accuracy. Estimated corrosion rates listed in the table are based on the results of in-pile loop and autoclave experiments.

The work which remains to be completed before the design can be proved acceptable and the experiment constructed includes the following:

1. Determinations of the uncertainties introduced into the weight results by the ear-cutting operation. Mockup specimen assemblies will be employed, and the cutting and weighing operations will be carried out in the Postirradiation Examination Group of Metallurgy.

2. Construction of a mockup of the specimen and holder assembly and testing of this in the mockup of the HRT core. This testing will be carried out by members of the Engineering Development Section of the Reactor Division.

Table 10.1. Estimated Power Densities, Temperatures, Solution Velocities, Corrosion Rates, and Probable Errors in Rate Measurements for HRT Core Specimens at 5-Mw Core Power and Entrance Temperature of 250°C

Station	Average Distance from Core Center (in.)	Average Solution Velocity (fps)	Average Solution Temperature (°C)	Power Density at 5 Mw (w/ml)	Corrosion Rate (mpy)	Days for ±10% Probable Error	
						a	b
A	43	16	250	0		-	-
B	27	16	250	(4)[c]	(3)	(23)	(65)
C	21	16	250	~15	~6	~10	~29
D	13	15	254	17	7	8	25
E	8	13	260	21	9	7	20
F	3	11	266	24	11	5	16
G	2	9	272	24	13	4	14
H	7	7	278	22	14	4	12
I	12	6	283	18	14	4	13

[a] Assuming uncertainty in specimen thickness measurements of ±1 mil and in measurements of length of ears removed of ±4 mils.

[b] Assuming uncertainty in specimen thickness measurements of ±2 mils and in measurements of length of ears removed of ±4 mils.

[c] Assumed value; Vondy's data do not extend this far from core center.

10.4 SORPTION OF URANIUM ON HYDROUS ZIRCONIA IN UO_2SO_4 SOLUTIONS

Investigations were continued of the sorption of uranium on hydrous zirconia in uranyl sulfate solutions at elevated temperatures, using an autoclave for batch-type exposures.

Most of the experiments were with an oxide purchased from City Chemical Co. and then pretreated by heating for 2 hr in air followed by storage in capped bottles. This oxide (designated AF oxide) when used contained about 55 wt% water and 1.7 wt% sulfate. The surface area of the ZrO_2, as determined by nitrogen absorption, was 275 m^2/g. After autoclaving in water or uranyl sulfate solution the surface areas are less, and values in the range 85 to 220 m^2/g have been found for the dried but unwashed material.

Other investigators have used the City Chemical oxide, with somewhat similar pretreatments, in sorption experiments at temperatures of 250, 100, and 25°C.[7,8] The results of the previous work at high temperature showed that the total and relative amounts of uranium sorbed from solutions of several different uranium concentrations are similar to those of the in-pile Zircaloy-2 films and scales, as inferred from corrosion and scale analyses data. Other, higher-temperature pretreatments led to oxides showing smaller surface areas and lower water contents and to apparently lesser changes in the oxide during subsequent exposure in uranyl sulfate solutions. However, the amounts of uranium sorbed were less than on the air-dried material and appeared to be out of line with those occurring in-pile. Since a major objective of this work is to explain and control in-pile sorption on oxides, it appeared worth while to study the air-dried material in more detail.

Some sorption experiments have also been made with a material prepared by autoclaving portions of the as-received oxide in water at 300°C for 4 hr, air drying at 110°C, and then storing in capped bottles. This oxide (designated WF oxide) contains about 5% H_2O, 3.6% SO_4^{--}, and the ZrO_2 has a surface area of 76 m^2/g. This material apparently does not undergo much change during exposure; therefore, studies with this material may help separate effects which result from changes with the AF oxide.

The experiments which have been carried out fall into three groups. The experiments and results in each group are briefly described and discussed in the following.

Each sorption experiment employed a water solution of uranyl sulfate with 0.02 *m* H_2SO_4. The exposures were made in a titanium autoclave equipped with a centrifuge cone for separation of solution and oxide at temperature. Five milliliters of solution and 0.5 g of oxide were charged in each case. The oxide residue samples employed in surface-area measurements were dried but not washed.

10.4.1 Sorption and Oxide Properties as a Function of Exposure Time

The AF oxide is known to change in area, crystallite size, and water content during exposure, and some column results reported by Banter[9] indicated that the amounts of sorbed material change with the duration of exposure. Information on the sorption and oxide properties as a function of time thus appeared desirable for the evaluation of experimental techniques and results. Therefore two sorption experiments at 280°C were made, one using the AF oxide and an initial uranium concentration of 45 g/liter, and the other with WF oxide and a uranium

concentration of 30 g/liter. The autoclaving time was varied in each series from 10 min to 17 hr. The amounts of uranium and sulfate sorbed, the pH's of the final solutions, and the surface areas of the residues are given in Fig. 10.1. The sulfate values include the amounts in the original oxide.

The AF oxide results show that significant changes in sorption occurred during the exposures but that, with the exception of pH, the parameters measured were nearly constant after 2 to 4 hr. The WF oxide results indicate that uranium and sulfate sorption and surface areas did not change with time after the initial 30-min exposure. The pH results for the WF oxide indicate a small increase in acidity during the first 4-hr exposure and an equal decrease some time thereafter, as shown by the 17-hr result.

The changes in sorption on the AF oxide with time are almost certainly a result of the sintering and/or dehydrating of the oxide which proceeds during exposure, although the magnitudes of some of the observed changes were probably affected by the changes in solution composition. For example, the pH results show that much of the excess acid was sorbed during the early portion of the exposure, and the uranium sorption in the resulting solution may have been greater than that which would have occurred at the initial acidity. (It may be noted in passing that large sorption of acid during the initial exposure can and does affect the two-liquid-phase temperature of the solution. For example, in quartz-tube stability tests with a 40-g/liter solution and AF oxide in the ratio 0.1 g/ml, the observed two-phase separation temperature was about 10°C less than that of the solution without oxide.) The measured surface areas are probably fairly representative of the relative areas of the oxide at different exposure times. However, the areal and sorption data are considered inadequate to establish whether a direct relationship exists between the two factors. This inadequacy results partly from the probable effects of solution changes on the sorption in the experiments to date and partly from the fact that the relationship between the measured and true surface areas is unknown. There are some indications in these and other data that the uranium in the residues affects the measured areas. More area measurements of washed-oxide residues will be required to evaluate this relationship.

10.4.2 Temperature Dependence of Uranium and Sulfate Sorption in the Range 250 to 325°C

Sorption as a function of uranium concentration was measured at 250, 280, 300, and 325°C on AF oxide, employing exposure times of 4, 4, 2, and 3 hr, respectively. The amounts of uranium sorbed and the ratios of uranium to sulfate are plotted vs uranium concentration in Fig. 10.2. The U/SO_4 ratio plotted includes the ratio, 39 mg of sulfate per gram of ZrO_2, in the original oxide. The range of uranium concentration employed was determined by estimated solution stability limits in these solutions with the 0.02 *m* excess H_2SO_4. The results for uranium sorption on WF oxide in three experiments at 250 and 280°C are also given in Fig. 10.2.

The amounts of uranium sorbed on the AF oxide at 300 and 325°C were in near agreement with those at 250°C, while the sorption at 280°C was somewhat greater. The amounts of sulfate sorbed (including the sulfate impurity) showed a lesser increase with concentration in solution than did the uranium sorption, and the sulfate sorbed varied rather little with temperature. The U/SO_4 ratio curves, therefore, tend to parallel the uranium sorption curves. The 250°C uranium sorption isotherm essentially agrees with the data of Banter[10] when both data are expressed on a per-gram-of-ZrO_2 basis. (The oxide employed by Banter contained only 17% water.) Uranium sorption on the WF oxide was less than that on

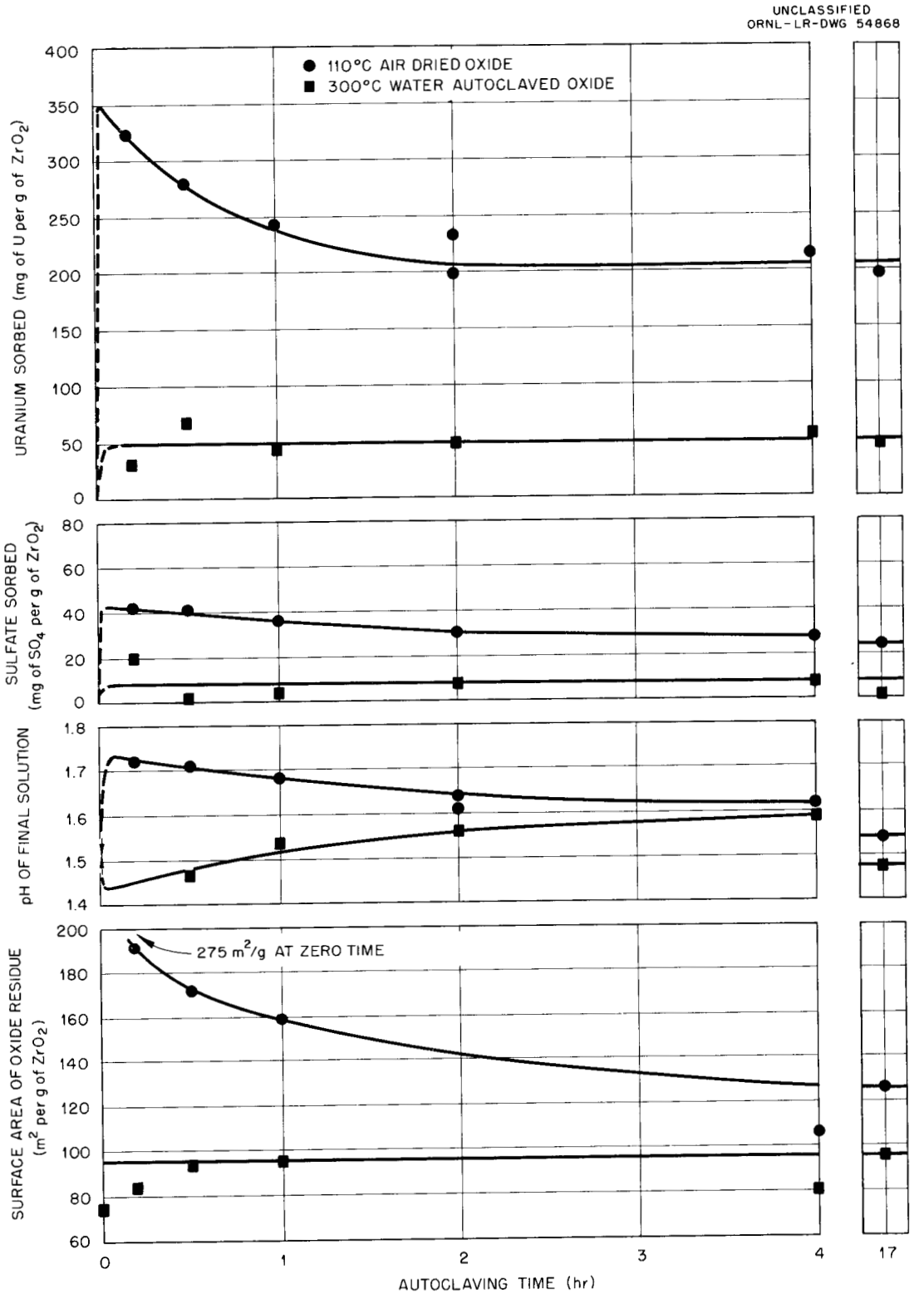

Fig. 10.1. Sorption on Air-Dried and Water-Autoclaved Oxides at Various Exposure Times at 280°C.

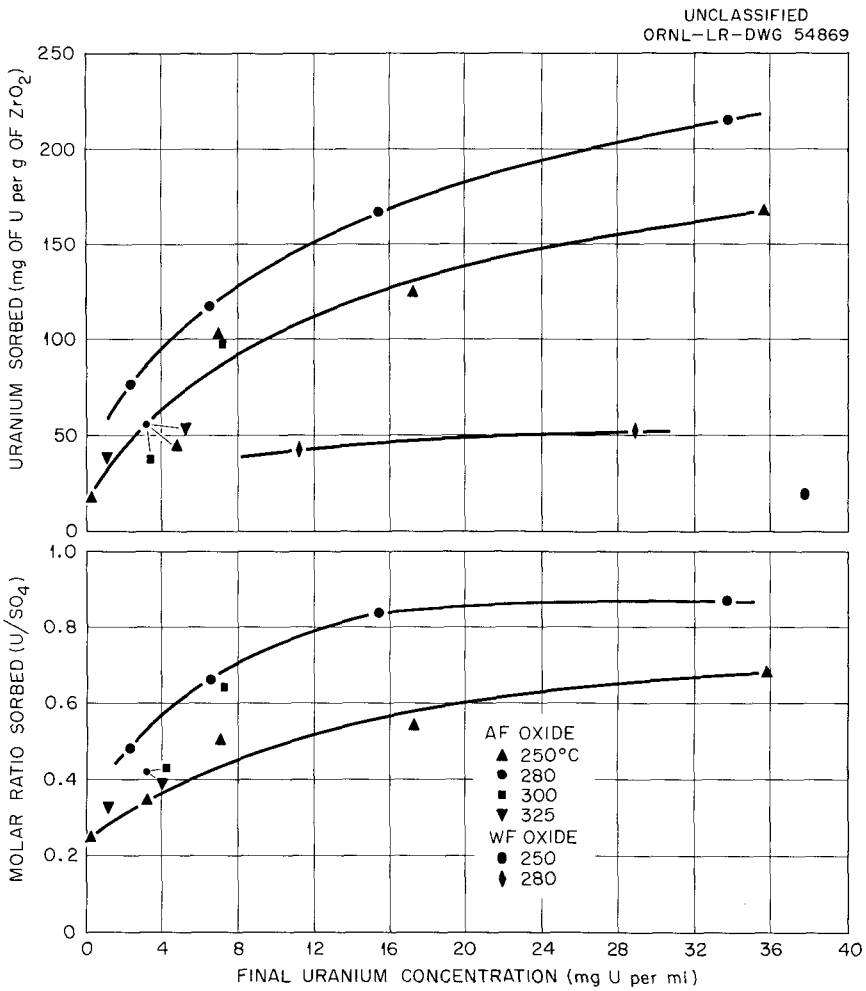

Fig. 10.2. Sorption Isotherm at 250, 280, 300, and 325°C with AF Oxide.

the AF material at the respective temperatures. However, the increase in sorption observed upon increasing the temperature from 250 to 280°C was much greater.

No satisfactory interpretation of these temperature effects and of the differences between the AF and WF oxide can be given at present. Among the factors which are believed to be important and which are being investigated are: surface area of the oxides, exposure times, changes in solution composition as a result of sorption, and differences between the species sorbed on the AF and WF oxide.

10.4.3 Elution of Oxide Residues

Elution experiments with some of the AF and WF oxide residues were made in order to aid in the characterization of the sorption and, in particular, to help elucidate the differences between the sorption properties of these oxides. Some of these experiments were made in a column, and others were made of the batch-washing type.

The column experiments were made with an AF oxide residue recovered after exposure in a 40-g/liter solution at 280°C for 4 hr and with a WF oxide residue from a similar exposure. Each dry residue was put in a column and eluted successively with 5-ml portions of 0.02, 0.1, and 1.8 *M* H_2SO_4. The batch experiments were with residues from 2-hr 280°C exposures of AF oxide in a 45-g/liter uranium solution and with a WF oxide in a 30-g/liter solution. The residues were washed successively with three 5-ml portions of each of the following eluents: H_2O, 0.1 *M* HCl, and 0.1 *M* KCl.

The data from these tests are given in Fig. 10.3. First, the amounts of uranium as indicated by the sorption experiment are plotted, next the amounts in the residues after rinsing from the autoclave and drying (as shown by the summation of material in washings and final residue), and, successively, the amounts left in the residue after each successive washing are given.

The results show that almost all the uranium is easily washed from the WF oxide, but that some uranium remains in the AF oxide even after extensive washing. It thus appears that part of the sorption on the AF oxide is the result of a process which does not occur on the WF oxide. It can be speculated that this process may be occlusion of uranium associated with sintering of AF oxide, or, possibly, compound formation.

It may be noted that the retention of uranium on the AF oxide provides additional evidence that sorption on this material is similar to that observed on in-pile Zircaloy-2 films and scales, since appreciable amounts of uranium are found on the in-pile materials after washing with water.[11,12]

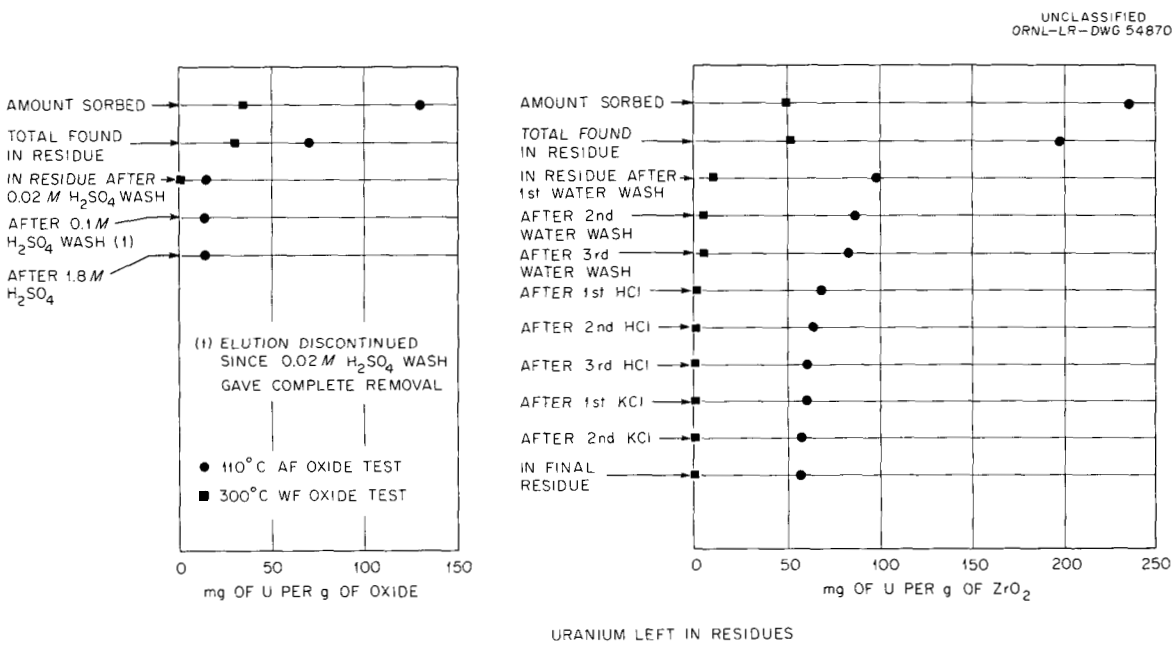

Fig. 10.3. Batch and Column Elution of Oxide Residues.

REFERENCES

1. G. H. Jenks, A Model for the Effects of Irradiation on Zircaloy-2 Corrosion and a Review and Correlation of In-Pile Zircaloy-2 Data, ORNL report (to be published).

2. G. H. Jenks and R. J. Davis, Relationship Between Uranium Deposition and Copper Concentrations in In-Pile Autoclave Tests of Zircaloy-2 Corrosion, ORNL CF memorandum (to be published).

3. J. R. Engel et al., Summary of HRE-2 Run 13 (Initial Power Operation), ORNL CF-58-10-115 (Oct. 29, 1958).

4. J. E. Baker and G. H. Jenks, HRT Core Corrosion Experiment (Status), ORNL CF memorandum (to be published).

5. C. G. Lawson, personal communication to G. H. Jenks.

6. D. R. Vondy, personal communication to J. E. Baker.

7. J. C. Banter and S. H. Wheeler, Adsorption of Uranium on Hydrous Zirconium Oxide from Uranyl Sulfate Solutions at Elevated Temperatures, ORNL report (to be published).

8. G. Goldstein, Sorption of Uranium on Zirconium Oxide, ORNL report (to be published).

9. G. H. Jenks et al., HRP Quar. Prog. Rep. May 1-Oct. 31, 1959, ORNL-2879, p 148-9.

10. G. H. Jenks et al., HRP Quar. Prog. Rep. Jan. 31, 1957, ORNL-2920, p 79.

11. G. H. Jenks et al., HRP Quar. Prog. Rep. Oct. 31, 1957, ORNL-2432, p 123.

12. B. E. Dearing, "Adsorption and Fixation of Uranium on Zircaloy in Autoclave Tests," p 5 in Uranium Surface Contamination on Nuclear Reactor Fuel Elements, ed. by W. M. Cashin, KAPL-2061 (Oct. 23, 1959).

PART IV. SLURRY FUELS

11. THORIA-PELLET IRRADIATIONS

J. P. McBride

A 2900-hr irradiation of a settled bed of 50 thoria pellets in D_2O was completed (experiment C-43-3). It was done in the LITR at a thermal-neutron flux of $\sim 2 \times 10^{13}$; the temperature was 250°C. The pellets were prepared by treating 1400°C-fired Davison Chemical Co. pellets with dibasic aluminum nitrate and refiring at 1750°C. When the irradiation autoclave was opened, 20 of the pellets were found to have broken into fragments and fines. The remainder had practically the same bulk and pycnometric densities as the original material (Table 11.1) but showed some damage from the chipping out of surface fragments and the breaking off of spherical segments (Fig. 11.1). All surfaces appeared to be quite porous.[1] A substantial quantity of a black vitreous substance was found in the upper half of the irradiation autoclave (Fig. 11.2). Pellets removed from a laboratory control experiment showed no apparent damage, and there was no evidence of the black vitreous material.

These pellets are inferior to pellets now being manufactured,[2] and the radiation effect, while real, may not necessarily be the same for the best thoria pellets now available. A second in-pile test on pure thoria pellets that showed excellent out-of-pile integrity characteristics is now under way.

Table 11.1. Thoria-Pellet Irradiation Data

Pellets irradiated 2900 hr in D_2O at 250°C
at a thermal-neutron flux of $\sim 2 \times 10^{13}$

Pellets	Average Weight (g)	Average Volume (cc)	Bulk Density (g/cc)	Pycnometric Density (g/cc)
Control	0.43	0.059	7.3	9.2*
Unirradiated	0.43	0.060	7.2	
Irradiated	0.38	0.056	6.8	8.5**

*Measured pycnometrically in water after drying at 110°C. A pycnometric density measurement on the control pellets before drying showed a density of 9.7 g/cc, indicating that heating at 250°C had resulted in filling with water those pores not ordinarily filled during the usual density measurements made at room temperature.

**By weighing in air and then in water to constant weight.

PIE-309

Fig. 11.1. Irradiated Thoria Pellets.

PIE-308

Fig. 11.2. Black Vitreous Material Recovered from Thoria-Pellet Irradiation Experiment C-43-3.

Attempts to identify the black vitreous material, which may have represented as much as 0.5 wt % of the solids in the bomb, have so far been unsuccessful. The material as recovered from the irradiation autoclave had a density of 1.18 g/cc. Loss in weight on ignition by flame firing was 76%. Ignition changed the color from a glossy black to a dull brown. Spectrographic analysis of the samples as received showed a small amount of thorium, but no spectrum could be found after ignition. The sample as received showed no x-ray diffraction pattern and, after ignition, only two faint and unidentifiable lines.

REFERENCES

1. R. E. McDonald, Metallurgy Division.

2. S. A. Reed, TBR Blanket Materials Studies: Compendium of Results of Evaluation Tests of Experimental Thoria Pellets, ORNL CF-60-9-91 (Sept. 15, 1960).

12. DEVELOPMENT OF GAS-RECOMBINATION CATALYST

J. P. McBride
L. E. Morse
W. L. Pattison

Work on the development of a gas-recombination catalyst for use in aqueous oxide slurries for the recombination of radiolytic gas continued with a re-evaluation and recalibration of the gas-injection apparatus[1] and further studies with slurries containing the sol-prepared palladium catalyst.[2]

12.1 GAS-INJECTION APPARATUS

Recalibration of the gas-injection equipment showed a significant holdup of gas in the capillary tubing that connects the gas-charging system to the reaction autoclave. This holdup under certain conditions amounted to as much as 80% of the gas charged and led to several erroneous conclusions as to the activity and properties of the palladium catalyst being used in the gas-recombination work[3,4] and obscured the true kinetics of the gas-recombination process.

Re-evaluation of the gas-recombination data as a result of the recalibration indicates that

(1) there is little or no deactivation of the catalyst under excess oxygen;

(2) the apparent threshold partial pressure for hydrogen to react in the presence of excess oxygen is not real, and reaction is obtained even at very low hydrogen partial pressures;

(3) the recombination of the oxygen and hydrogen in the reaction vessel is complete, and the apparent stoppage of reaction when significant partial pressures of both hydrogen and oxygen were present in the reaction vessel is also not real;

(4) the radical increase in catalyst specific activity when excess hydrogen is present, while real, may be consistent with the kinetics of the recombination process and does not necessarily indicate a change in the nature of the catalyst as previously surmised; and

(5) the solubilities of both oxygen and hydrogen in the slurry catalyst system appear consistent with those predicted from the Henry law constants obtained at BMI[5] and ORNL.[6]

The capillary tubing that connects the reaction autoclave, the Baldwin pressure gauge, and the gas-charging valve is 4 ft long, with a volume of 0.27 ml, and there is an additional 0.16-ml volume in the valve and fittings. The gas space in the reaction autoclave is about 7 ml at temperature. When the reaction autoclave containing slurry is operated at high temperatures, the capillary gradually fills with condensate. When either oxygen or hydrogen is charged to the system, the water is forced from the capillary. A portion of the gas at charging pressure is trapped in the capillary by a plug of condensate which

forms near the reaction vessel and is virtually unavailable for reaction except by diffusion through the plug. Subsequent additions of gas force the trapped gas into the autoclave but again leave a holdup in the capillary.

The equipment was calibrated with oxygen (Table 12.1). The data show that on the initial injection of oxygen, 80% of the gas charged was held up in the cold capillary. As more oxygen was added and the partial pressure of oxygen increased, the relative holdup, of course, decreased. If hydrogen should be charged after the oxygen is added, it is apparent that the fraction of hydrogen entering the reaction vessel would decrease with increasing (partial) oxygen pressure and that more or less pure hydrogen would be held up in the charging capillary.

Table 12.1. Calibration of Gas-Injection Apparatus

Volume of autoclave: 16.75 ml
Volume of gas-charging line: 0.42 ml
Volume of H_2O charged (22°C): 7.52 ml
Temperature: 280°C
Autoclave gas space at 280°C: 6.75 ml

Number of Injections	Oxygen Injected (moles)	Equilibrium Pressure (psi)	Dissolved* Oxygen (moles)	Oxygen in Gas Phase (moles)	Oxygen in Gas-Charging Line (moles)	Volume (ml)
	x 10^{-3}		x 10^{-3}	x 10^{-3}	x 10^{-3}	
0	0	917				
1	1.076	935	0.033	0.182	0.861	0.33
2	0.925	993	0.104	0.587	0.234	0.40
3	0.812	1046	0.092	0.536	0.184	0.44
4	0.887	1113	0.112	0.678	0.097	0.45
5	0.944	1183	0.101	0.708	0.135	0.46
6	1.020	1260	0.107	0.779	0.134	0.47
7	1.076	1342	0.147	0.830	0.099	0.47
8	1.303	1432	0.211	0.911	0.181	0.49
9	2.417	1596	0.293	1.659	0.465	0.54
10	2.039	1756	0.290	1.618	0.131	0.52
Totals	12.499		1.490	8.488	2.521	
Average	1.250		0.149	0.849	0.252	0.46
			Over-all Balance After Cooling to 94°C			
	12.499	573	0.278	11.59	0.631	0.40

*Calculated from data of ref. 5.

12.2 PALLADIUM CATALYSIS

Further work on the kinetics of hydrogen and oxygen recombination in a slurry containing the sol-prepared palladium catalyst suggests a probable first-order dependence of rate on the hydrogen partial pressure and a 0.5-order dependence on oxygen partial pressure. Previous data have been obscured by gas holdup in the gas-charging capillary tubing mentioned above, and the present results take into account the gas-pressure corrections that are required because not all the gas charged to the system actually entered the reaction vessel.

Three series of experiments were completed on a sample of pumped slurry from the out-of-pile testing of the in-pile slurry loop (L2-26S-6-4).[7] This slurry contained thorium - 0.5% uranium oxides in a concentration of 483 g of Th per kg of D_2O and 640 ppm of palladium (based on thorium). The slurry had been pumped several hundred hours under oxygen and had been subjected to deuterium-oxygen reaction tests at 280°C during the loop operations. In two series of experiments the initial oxygen pressure was held constant at 215 and 320 psi above steam (280°C) while the deuterium partial pressure was varied (Table 12.2). In both cases the initial reaction rate showed first-order dependence on the deuterium partial pressures from 0 to 400 psi (Fig. 12.1).

In a third series of experiments (Table 12.3) the initial deuterium pressure was confined to a relatively narrow range of partial pressures (35 to 100 psi) above steam at 280°C, and the initial oxygen pressure was varied from 113 to 765 psi (Table 12.3). The rate data were normalized by dividing the initial reaction rate by the initial hydrogen partial pressure and plotted against the 0.5 power of the oxygen pressure (Fig. 12.2). A fairly good linear fit was obtained except at the low oxygen partial pressures, indicating a probable 0.5-order dependence of the reaction rate on the oxygen partial pressure.

After each recombination experiment, the reaction autoclave was cooled to 98°C and vented to remove residual gas. The autoclave was then heated to 280°C, the oxygen added first, and then the deuterium. The gas holdup volume in the charging capillary was ~0.4 ml. Corrections for the gas pressure actually in the reaction autoclave were made by assuming that the oxygen held in the charging capillary was completely charged to the bomb during the deuterium addition and that there was a holdup of pure deuterium in the capillary after the deuterium was added. The apparent decrease in rate with increasing oxygen pressure indicated in Fig. 12.1 and the fact that the rate data obtained at a constant 215-psi oxygen partial pressure do not extrapolate to zero at zero deuterium partial pressure may have resulted from a partial mixing of the deuterium and oxygen in the charging capillary and a consequent holdup of both oxygen and deuterium in the capillary. Deviation of the rate data of Fig. 12.2 at low oxygen partial pressures may also have resulted from such a condition. The use of a standard operating procedure and the consistency of the rate data obtained suggest that while the gas-pressure corrections are semiquantitative, the rate dependences illustrated in Figs. 12.1 and 12.2 are probably real.

The experimental procedures and/or apparatus will be modified to prevent holdup of gas in the charging capillary, and further work on the reaction kinetics will then be carried out.

Table 12.2. Initial Reaction Rates for D_2-O_2 Mixtures in an Aqueous Thorium Oxide - 0.5% Uranium Oxide Slurry with a Palladium Catalyst at Constant Oxygen Partial Pressures

Slurry: 483 g Th/kg D_2O; 640 ppm Pd (based on thorium)
Temperature: 280°C

Oxygen Charged* (moles)	Deuterium Charged* (moles)	Corrected Deuterium Partial Pressure* (psi)	Initial Reaction Rate (psi/min)
x 10^{-3}	x 10^{-3}		
		P_{O_2} = 215 psi	
2.7	3.0	89	4.6
2.7	2.0	0	2.2
3.0	4.9	184	8.4
2.9	4.0	134	7.6
3.0	2.2	49	3.6
3.0	3.5	114	6.1
2.8	6.7	274	10.9
		P_{O_2} = 320 psi	
4.4	0.8	0	0
4.3	1.5	0	0
4.1	2.5	28	1.3
4.0	3.2	78	2.4
4.0	4.8	178	5.4
4.0	6.2	288	8.7
4.1	8.1	408	11.8
4.3	10.5	593	22.5
4.1	8.9	493	16.2

*Oxygen charged first, then deuterium, and pressure corrected assuming that all oxygen entered the reaction autoclave and that deuterium was held up in the capillary-gas-charging line; autoclave gas phase (280°C), 6.8 ml; gas-charging-line volume, 0.56 ml.

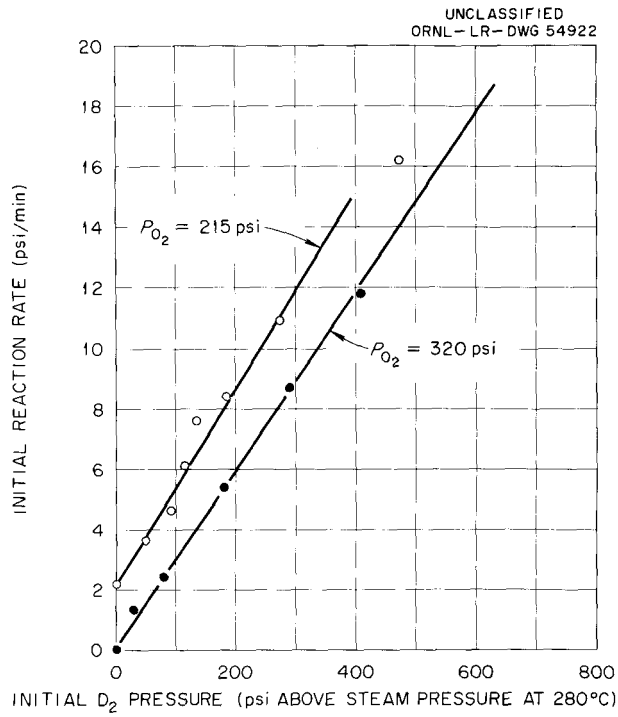

Fig. 12.1. Initial Reaction Rates of D_2-O_2 Mixtures in an Aqueous ThO_2–0.5% U Oxide Slurry with a Palladium Catalyst, at Constant Initial Oxygen Pressures. Temperature, 280°C.

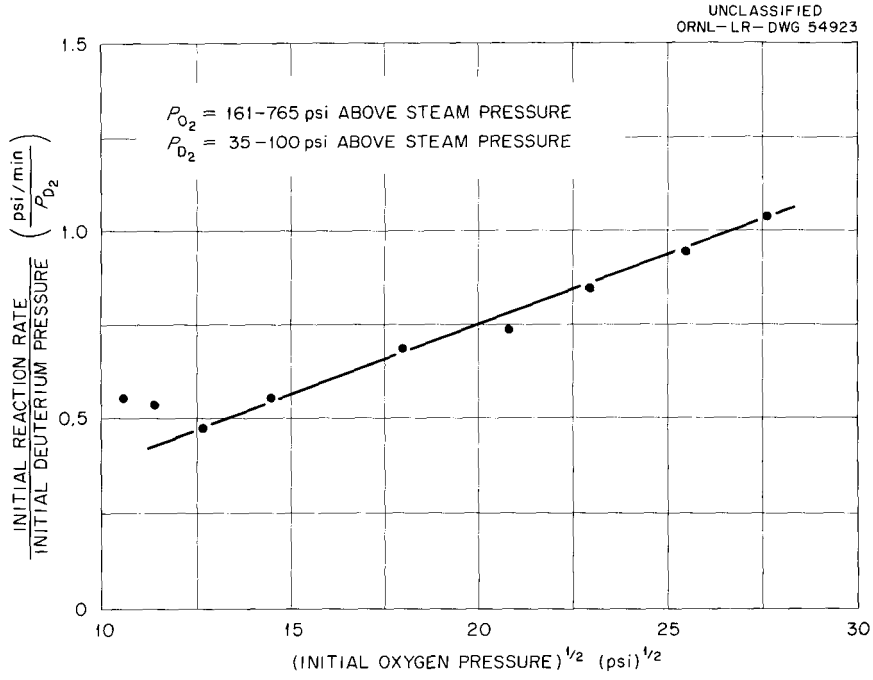

Fig. 12.2. Reaction Rates of D_2-O_2 Mixtures in an Aqueous ThO_2–0.5% U Oxide Slurry with a Palladium Catalyst at 280°C.

Table 12.3. Initial Reaction Rates for D_2-O_2 Mixtures, Normalized to P_{D_2} of 1 psi in an Aqueous Thorium - 0.5% Uranium Oxide Slurry with a Palladium Catalyst

Oxide Slurry: 483 g Th/kg D_2O; 640 ppm Pd (based on thorium)
Temperature: 280°C

Oxygen Charged (moles)	Deuterium Charged (moles)	Corrected Partial Pressures (psi)		Initial Reaction Rates (psi/min)	Ratio of Initial Reaction Rates to Deuterium Partial Pressure $[(psi/min)/P_{D_2}]$	$(\text{Oxygen Partial Pressure})^{1/2}$ $(psi)^{1/2}$
		Oxygen	Deuterium			
x 10^{-3}	x 10^{-3}					
4.2	3.0	324	78	5.3	0.068	18.0
2.8	2.9	211	89	4.9	0.055	14.5
5.4	2.9	433	67	4.9	0.073	20.8
2.0	2.9	461	94	4.4	0.047	12.7
6.6	2.8	527	58	4.9	0.084	23.0
8.4	2.8	649	46	4.4	0.094	25.5
1.7	3.0	130	100	5.1	0.051	11.4
1.5	3.1	113	99	5.4	0.055	10.6
10.1	2.8	765	35	3.6	0.103	27.7

*Oxygen charged first, then deuterium. Pressures corrected by assuming all oxygen entered reaction autoclave and deuterium held up in the capillary gas-charging line; autoclave gas volume at 280°C, 6.8 ml; gas-charging-line volume, 0.56 ml.

REFERENCES

1. J. P. McBride and L. E. Morse, HRP Quar. Prog. Rep. Oct. 31, 1959, ORNL-2879, p 173-179.

2. J. P. McBride and L. E. Morse, HRP Quar. Prog. Rep. Apr. 30, 1960, ORNL-2947, p 87-90.

3. J. P. McBride and L. E. Morse, HRP Quar. Prog. Rep. July 31, 1960, ORNL-3004, p 85-88.

4. Chem. Tech. Ann. Prog. Rep. Aug. 31, 1960, ORNL-2993, p 121.

5. H. A. Pray, C. E. Schweickert, and B. A. Minnich, Ind. Eng. Chem. 44, 1146-51 (1952); also, BMI-T-25 (May 15, 1960).

6. H. F. Soard, Solubility of Oxygen and Hydrogen in Thorium Oxide Slurries, ORNL CF-60-3-153 (Mar. 25, 1960).

7. E. L. Compere et al., HRP Quar. Prog. Rep. Apr. 30, 1960, ORNL-2947, p 107.

13. SLURRY CORROSION AND BLANKET MATERIALS TESTS

E. L. Compere
J. M. Baker
V. A. DeCarlo
T. Hikido[1]
R. A. Lorenz
H. C. Savage
R. A. McNees[1]
S. A. Reed
A. J. Shor
L. F. Woo

13.1 THORIA-PELLET TEST PROGRAM

13.1.1 Introduction

Ball-mill tests have served as one rapid and reproducible method for determining the relative integrity of thoria[2,3] and urania[4] experimental pellet preparations. In the past six months experimental batch preparations have consisted of about 10 to 50 pellets. With the limited number of pellets and the rather wide variations in the quality of the batches, it was not possible to make a critical evaluation of the effect of test variables on pellet wear or to relate wear rates with some known physical properties of the pellets. Recently one experimental batch contained a sufficient number of pellets to permit initiation of a systematic study of several pertinent ball-mill-test variables and to gain some knowledge of the size distribution of the particles which were rubbed off the pellets.

13.1.2 Effects of Operational Variables

The effects of operational variables were studied, using rotational speed of the mill, mill volume, and pellet and water loadings as the variables. Pellets (from batch P-39)[2] used for the tests were fabricated as right cylinders with hemispherical ends, 0.2 in. in diameter by 0.2 in. in height. The average grain size of the ThO_2 used to prepare the pellets was 7μ , and the pellets had been fired for 4 hr at 1750°C.

All tests were performed in a rubber-lined mill, 3.75 in. in ID, which had a capacity of 800 ml. A fresh charge of pellets was used in each test. Results of the test series are presented in Fig. 13.1.

Tests were run with four different loadings (10, 20, 50, and 100) of pellets at three different rotational speeds: 100, 150, and 200 rpm. Also one series of tests was run at 150 rpm, using the four different pellet loadings in a mill of the same diameter but of half the length (400-ml capacity). Except for the series using a mill of 400-ml capacity, each point on the plot in Fig. 13.1 represents the average of two 1-hr tests at a given set of conditions. It will be noted that the weight-loss rates of the pellets were proportional to the number of pellets and to the rotational speed of the mill and that rates increased with increased mill speed and pellet charge. However, the weight-loss rates of the pellets were essentially unaffected by the amount of water charged to the mill or by changing the length of the mill.

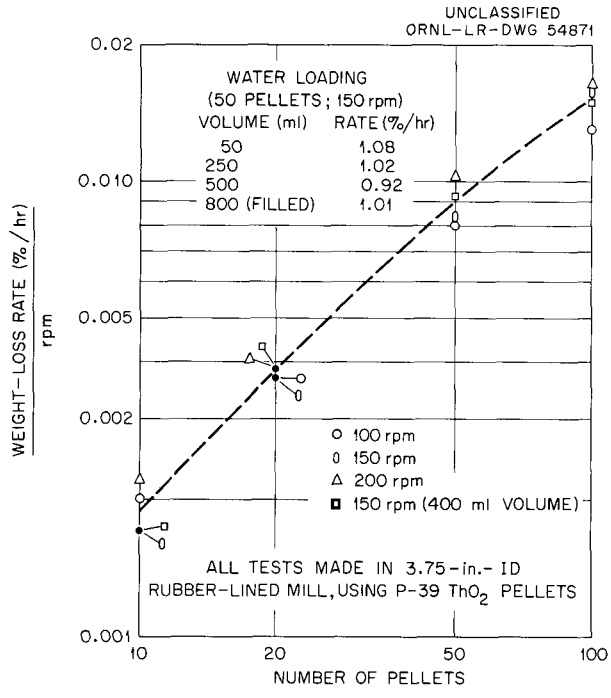

Fig. 13.1. Effects of Operating Variables on Attrition Rates of ThO_2 Pellets in Ball-Mill Tests.

13.1.3 Size Distribution of Fines

The size distribution of fines rubbed off pellets during ball-mill tests was the objective of a second test series. Such a study afforded some insight into the attrition process, that is, whether the individual grains were being released from the pellets due to impact, if chipping occurred, or whether a uniform wearing of the surface was taking place.

The tests were conducted by using approximately 60 (36 g) new P-39 pellets in a mill which was filled with water (800 ml). The mill was rotated at 150 rpm for four consecutive 1-hr periods. The water and rinses which contained the fines were combined after each 1-hr test and then submitted for particle-size-distribution analyses, using the Andreasen pipette method. The results of the tests are shown in Fig. 13.2.

The pellets had lost approximately 5% of their initial weight after the fourth test. According to the plots in Fig. 13.2, the average mean diameter of the particles was about 2μ and about 80% of the particles were less than 6μ in size. Since the grain size of the initial thoria used for preparing the pellets was 7μ, and since some grain growth would be expected as a result of the high firing (1750°C) of the pellets, one would conclude from the size range of the fines that attrition was due principally to wear of material from the surface of the pellets rather than from dislodging the grains or from gross chipping. Microscopic examinations of the postrun pellets revealed some localized chipping at the malformed ends of the pellets at the intersection of the cylindrical and hemispherical sections; however, no chipping was noted over the general surface of the specimens. Optical microscopy of the fines revealed a small number of fragments of the approximate size range indicated by the particle-size-distribution

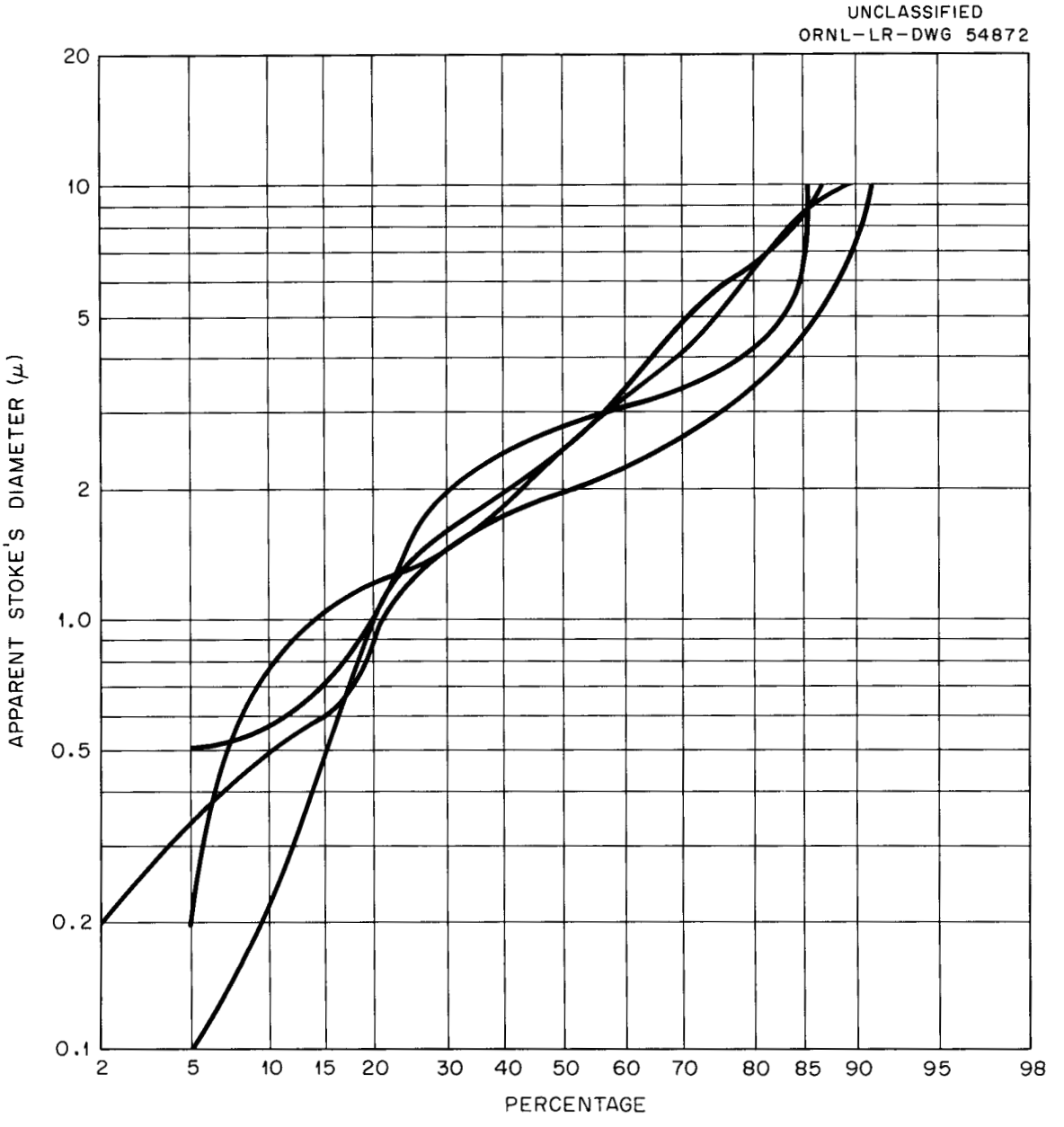

Fig. 13.2. Particle-Size Distribution of Material Rubbed Off the P-39 ThO_2 Pellets During Ball-Mill Tests.

data. The results of these tests are in accord with findings of other investigators who have made similar studies with UO_2 pellets.[5]

13.1.4 Evaluation of Experimental Pellets

Samples of four new pellet preparations were tested recently to determine their relative integrity and wear rates. One group of samples which was prepared by the Ceramics Group of the ORNL Metallurgy Division consisted of one preparation (P-82) of pure ThO_2 pellets fabricated as right cylinders with domed ends, 0.219-in. diameter x 0.205-in. height, and two samples (P-83 and P-84) of the same pellets which had been coated with ~0.3 mil of zirconium by means of an

experimental electron-beam vaporization technique. Detailed test data for the three preparations have been reported elsewhere.[6]

The fourth sample (P-85 Numec) was obtained from a batch procured from Nuclear Materials and Equipment Corp. The pellets were of pure thoria, fabricated as right cylinders with domed ends, 0.159-in. diameter x 0.162-in. height.

Pellets from each batch were subjected to two 1-hr spouted-bed tests (10 pellets, 0.2 fps superficial velocity) before and after autoclaving. Static autoclave tests were conducted in the usual manner by exposing the pellets, submerged in water, for 72 hr at 260°C. New pellets from each of the uncoated preparations were also subjected to two 1-hr ball mill tests with the mill operated at 150 rpm. There were not enough coated pellets for ball-mill tests. The results are summarized in Table 13.1.

Table 13.1 Summary of Evaluation Tests of Experimental Zirconium-Coated and Uncoated ThO_2 Pellets

Batch Code	Average Weight-Loss Rates (%/hr)			
	Static Autoclave (72 hr, 260°C)	Spouted Bed		Ball Mill (150 rpm)
		Preautoclave	Postautoclave	
P-82*	1×10^{-4}	0.25	0.49	6.1×10^{-2} (10 pellets)
P-83 (Zr-coated)*	2.7×10^{-2}	0.36	0.63	
P-84 (Zr-coated)*	2.5×10^{-2}	0.25	0.56	
P-85 (Numec)**	1.1×10^{-3}	1.27	1.50	1.5 (100 pellets)

*Prepared by Ceramics Group, ORNL Metallurgy Division.
**From Nuclear Materials and Equipment Corp.

The following information supplements the tabulated data:

1. The weight-loss rates of the ORNL P-82 unclad ThO_2 pellets in the autoclave and dynamic tests were lower than rates obtained with other experimental preparations prepared by similar techniques.[3]

2. Penetration of the thin cladding of zirconium was observed with the coated pellets after the initial 1-hr spouted-bed tests. Major wear occurred at the junction of the cylindrical and hemispherical sections of the pellets, and it became progressively more pronounced during the second 1-hr spouted-bed test. Flakes of the zirconium which had spalled off the pellets were found in the autoclaves.

3. The Numec (P-85) pellets displayed relatively poor attrition resistance, compared with the P-82 preparation. Their inferior integrity was attributed to numerous fine surface cracks and isolated fissures, which in some cases penetrated nearly a third of the way into the pellet, as shown in Fig. 13.3. The pellets also contained more and larger pores than most preparations which have been examined recently.

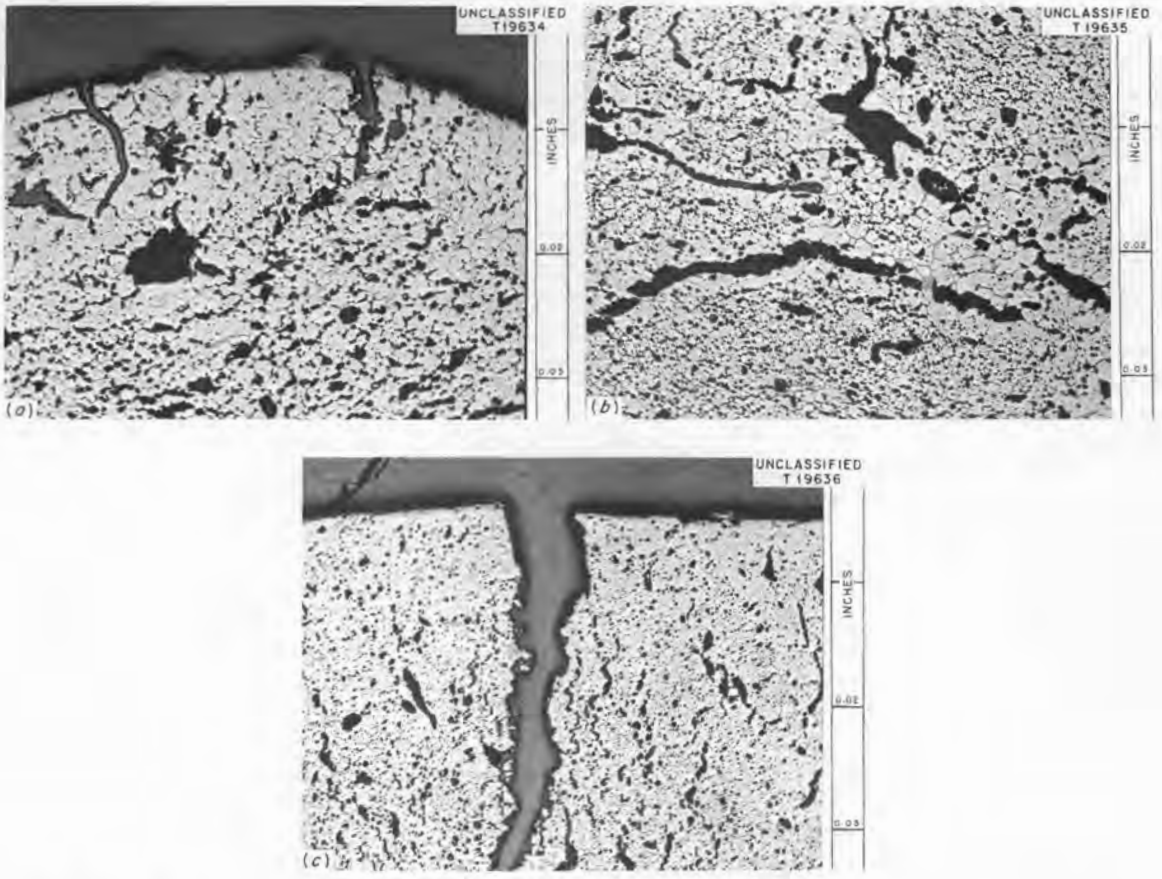

Fig. 13.3. Experimental ThO_2 Pellets from Nuclear Materials and Equipment Corp. As polished. (*a*) Internal pores and voids; (*b*) surface cracks; and (*c*) fissure. 100X. Reduced 16%.

13.2 IN-PILE AUTOCLAVE SLURRY-CORROSION STUDIES

13.2.1 Development of Al_2O_3 Slurry Capillary Filter

An Al_2O_3 filter for application between Zircaloy-2 slurry autoclaves and the attached water-filled capillary lines leading to pressure instruments has been fabricated as a result of the development of Al_2O_3 - Zircaloy-2 brazing procedures. In recent in-pile slurry autoclave experiments,[7-9] the formation of a slurry plug in the capillary line led to quite slow responses of the pressure cell. In some cases the experiment was terminated because potential changes in radiolytic-gas level could not have been sensed fast enough to satisfy safety criteria.

A porous, 100% Al_2O_3 (Coors Porcelain Co., AP-100 body) tube, 0.13-in. OD x 0.07-in. ID x 0.25-in., was pretested by exposure in a static autoclave for eight weeks to 280°C water, with a resultant weight loss of 0.24%. Subsequently one end of the tube was brazed coaxially to the 0.052-in. hole to the pressure capillary tap in the Zircaloy-2 autoclave closure. A Zircaloy-2 cover was brazed to the other end of the Al_2O_3 tubing. The brazing (by the HRP Metallurgy Section and the Welding and Brazing Laboratory of the ORNL Metallurgy Division, Fabrication Section) was carried out in a vacuum furnace, using an alloy containing 48% Zr, 48% Ti, and 4% Be.

The brazed filter assembly satisfactorily separated slurry from water, with no visible solids carry-over and no evidence of plugging. Exposure of the assembly to 280°C water for 64 hr did not result in attack of the joint or any appreciable corrosion. A weight gain of 2 mg was observed; the assembly weighed 18 g and the filter tubing approximately 100 mg. Further testing is being carried out, using the filters as components in slurry autoclave experiments.

13.3 IN-PILE SLURRY LOOP

13.3.1 In-Pile Operation

Operation of the first in-pile slurry loop (L-2-27S),[10,11] installed in LITR beam hole HB-2, was satisfactorily completed after 3115 hr of slurry circulation, of which 2220 hr (July 19 to Oct. 19, 1960) were with continuous in-pile operation, and 1839 hr under irradiation at 3-Mw LITR power. At the time of insertion, the circulating slurry inventory was 1350 g of thorium per kg of D_2O (980 g of thorium per 280°C liter). The slurry contained 0.5 wt % of enriched uranium, based on thorium, and 0.019 m palladium (ref 12) as a recombination catalyst. The 5-gpm loop was operated at 280°C under an oxygen atmosphere, with slurry velocities in the piping of 6 to 8 fps. During the irradiation, withdrawal of six samples reduced the circulating inventory concentration to 960 g of thorium per kg of D_2O (735 g of thorium per 280°C liter). Six terminal samples involving a tracer experiment to verify the circulating inventory were also withdrawn. Sampling procedures operated entirely without difficulty.

Before removal from the reactor, the thorium oxide remaining in the loop (450 g of Th per kg of D_2O) was flushed to a slurry holdup tank located in a shielded, external equipment chamber. Radiation measurements of the loop during removal from the reactor indicated that practically all the thorium oxide and associated fission products had been removed by the flushing operation. The ease with which the slurry was removed indicated that there was no caking of the slurry on the inside surface of the loop. This will be verified by visual examination of the loop components when it is dismantled in the hot cells.

13.3.2 Slurry Circulation

Evidence as to whether all the slurry inventory of the loop was actually circulating is presently incomplete. However, complete removal of solids from the sample carrier was obtained only after repeated flushing in the hot cell. Material balances on these flushings are not complete. No direct evidence of loss of thoria from circulation was seen during in-pile operation, according to pump power, or fission- and gamma-heat measurements. No significant changes in core "nose" piping temperatures were observed, implying that no deposits occurred in the maximum-flux region. The ease of final slurry draining and the lack of retention of activity in the pressurizer and pump regions implied no permanent buildup of solids there. Partial plugging of the sintered stainless steel filter[13] (8-μ mean pore diameter) occurred during early in-pile operation; flow decreased from 3 to 4 cc/sec to 0.3 to 0.4 cc/sec. This may have been due partially to corrosion but may also have been due to some plugging by slurry as the particles degraded. The radioactivity noted in the filter region during withdrawal was slightly higher (3 R at 1 ft) than that noted on piping and pressurizer regions on either side (1.2 R at 1 ft). Since 1 ml of slurry as sampled read more than 10 R at 1 ft, no noteworthy deposits are implied.

A slow decrease (days) of 2 to 4° in core outlet temperature occurred frequently during in-pile operation. The original spread between outlet and inlet temperatures returned during reactor shutdowns. In one case, the spread was immediately restored when slurry flow was increased by increasing the pump-current frequency from 60 to 80 cps. Since inlet and outlet thermocouples are on the bottom of the piping, any accumulation of solids or sludge could have caused such a decline by decreasing heat transfer to the thermocouple.

13.3.3 Slurry Corrosion

The definitive corrosion determination will be made by examination of test specimens after hot-cell disassembly of the loop. A total of 48 specimens of Zircaloy-2, titanium, and type 347 stainless steel, each 1/4 x 5/8 x 1/16 in., were placed in similar arrays in the core nose, core rear, and loop rear positions, thus affording three levels of radiation intensity. Specimen holders permitting flow at 8 and 22 fps were placed in each location. In the core region these were perpendicular to the radiation gradient.

Generalized corrosion of the stainless-steel slurry-circulating system, including pump casing, loop piping, core piping, and filter internal area, based on iron pickup by the circulating slurry, was 0.4 mpy during 820 hr of preirradiation circulation and 0.4 mpy during the next 1279 hr, which included 1042 hr of full-power irradiation. Total generalized loop corrosion based on oxygen loss or chromium buildup exceeded the values based on iron pickup. However, internal areas of the pressurizer and filter were involved in the oxygen and chromium values. The filter internal area, though certainly greater than the other loop areas combined, has not been determined; so a rate of corrosion is not cited. Oxygen-partial-pressure reduction and chromium buildup were in fair agreement. Rate of oxygen consumption increased for a period after irradiation began but then became quite low as the experiment continued.

13.3.4 Radiochemical Considerations

Analyses of Cs^{137}, Zr^{95}, and Ce^{144} (fission products) and Pa^{233} activity are under way as a basis for the determination of average flux, burnup, $\phi\sigma_{abs}$ for Th^{232}, and solids-liquid activity distribution ratios. Table 13.2 summarizes the distribution of the fission products obtained to date. It will be noted that although some scatter exists, only Cs^{137} showed appreciable tendency to be carried by the liquid phase.

Table 13.2. Molar Distribution Ratios of Fission Products

Hours at 3 Mw	Molar Distribution Ratios (Solids/Liquid)			
	Cs^{137} (γ)	Zr^{95} (γ)	Ce^{144} (β)	Pa^{233} (γ)
155	1.87	1,910	>590	>116,000
448	1.07	3,830	>550	18,400
608	1.30	473	509	> 76,000
1042	0.56	10,400	175	8,470

Radiochemical data (Table 13.3) for the fourth in-pile sample (1200 hr in-pile) were chosen for an estimate of the flux. After 1042 hr of irradiation at 3-Mw reactor power, the burnup was computed as 0.2 at. % of U^{235}. Based on Cs^{137} analyses and assuming a U^{235} cross section of 582 barns, the neutron flux averaged over the loop main stream was 0.88×10^{12}, giving an nvt of 3.3×10^{18} at the sample time. Analysis of the Pa^{233} yield, neglecting protactinium burnup, gave a value for $\phi\sigma_{Th}$ of 10.4×10^{-12}. Using the computed value for the flux, the absorption cross section for Th^{232} was estimated as 11 barns. Such a value is compatible with a nominal 7 barn (2200 m/sec) cross section, if a 50% resonance correction, deemed reasonable, is assumed.

Table 13.3. Radiochemical Data and Results of Nuclear Calculations (1042 hr at 3 Mw)

	Disintegrations per Minute per Gram of Solids	Fissions per Gram of Solids
Cs^{137}[a]	4.1×10^{7}	1.8×10^{16}
Zr^{95}[b]	5.1×10^{9}	1.0×10^{16}
Ce^{144}[c]	1.5×10^{9}	1.4×10^{16}
Pa^{233}	9.4×10^{11}	
Burnup of U^{235},[c] at. %	0.19	
nvt	3.3×10^{18}	
Average ϕ (main stream)	0.88×10^{12}	
$\phi\sigma_{Th^{232}}$	10.4×10^{-12}	
$\sigma_{Th^{232}}$	11 barns	

[a] Corrected for Cs^{137} in liquid.
[b] Nuclides in liquid negligible.
[c] Based on Cs^{137}.

13.3.5 Radiolytic Gas

Partial-pressure measurements indicated that the radiolytic gas level remained below 10 psi during the in-pile period. Recombination as a result of pile gamma radiation was estimated to be sufficient to account for the estimated production rate of 0.08 mole/liter-hr (ref 14), using a G value[15] of 5 molecules of D_2 per 100 ev.

Low flow rates through the filter[16] implied a rate of gas transfer between main stream and pressurizer characterized by a half life of at least 60 min. Consequently, experiments using transients to determine the catalytic activity of the palladium added as recombination catalyst were not deemed meaningful.

13.3.6 Particle Integrity

There appeared to be substantial degradation of slurry particle size as irradiation proceeded (Fig. 13.4). The average diameter decreased from an original value of 1.7μ prior to irradiation to a value of 0.3μ after 1460 hr of irradiation (2716 hr of slurry circulation). Concurrently, the surface area increased from 1.5 to 25 m^2/g. As indicated in Fig. 13.4, substantial effects on particle characteristics were initiated when irradiation began and had not necessarily ceased at the time irradiation was terminated. As shown below, there was an associated effect on settling properties. Clearly, irradiation

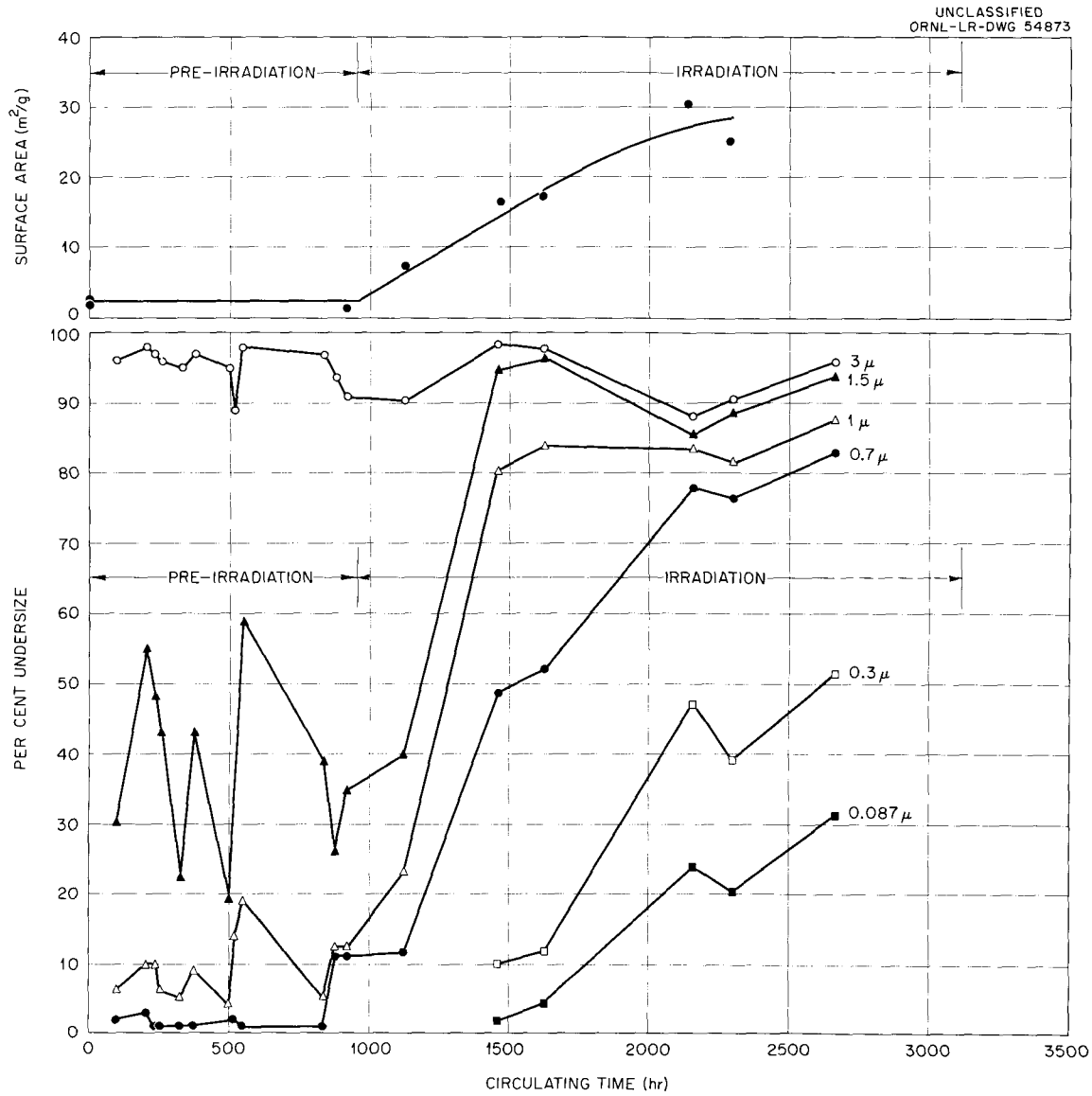

Fig. 13.4. Effect of Irradiation and Circulation on Slurry Particle-Size Distribution and Surface Area.

of the experiment resulted in appreciable particle degradation. However, it is of interest to consider observations on similar slurries in relevant earlier in-pile autoclave[17] and unirradiated loop[18] experiments.

In-pile autoclave experiment[17] L6Z-122S, with thoria - 0.5% urania of an original mean diameter of 0.8μ (5% below 0.3μ), irradiated for 681 hr (nvt = 1.3 x 10^{19}) showed a postirradiation mean diameter of 0.6μ (41% below 0.2μ). Also, circulation[18] in out-of-pile loop run L-2-26S-4 of thoria - 0.5% urania (natural) batch DT-18, prepared in parallel with the present in-pile batch DT-22 (enriched uranium), resulted in degradation from the 1.9-μ original mean diameter to a mean diameter of 0.7μ during ~1400 hr of circulation.

It may further be noted that the present loop run has subjected the slurry to more passes through the pump (a major degradation cause) by its short cycle time than any other ORNL slurry run.

Thus a reasonable conclusion may be that radiation served as a definite cause of degradation, but acted in combination with pumping. Effects on loop operation which could be attributable to the degradation might include filter plugging, incomplete sample draining, possible (as yet uncertain) loss of solids from circulating inventory, and association with the core inlet-outlet temperature difference mentioned above. As yet, the association of degradation with these effects is not fixed. No other gross effects on loop operation attributable to degradation were noted.

13.3.7 Settling Observations

Direct determinations of settling rate at room temperature were made with slurry in 25-ml tapered-bottom centrifuge cones directly after draining from the sample carrier. Volumes of 8 to 11 ml were used; the settling normally occurred in the straight portion. The solids interface subsided in an exponential fashion to a final settled-bed volume; values cited represent 1 to 3 days of settling.

In general, as irradiation of the experiment continued, the settling became slower, as evidenced (Table 13.4) by both initial rates and by subsidence "half

Table 13.4. Room-Temperature Settling Rates of In-Pile Slurry Loop Samples

Slurry circulation, hr	0	0-810	1076	1412	2110[a]	2251	2712
Radiation, hr	0	0	155	448	1042	1150	1460
	Original Batch DT-22	Mixed Y-12 Samples					
Concentration, g Th/kg D_2O	960	965	795	660	545	375	440
Concentration, vol. % solids	11.2	11.2	9.4	7.9	6.6	4.6	5.4
Settling rate,[c] cm/min x 10^3	25	52	33	27	2.7[b]	0.8	0.8
Subsidence half life, min	12	19	28	31	-	110	120
Final settled bed, vol. % solids	14	20	21	14	8	6	7

[a] Sample did not exhibit sharp solid-liquid interface.
[b] Settling rate after 105 min.
[c] Initial settling rate; extrapolated to zero settling time using semilogarithmic plot.

life". Also, the solids content of the settled bed diminished. It is implied that the slurry became more flocculated and was settling under highly hindered conditions. Such behavior is compatible with the degradation cited above.

REFERENCES

1. Ceramics Group, ORNL Metallurgy Division.
2. E. L. Compere et al., HRP Quar. Prog. Rep. Apr. 30, 1960, ORNL-2947, p 92.
3. E. L. Compere et al., HRP Quar. Prog. Rep. July 31, 1960, ORNL-3004, p 89.
4. M. R. Scheve, Liquid Fluidized Bed Reactor Study, First Quar. Prog. Rep. (Feb., 1960), MND-LFBR-2303, p 10.
5. E. L. Compere et al., Report On Trip to The Martin Company, August 31, 1960, ORNL CF-60-9-63.
6. S. A. Reed et al., Summary of Evaluation Tests of Experimental Zirconium-Clad ThO_2 Pellets, ORNL CF-60-11-15 (Nov. 1960).
7. E. L. Compere et al., HRP Quar. Prog. Rep. Apr. 30, 1959, ORNL-2743, p 143.
8. E. L. Compere et al., HRP Quar. Prog. Rep. Apr. 30, 1960, ORNL-2947, p 99.
9. E. L. Compere et al., HRP Quar. Prog. Rep. July 31, 1960, ORNL-3004, p 93.
10. H. C. Savage et al., HRP Quar. Prog. Rep. Apr. 30, 1960, ORNL-2947, p 101-107.
11. H. C. Savage et al., HRP Quar. Prog. Rep. July 31, 1960, ORNL-3004, p 96-97.
12. J. P. McBride, L. E. Morse, HRP Quar. Prog. Rep. Apr. 30, 1960, ORNL-2947, p 87.
13. J. M. Baker et al., 5-gpm In-Pile Thorium Oxide Slurry Loop Development Runs 14-16 In Loop L-4-24S, and Filtration of Thorium Oxide Slurry With Sintered Filters, ORNL CF-60-3-39, (Mar. 7, 1960).
14. E. L. Compere et al., HRP Quar. Prog. Rep. Apr. 30, 1960, ORNL-2947, p 107.
15. C. J. Hochanadel, The Radiation Induced Reaction of Hydrogen and Oxygen In Water at 25° to 250°C, ICPUAE, P/739, Rev. 1, 1955.
16. E. L. Compere et al., HRP Quar. Prog. Rep. July 31, 1960, ORNL-3004, p 97.
17. E. L. Compere et al., HRP Quar. Prog. Rep. Oct. 31, 1959, ORNL-2654, p 139.
18. H. C. Savage et al., HRP Quar. Prog. Rep. Jan. 31, 1960, ORNL-2920, p 111.

PART V. FUEL MANUFACTURE

14. THORIUM OXIDE PRODUCTION

O. C. Dean P. A. Haas
V. L. Fowler
C. C. Haws
A. T. Kleinsteuber

14.1 PREPARATION OF THORIUM OXIDE PRODUCTS

14.1.1 Preparation of Spherical Pellets for Pebble-Bed Blanket

Fabrication factors influencing the integrity of spherical thoria pellets prepared by automatic pressing and calcination of DT-100, oxalate-precipitated ceramic-grade ThO_2 powder, were studied.[1] The integrity was evaluated on the basis of freedom from visible cracks and loss of particles when subjected to a standard spouting-bed attrition test.[2]

Visible cracks were of two types, those appearing at the junction of the spherical cap and the cylindrical sections of the pressed pellet (capping) and those parallel to the axis of the pellet (top and side cracking). Capping was due to strains induced by adherence of the powder to the punch face and to the variation in powder density through the cap, a result of the high-domed shape of the ball punch face. The incidence of capping was decreased 90% by a combination of three factors: (1) increasing the radius of curvature of the 1/4-in. ball-face punch from 0.144 to 0.25 in.; (2) increasing the percentage of Carbowax binder-lubricant or changing the kind used: and (3) increasing the firing temperature of the ThO_2 powder from 800 to 1200°C prior to granulation and automatic pressing.

Top and side cracking were attributed to strains induced during calcination of the press-formed pellets. The incidence of this type of cracking was decreased by increasing the density of the powder grains formed by granulation prior to pressing and by including a 2-hr soaking at 1200 to 1300°C before increasing the temperature to the final 1750°C. The pour density of powder grains was increased from 2.14 to 2.77 g/cc by increasing the pressure on the powder in the granulation step or by increasing the powder firing temperature prior to granulation from 800 to 1200°C (Table 14.1). The effect of soaking appeared to be optimum in a powder of grain density 2.5 to 2.7 g/cc.

The final attrition rates, based on a series of six 1-hr tests in the spouting bed for each sample, were lowered by the modified calcination program, which included soaking, and by holding the pour density of granulated powder between 2.5 and 2.7 g/cc. The fired density of the pellets also increased when granulated-powder densities were in this range.

Table 14.1. Effects of Variations in Fabrication Procedure on Density, Cracking, and Attrition Resistance of ThO_2 Pellets

Pour Density of Powder Grains (g/cc)	Pellet Calcination Program*		Average Fired Density of Pellets (g/cc)	% of Samples with Visible Cracks	Attrition Rate (%/hr)
	Soaking 1.5 to 2 hr at 1200 to 1300°C	Direct Firing to 1750°C for 4 hr			
2.14	No	Yes	8.84	67	1.02
	Yes		8.74	33	0.86
2.42	No	Yes	8.50	67	1.12
	Yes		8.89	0	0.91
2.48	No	Yes	8.82	67	1.41
	Yes		8.80	0	0.90
2.50	No	Yes	8.73	67	0.34
	Yes		8.74	0	0.30
2.65	No	Yes	9.03	67	0.46
	Yes		9.15	0	0.36
2.77	No	Yes	9.29	0	0.27
	Yes		9.34	16	0.55

*Pellets having been soaked at 1200 to 1300°C, the temperature was then increased to 1750°C for 2 to 3 hr.

14.1.2 Preparation of Pebbles from Calcined Thorium-Uranium Oxide Gel Fragments

Uranium-thorium oxide fragments containing 5 mole % uranium, prepared by the sol-gel process and fired[3] to 1300°C in hydrogen, were rounded by attrition in a ball mill for several hours. Although the fragments were still jagged, a series of six 1-hr tests in the spouting bed showed attrition losses of 2.1 %/hr, initially, to 0.3%, finally, for pellets nominally 1/8 to 1/4 in. in diameter. These results seem to indicate that thoria pellets of high integrity can be made by the gel method.

14.1.3 Coating of ThO_2 Pellets with Metals and Oxides

The feasibility of coating ThO_2 pellets with Ni, Cr, Al_2O_3, Ta_2O_5, ZrO_2, or TiO_2 by the plasma-jet apparatus was studied. Powders, -325 mesh, fluidized by argon or argon-hydrogen mixtures, were passed through the arc and deposited on the pellets held in the jet stream 3 to 5 in. distant from the hot exit. The arc was struck in argon or argon-hydrogen at 25 v and at 325 or 700 amp. At the higher powers, pellets were successfully coated with the above metals and oxides.

Only the nickel-coated pellets, which had been postannealed at 1200°C in hydrogen, showed greater resistance to attrition in the spouting-bed test than did the original thoria pellet. For the first two of six successive 1-hr tests, the nickel-coated pellets showed weight losses of 0.07 and 0.04 %/hr. After the third hour, the coat stripped from the pellet, evidently having sheared at sharp edges in the thoria pellet.

14.2 DEVELOPMENT OF OXIDE PREPARATION

14.2.1 Flame-Calcination Development

Experimental development of flame-preparation techniques for slurry-blanket materials was completed by a material-balance run and other runs (Table 14.2). The recovery for a 24-hr run with a feed input of 14.8 kg of thorium as $Th(NO_3)_4$ in water represented 94% of the feed thorium (Table 14.3). Rounded product particles of 1.35-μ mean diameter were produced. All effluent streams were carefully sampled; the unaccounted for 6% is larger than would be expected from normal analytical uncertainties; however, it is believed due to incomplete drying of the sample, as shown by weight losses on ignition. The thorium was recovered as 40% product and 54% furnace-wall and trap material, from which product recovery would be low.

Results from the flame calcination of thoria sols show that the larger particle sizes for runs 108 and 115 were due to the increase in thoria sol concentration from 1 to 2 *M* instead of being due to the absence of alumina from the sols. Both concentrations gave rounded particles (Fig. 14.1), although the product from the 1 *M* sol showed more regular shapes. Increased temperatures within the 1500 to 1600°C range for sol feeds gave smaller surface areas (Table 14.2) and may have slightly increased the roundness of the particles, as shown on microphotographs.

Table 14.2. Conditions and Product Characteristics for Flame-Calcination Runs

Feed solvent: H_2O
Feed rate: 30 cc/min

Run No.	Reflector Temperature[a] (°C)	Feed Concentrations (g/liter)			Product Surface Area (m^2/g)	Product Mean Diameter (μ)
		$Th(NO_3)_4 \cdot 4H_2O$	ThO_2 (as a sol)	$Al(NO_3)_3 \cdot 9H_2O$		
108	1500		528	8	2.2	3.9
109	1000	920		83	5.6	2.2
111	1500	920		83	1.1	1.35
112	1600	920		8.3	1.8	1.0
113	1600[b]				0.84	1.8
114	1550		264		1.1	2.0
115	1525		528		0.98	4.6
116	1625[c]	600			3.6	0.9
117	1600		264		0.90	2.7

[a]These temperatures and those mentioned in the text were measured by a thermocouple in contact with the outside of the reflector tube; flame temperatures would be higher.

[b]Feed of 95% ThO_2 - 5% Al_2O_3, as a slurry in methyl alcohol (200 g/liter). This slurry was classified product from run 109.

[c]Feed solvent was methyl alcohol instead of water.

Table 14.3. Thorium Material Balance for Run 111

Thorium analyses on a weight basis

Input

Feed Salt: (36.8 kg $Th(NO_3)_4 \cdot 4H_2O$)(0.401 g Th/g salt) = 14.75 kg of thorium

Feed Solution: (66.14 kg solution)(0.228 g Th/g solution) = 15.09 kg of thorium

Output

Location	Weight (kg)	Thorium (%)	Wt of Thorium (kg)	% of Feed Thorium*
Product (recycle stream)	5.17	85.14	4.40	29.8
Trap	7.89	76.9	6.06	41.1
Furnace Wall	2.35	82.7	1.95	13.2
Filter bags	0.90	84.3	0.76	5.2
Product (recycle holdup)	0.59	81.4	0.48	3.3
Product (recycle supernatant)	192.2	0.117	0.23	1.6
Off-gas			0.00	0
Total			13.88	94.2

*Based on feed-salt input of 14.75 kg of thorium.

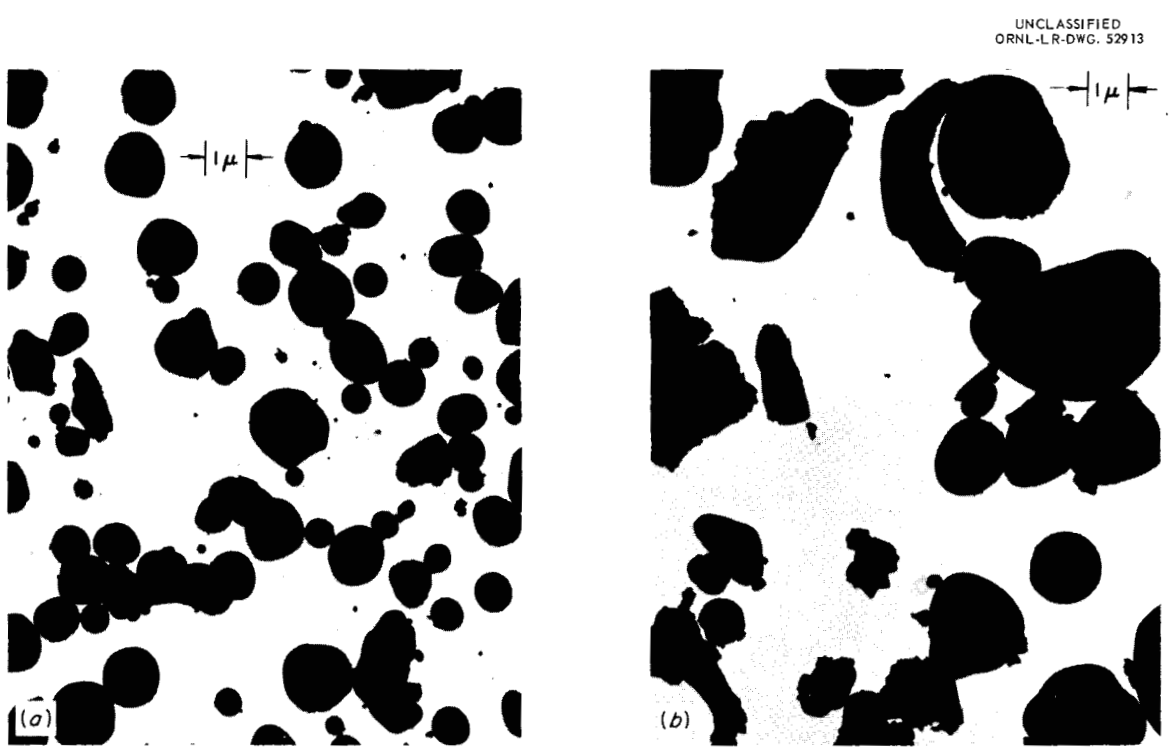

Fig. 14.1. Product from Flame Calcination of Thoria Solutions. (*a*) Run 117: 1 *M* thoria solution calcined at 1600°C; product of 2.7-μ mean diameter and 0.90-m^2/g surface area. (*b*) Run 115: 2 *M* thoria solution calcined at 1525°C; product of 4.6-μ mean diameter and 0.98-m^2/g surface area.

Some alumina appears necessary for obtaining rounded particles from the flame denitration of $Th(NO_3)_4$ solutions at temperatures which are practical with the present equipment. The product without aluminum nitrate in the feed does not show the rounded particles obtained with feed concentrations calculated to give 0.5 wt % Al_2O_3 in the ThO_2 (Fig. 14.2). The surface areas of both products are low, considering their small mean particle diameters.

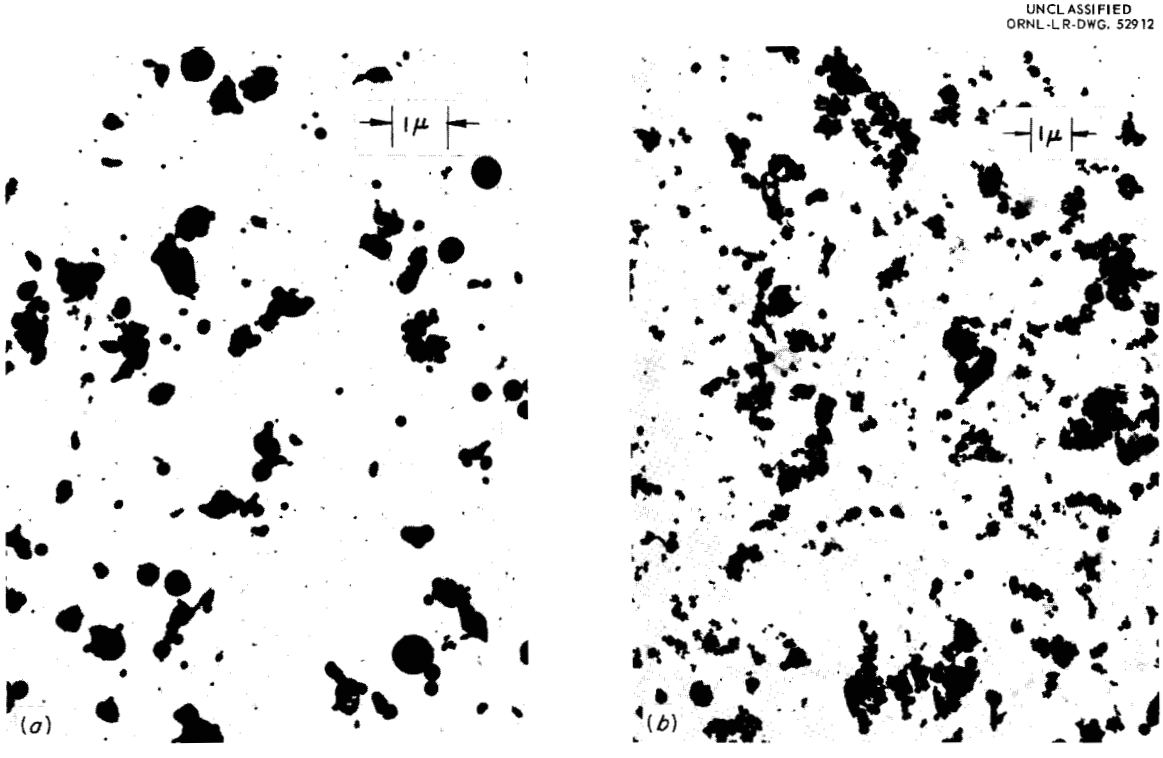

Fig. 14.2. Effect of 0.5 wt % Al_2O_3 in ThO_2 from Flame Denitration at 1600 to 1625°C. (*a*) Run 112: 1600°C, feed of 920 g/liter of $Th(NO_3)_4 \cdot 4H_2O$ and 8.3 g/liter of $Al(NO_3)_3 \cdot 9H_2O$ in CH_3OH; product of 1.0-μ mean diameter and 1.8-m^2/g surface area. (*b*) Run 116: 1625°C, feed of 600 g/liter of $Th(NO_3)_4 \cdot 4H_2O$ in CH_3OH; product of 0.9-μ mean diameter and 3.6-m^2/g surface area.

The irregularly shaped particles of ThO_2 - 5 wt % Al_2O_3 obtained by flame denitration at 1000°C can be re-fed as a slurry and calcined at 1600°C to give rounded particles (Fig. 14.3). The product from run 109 was classified to avoid plugging by any large particles; this may be the cause of the decrease in particle size from 2.2- to 1.8-μ mean diameters. The surface area of 0.84 m^2/g after the 1600°C calcination is the lowest obtained for a flame-calcination product.

UNCLASSIFIED
ORNL-LR-DWG. 52911

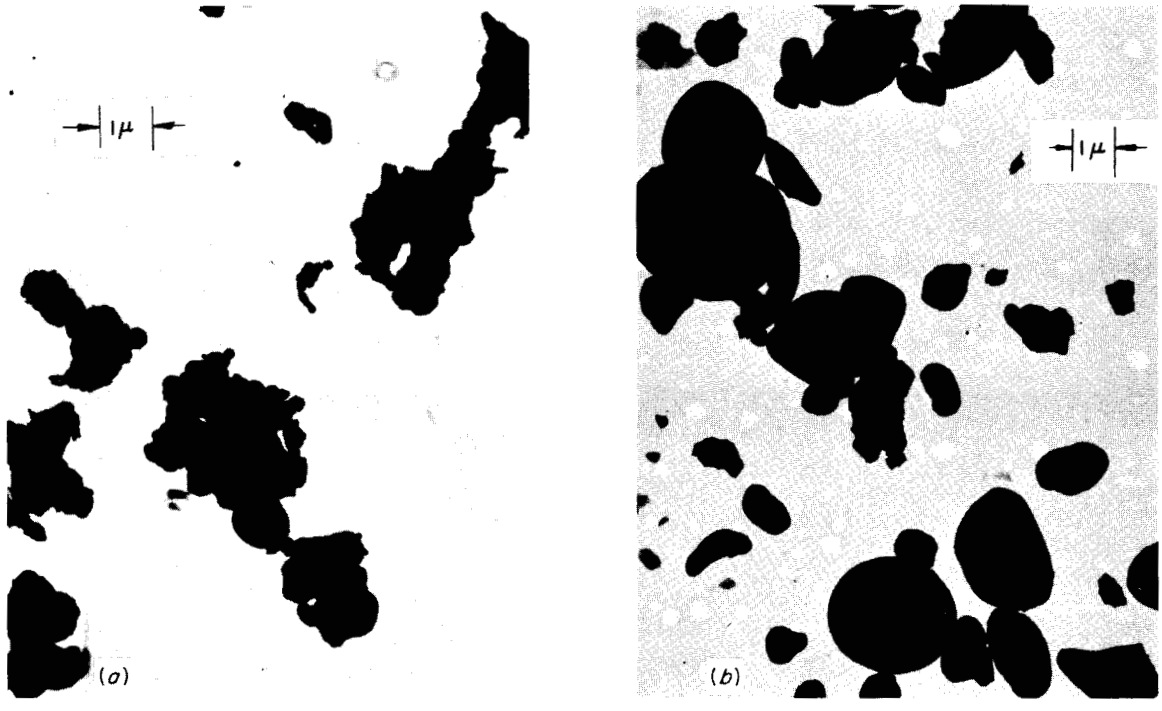

Fig. 14.3. Effects of Flame Calcination at 1600°C on Flame-Denitrated ThO_2-Al_2O_3 Prepared at 1000°C. (*a*) Run 109: 1000°C, feed of 920 g/liter of $Th(NO_3)_4 \cdot 4H_2O$ and 83 g/liter of $Al(NO_3)_3 \cdot 9H_2O$ in H_2O, product of 2.2-μ mean diameter and 5.6-m^2/g surface area. (*b*) Run 113: 1600°C, feed of 200 g/liter of slurry in CH_3OH of classified run-109 product; product of 1.8-μ mean diameter and 0.84-m^2/g surface area.

REFERENCES

1. A. T. Kleinsteuber and O. C. Dean, Optimization of Fabrication Procedures for Preparation of Spherical Pellets from DT-100 ThO_2, ORNL CF-60-10-96 (Oct. 1960).

2. E. L. Compere et al., HRP Quar. Prog. Rep. Apr. 30, 1960, ORNL-2947, p 92.

3. S. D. Clinton et al., Preparation of High Density Oxides and Vibratory Compaction in Fuel Tubes, ORNL-2965, in press.

PART VI. METALLURGY

15. METALLURGY

A. Taboada

F. W. Cooke J. W. Tackett
R. A. McNees A. J. Taylor

15.1 THORIA-PELLET FABRICATION

One alternative blanket material for use in a thermal breeder reactor is a bed of small ThO_2 pellets capable of being pumped into and out of the blanket region of the reactor and of such quality as to resist mechanical, chemical, and radiation damage. Since large quantities of such pellets, possibly as much as 27 tons, would be needed for a blanket loading, an economical and reliable method for pellet production is needed. Therefore a study has been undertaken to determine the factors influencing the fabrication characteristics and integrity of pellets formed by pressing and sintering.

In initial tests, an ordinary batch of thorium oxide (D-40, produced by the Thorium Oxide Pilot Plant for slurry use) could not be pressed on an automatic press to the required green density without the formation of extensive laminations. To improve this situation the oxide was modified by calcining to 1425°C followed by wet ball-milling in a steel mill, leaching with acid to remove the abraded iron, mixing with 2% Carbowax, prepressing to 15,000 psi, granulating, and sizing to -35 +100 mesh.

Using this modified D-40 powder, 3.5 kg of rounded-end pellets were produced, without laminations, on a single-action Stokes automatic press at green densities up to 6.3 g/cm^3. At higher green densities (6.7 g/cm3) laminations appeared at the junction between the upper dome and the cylindrical portion of the pellet. The sintered density after firing to 1650°C ranged from 9.0 to 9.3 g/cm^3. The roughness formed at the juncture of the dome and the cylinder was removed by first firing the pellets to 1450°C, cooling, wet tumbling, drying, and refiring to 1650°C.

Samples of the best pellets from this batch had a sintered density of 9.14 g/cm^3 and were submitted to the Chemical Technology Division for in-pile testing and to the Reactor Division for mechanical testing.

Other methods for modifying Pilot Plant oxides were investigated because the high-temperature calcination method just discussed has not been entirely consistent in producing a satisfactory pressing powder. One method which has been tested on cylindrical pellets is to combine 1 to 2% of polyvinyl alcohol (PVA) with the powder to serve as a binder during pressing. In this manner, oxide DT-102, which laminated at a green density of 4.57 g/cm^3 without PVA, could be pressed to a green density of 5.57 g/cm^3 after 2% PVA had been added.

In the latter condition, a sound pellet with a density of 9.5 g/cm^3 was produced by firing at 1650°C for 2 hr. The usefulness of powders of this nature for automatic-press production of rounded-end pellets is now being investigated.

A thorium oxide powder which is unique in that it was prepared by calcination of thorium formate instead of oxalate has been formed into cylindrical pellets at a green density of 5.74 g/cm^3 and sintered to a final density of 9.40 g/cm^3. For this test, the powder was prepressed at 15,000 psi and then granulated. The as-received powder, however, is sufficiently free-flowing to be usable in the automatic press and has been formed into cylindrical pellets and fired to a density of 9.11 g/cm^3. The usefulness of thorium oxide powders produced by other methods is also being investigated.

Results of physical tests, described in Sec. 13.1 of this report, have shown that in some cases thoria pellets containing added alumina have higher densities and greater abrasion resistance than pellets of pure thoria. Figure 15.1 shows photomicrographs of both types of pellets and provides a basis for explaining observed behavior.

Figure 15.1(a) shows the effect of firing pure ThO_2 at 1600, 1800, and 2000°C. The main effect of increased sintering temperature is a growth of the angular, equiaxial ThO_2 crystals and a coalescence of pores (small black circles).

At 2000°C pore migration occurred, and many large pores are concentrated at the grain boundaries.

Figure 15.1(b) shows the effect of the addition of 20 vol % of Al_2O_3 to the ThO_2. At 1600°C a eutectic liquid apparently formed, and at 1800°C the amount of liquid phase (dark-gray areas) was increased. The coalescence of small pores into larger ones is more marked in this specimen than in pure ThO_2 after firing at 1800°C.

At 2000°C a substantial growth of the ThO_2 grains occurred, and the number of pores was greatly reduced, especially in the areas near the grain surfaces. The eutectic liquid apparently filled the interstices, forming a continuous coating around the ThO_2 crystals, and, upon cooling, solidified in a "divorced" fashion so that the grain-boundary material at room temperature is essentially a single phase. Petrographic examination indicated that the grain-boundary material consists mainly of crystalline Al_2O_3. It is this coating which, if obtained in an optimum amount, would afford protection against abrasion for the softer ThO_2 grains.

15.2 WELDING OF ZIRCALOY-2

Fabrication studies have been conducted on methods for constructing the proposed Zircaloy-2 replacement core vessel. Two primary fields of study were covered: (1) the attachment of inlet orifice vanes and (2) the determination of allowable preweld misalignment of vessel components.

15.2.1 Attachment of Inlet Orifice Vanes

Current designs of possible HRT replacement core tanks call for a double-walled Zircaloy-2 inlet region with closely spaced vanes located in the annulus to direct the inlet fuel stream tangentially against the outer core-vessel wall. The vanes would probably have a contoured shape, with a maximum thickness of 0.1

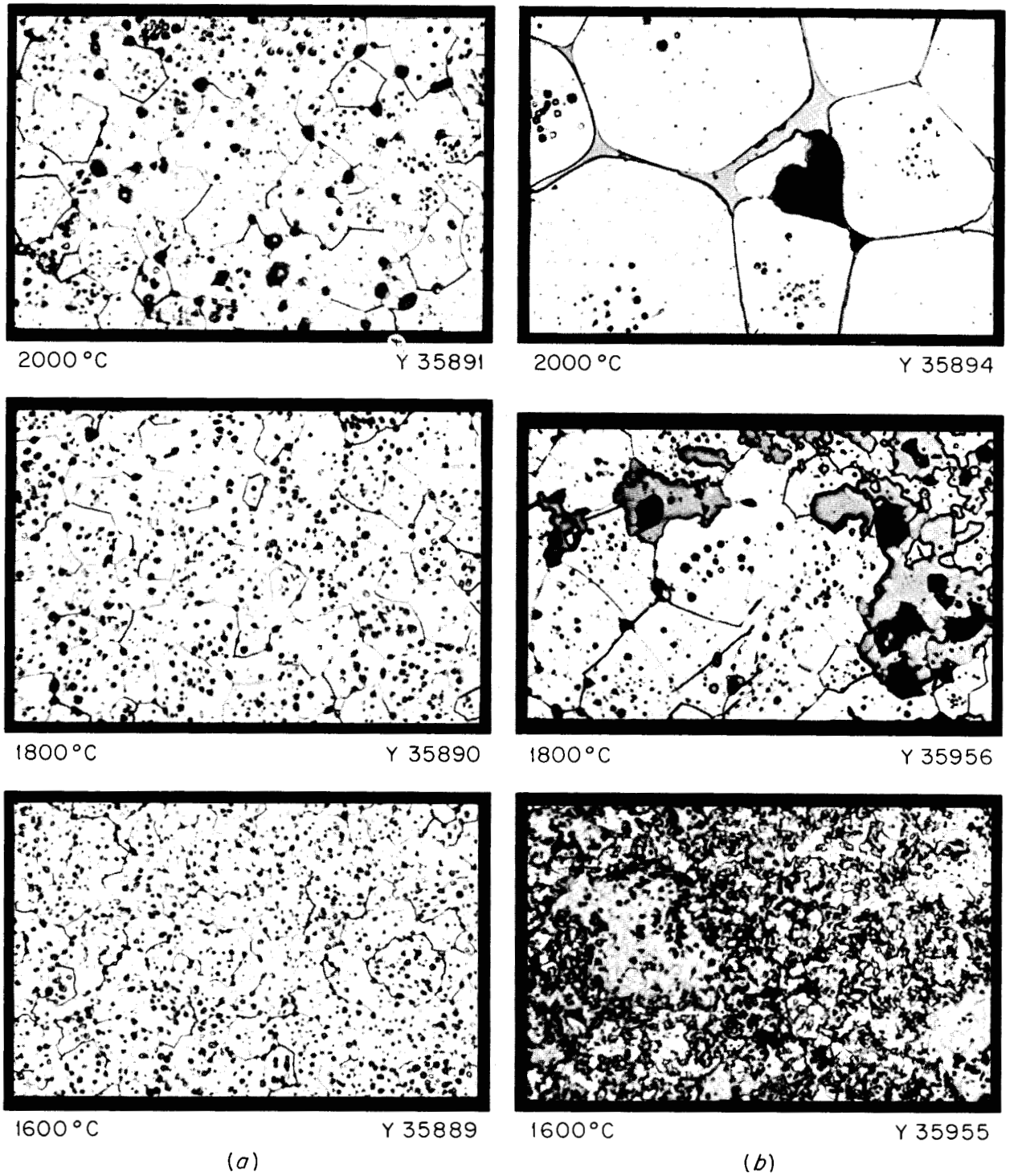

Fig. 15.1. Microstructures of (*a*) Pure ThO_2 and (*b*) ThO_2 Plus 20 vol % Al_2O_3 After Firing to 1600, 1800, and 2000°C in Air for 2 hr. Etchant: 16 *M* HNO_3, 0.01 *M* HF, at 121°C. 500X.

to 0.2 in. and a length of 0.5 to 1 in., spaced at intervals of twice the vane thickness. One means for placing these vanes in the desired locations in the annulus includes the fabrication of a circumferential, vaned insert and the subsequent butt-welding of this insert to the rest of the double-walled vessel. The studies have therefore been concentrated on the fabrication of vaned inserts.

During the current investigation, two methods of constructing the vaned-insert assembly have been evaluated. One method, involving spark-discharge machining, appeared promising, and a specimen made by this method is illustrated in Fig. 15.2. A second method consisted of machining the vanes so as to be integral with the outer wall and subsequently welding them to the inner wall in an inert-atmosphere chamber. Three test specimens demonstrating this method have been fabricated, each involving a different joint design for welding, as illustrated in Figs. 15.3, 15.4, and 15.5. A deliberate attempt was made during fabrication to obtain full penetration and crevice-free welds. However, this was obtained only in the joint design shown in Fig. 15.5.

15.2.2 Welding Misaligned Components

The present HRT core vessel was fabricated by welding together a network of preformed spherical sections. In order to reduce the cost of the replacement core vessel, it has been proposed that the weld fabrication be reduced to a minimum. In the case of a spherical vessel, two hemispherical sections preformed by hot spinning or forging would be joined by a single, circumferential, girth

Fig. 15.2. Zircaloy-2 Specimen Milled by Spark-Discharge Machining.

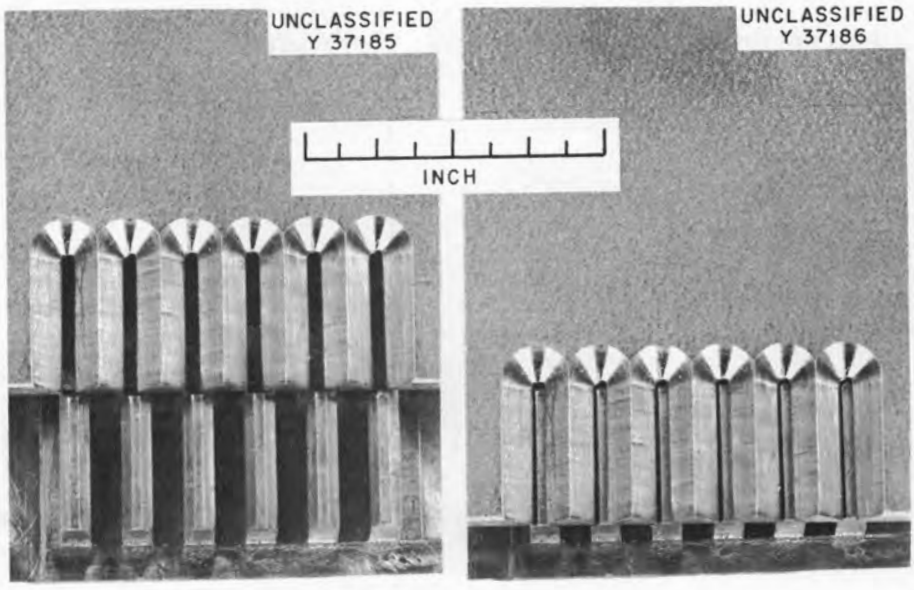

Fig. 15.3. First Welded-Assembly Joint Design.

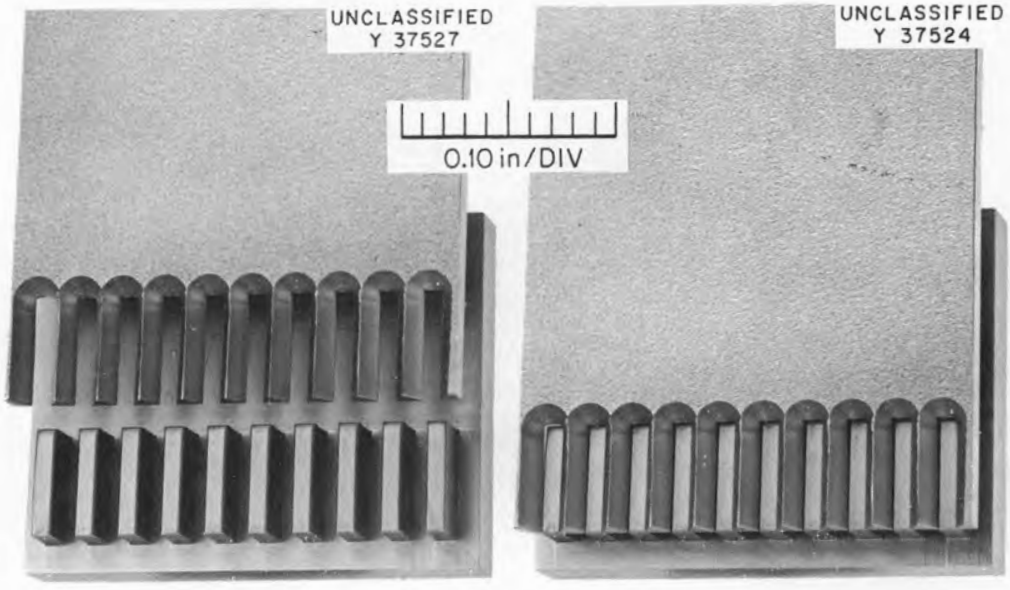

Fig. 15.4. Second Welded-Assembly Joint Design.

weld. However, it may be extremely difficult to obtain a perfect preweld fitup for the single girth weld. In a preliminary investigation of hot-spinning methods, it was indicated that a maximum of 0.060 in. of mismatch could be expected in the preweld fitup.

An investigation has therefore been conducted to determine the amount of misalignment which can be allowed in the preweld fitup to permit a sound, uncontaminated root pass with a hydrodynamically acceptable contour. Zircaloy-2 plate, 0.317 in. in thickness, was utilized for the complete study. On the basis of preliminary work, a J-beveled joint design was used, incorporating a

0.125-in. land. All root-pass welds were made by the inert-arc process, using automatic equipment and a trailer shield to prevent weld-metal contamination. No filler metal was added in the root-pass welds.

Using the welding conditions suitable for making welds in the aligned plates as a starting point, root passes were made with preweld offsets of 0.015, 0.030, 0.045, 0.060, 0.075, and 0.090 in. All root passes were sound, complete penetration was obtained and no significant weld-metal contamination occurred.

Figures 15.6 and 15.7 illustrate a typical root pass with a plate mismatch of 0.075 in., indicating the general soundness and gentle root-contour change. The remainder of the weld on several specimens was completed manually in an inert-atmosphere chamber, using filler metal. As would be expected, sound welds were made easily, and a photograph of such a joint is shown in Fig. 15.8.

The studies indicate that the production of satisfactory welds is feasible where the joint components are misaligned in the range of 0.075 to 0.090 in. However, suitable care must be taken to carefully control the welding variables and to provide adequate inert-gas shielding of the weldment.

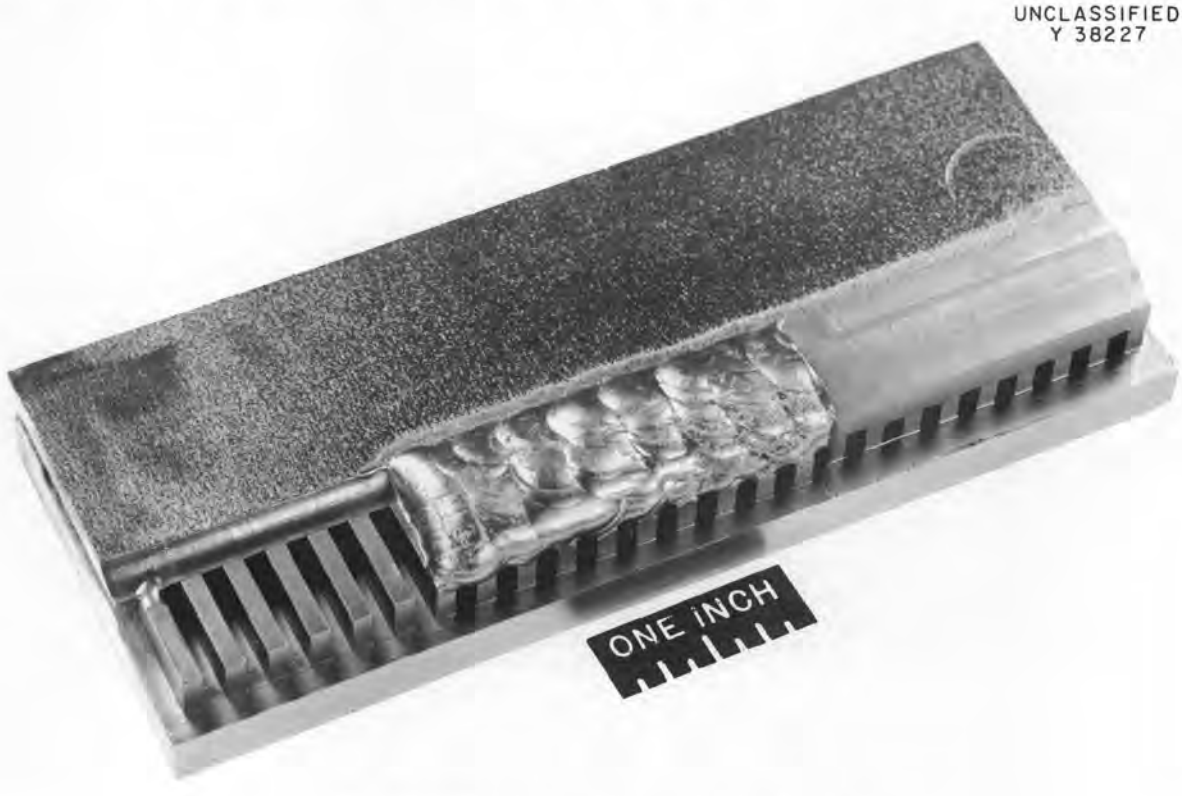

Fig. 15.5. Third Welded-Assembly Joint Design.

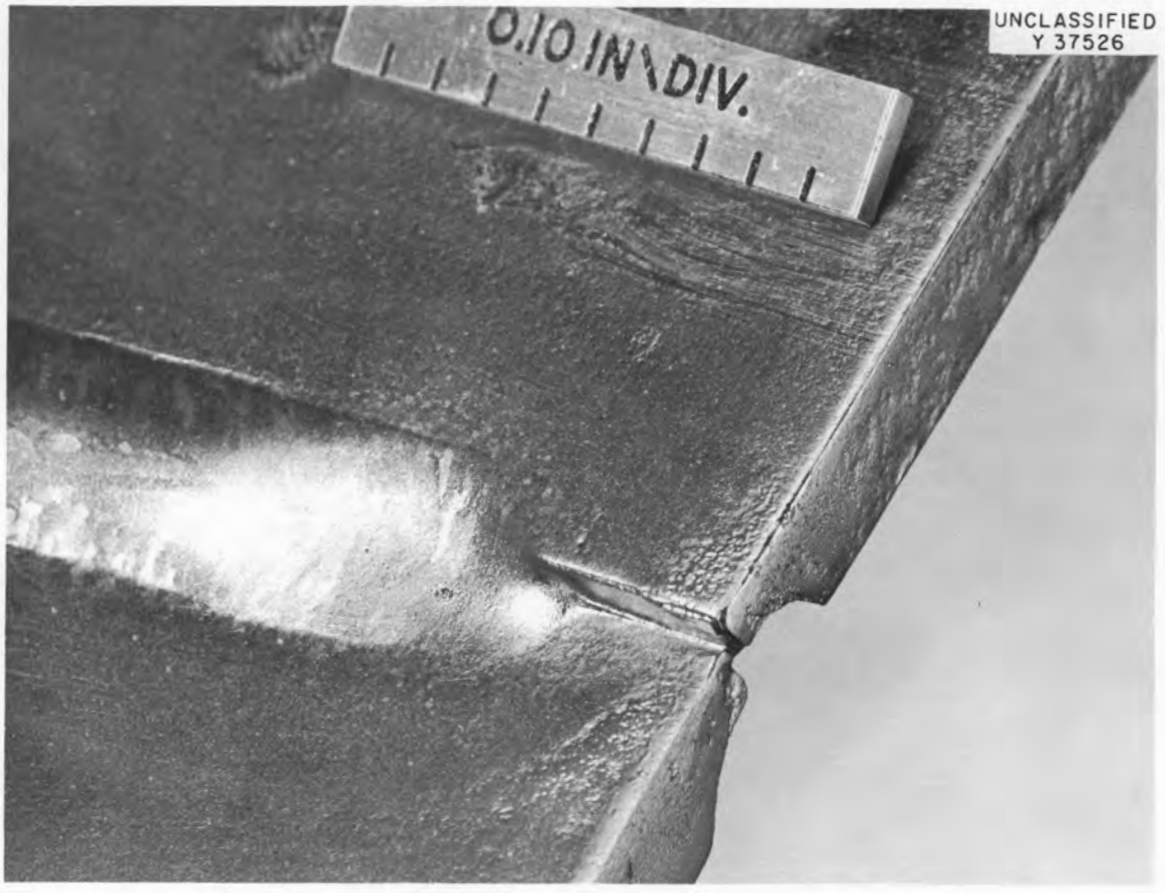

Fig. 15.6. Root Pass with Plate Misalignment of 0.090 in.

Fig. 15.7. Root-Pass Cross Section with Plate Misalignment of 0.075 in.

UNCLASSIFIED
Y-37594

Fig. 15.8. Completed Weld in Zircaloy-2 with a Misalignment of 0.075 in. Etchant: H_2O, HNO_3, HCl, HF solution. 4X.

PART VII. ANALYTICAL CHEMISTRY

16. ANALYTICAL CHEMISTRY

H. E. Zittel
D. L. Manning
G. Goldstein
T. C. Rains

16.1 AMPEROMETRIC TITRATION OF THORIUM

An amperometric method was developed for the estimation of thorium in slurries of ThO_2 and also in fuels for molten-salt reactors consisting of mixtures of the fluoride salts of Li, Be, Th, U, and Zr. In this method, which can be carried out by remote control, the thorium is titrated amperometrically with di-sodium ethylenediaminetetraacetic acid (EDTA) in a deaerated acetate-buffered medium at pH 4.5. A potential of 0.4 v vs the SCE is applied to a platinum-foil indicator electrode. Ferrous iron, added to serve as an indicator ion, is not oxidized at that potential. However, a ferrous-EDTA complex, formed after the titration of thorium is completed, is oxidized, producing an increase in the flow of current and, consequently, a break in the current-titrant curve at the end point. The end point is fixed by extrapolating lines drawn through the two straight segments of the titration curve to a point of intersection.

By control of the pH within the permissible range, 2.5 to 4.5, a number of interferences can be circumvented. At pH 2.5, Ce(III), Cr(III), and Al can be tolerated, but not at pH 4.5; the reverse is true for zirconium. Lithium, uranyl, Mn^{++}, and Mg do not interfere at either pH. Chloride, nitrate, and sulfate do not interfere in molar concentrations tenfold greater than the thorium. At pH 4.5, fluoride at a molar concentration equivalent to the thorium can be tolerated. Zinc, Ni^{++}, Cu^{++}, Fe^{+++}, Co^{++}, and VO^{++}, interfere in concentrations equimolar with that of the thorium. Phosphate interferes seriously and must be absent.

16.2 DETERMINATION OF THORIUM BY AN INDIRECT POLAROGRAPHIC METHOD

An indirect polarographic method, first described by Flaschka,[1] was adapted to the determination of microgram quantities of thorium in reactor materials. In this method, the thorium is reacted with Pb-ethylenediaminetetraacetate (Pb-EDTA), liberating one gram-atom of lead for each gram-atom of thorium reacting. The lead is then determined polarographically at a half-wave potential of -0.45 v vs the SCE. The reaction of thorium with Pb-EDTA and subsequent polarographic measurement are carried out in an acetate-buffered solution at pH 3.5. By this method, from 2 to 16 μg of thorium per milliliter can be determined with a coefficient of variation of about 6%.

Although the sensitivity of colorimetric methods is comparable with that of the polarographic method, the latter method, when applicable, offers the advantage that it can be more readily adapted to the analysis of radioactive materials by remote control.

Interference studies were made which revealed that, with the ORNL derivative polarograph, model Q-1673, 20 μg of thorium can be determined in the presence of 270, 80, and 10 μg of U, Cr, and Mo, respectively. Copper, Ni, and Fe, which appear to displace lead from Pb-EDTA, cannot be tolerated.

16.3 ELIMINATION OF INTERFERENCES IN THE FLAME-PHOTOMETRIC DETERMINATION OF CALCIUM

A method was found for inhibiting the interference of a number of anions in the flame-photometric determination of calcium. Nitrate, sulfate, and phosphate, introduced in the solvents used for the dissolution of samples of nuclear reactor materials, are known to suppress the radiant intensity of calcium when aqueous solutions are used in the flame-photometric determination of this element. The interferences can be reduced but not eliminated by using an oxyacetylene rather than an oxyhydrogen flame. If, however, a 20% ethylene glycol solution is used in aspirating the sample into the flame, nitric, sulfuric, or phosphoric acid up to 1 *M* do not interfere. When, however, the solution is made 0.1 *M* with phosphate by adding $(NH_4)_2HPO_4$, the calcium emissivity is reduced approximately 20% even though a medium containing ethylene glycol is used. This interference can be largely eliminated by adjusting the pH with nitric acid to fall within the range, 0.5 to 1.

The addition of ethylene glycol to the sample solutions not only eliminated the interference of phosphate in the determination of calcium but exerted a similar effect in the flame-photometric determination of several other elements, including barium and strontium.

REFERENCE

1. H. Flaschka, S. Khalafalla, F. Sadek, Z. Anal. Chem. 156, 321 (1957).

ORNL-3061
UC-80 - Reactor Technology
TID-4500 (16th ed.)

INTERNAL DISTRIBUTION

1. C. E. Center
2. Biology Library
3. Health Physics Library
4. Metallurgy Library
5-6. Reactor Division Library
7-9. Central Research Library
10-14. Laboratory Records Department
15. Laboratory Records, ORNL R.C.
16. G. M. Adamson
17. A. L. Bacarella
18. J. E. Baker
19. S. J. Ball
20. J. C. Banter
21. S. E. Beall
22. L. L. Bennett
23. A. M. Billings
24. D. S. Billington
25. E. P. Blizard
26. R. Blumberg
27. E. G. Bohlmann
28. S. E. Bolt
29. C. J. Borkowski
30. G. E. Boyd
31. J. C. Bresee
32. F. R. Bruce
33. J. R. Buchanan
34. W. D. Burch
35. C. A. Burchsted
36. S. R. Buxton
37. A. D. Callihan
38. W. L. Carter
39. G. H. Cartledge
40. R. H. Chapman
41. R. A. Charpie
42. R. D. Cheverton
43. C. J. Claffey
44. H. C. Claiborne
45. T. E. Cole
46. C. W. Collins
47. E. L. Compere
48. F. L. Culler
49. D. G. Davis
50. R. J. Davis
51. V. A. DeCarlo
52. W. K. Eister
53. L. B. Emlet (K-25)
54. J. L. English
55. D. E. Ferguson
56. D. F. Frech
57. J. H. Frye, Jr.
58. C. H. Gabbard
59. J. L. Gabbard
60. W. R. Gall
61. R. B. Gallaher
62. E. H. Gift
63. H. E. Goeller
64. A. T. Gresky
65. J. C. Griess
66. W. R. Grimes
67. E. Guth
68. R. H. Guymon
69. L. A. Haack
70. P. A. Haas
71. J. Halperin
72. P. H. Harley
73. R. J. Harvey
74. P. N. Haubenreich
75. D. N. Hess
76. J. W. Hill
77. E. C. Hise
78. A. Hollaender
79. P. P. Holz
80. H. P. House
81. A. S. Householder
82. S. Jaye
83. G. H. Jenks
84. D. T. Jones
85. E. V. Jones
86. J. E. Jones Jr.
87. W. H. Jordan
88. P. R. Kasten
89. C. P. Keim
90. M. T. Kelley
91. M. J. Kelly
92. F. Kertesz
93. J. O. Kolb
94. U. Koskela
95. K. A. Kraus
96. N. A. Krohn
97. J. A. Lane
98. C. G. Lawson
99. S. C. Lind
100. R. S. Livingston
101. R. A. Lorenz
102. M. I. Lundin
103. R. N. Lyon
104. J. L. Marsh (C&CC, South Charleston)
105. W. L. Marshall

106. J. P. McBride
107. H. F. McDuffie
108. H. A. McLain
109. J. R. McWherter
110. E. C. Miller
111. R. L. Moore
112. C. S. Morgan
113. K. Z. Morgan
114. L. E. Morse
115. J. P. Murray (Y-12)
116. M. L. Nelson
117. P. D. Neumann
118. A. R. Olsen
119. L. F. Parsly
120. P. Patriarca
121. F. N. Peebles
122. M. L. Picklesimer
123. H. B. Piper
124. B. E. Prince
125. L. R. Quarles
126. S. A. Reed
127. W. D. Reel
128. P. M. Reyling
129. S. A. Reynolds
130. L. Rice
131. D. M. Richardson
132. R. C. Robertson
133. W. Robinson
134. H. C. Roller
135. M. W. Rosenthal
136. H. C. Savage
137. C. E. Schilling
138. H. E. Seagren
139. C. H. Secoy
140. C. L. Segaser
141. E. D. Shipley
142. A. J. Shor
143. M. D. Silverman
144. M. J. Skinner
145. A. N. Smith
146. A. H. Snell
147. I. Spiewak
148. H. H. Stone
149. R. W. Stoughton
150. C. D. Susano
151. J. A. Swartout
152. A. Taboada
153. E. H. Taylor
154. W. Terry
155. P. F. Thomason
156. M. Tobias
157. W. E. Unger
158. W. C. Ulrich
159. R. Van Winkle
160. D. W. Vroom
161. R. E. Wacker
162. H. O. Weeren
163. A. M. Weinberg
164. S. H. Wheeler
165. E. P. Wigner (Consultant)
166. H. D. Wills
167. G. C. Williams
168. J. C. Wilson
169. R. H. Winget
170. C. E. Winters
171. C. H. Wodtke
172. L. F. Woo
173. F. C. Zapp
174. H. E. Zittel
175. ORNL - Y-12 Technical Library, Document Reference Section
176. HRP Director's Office, Y-12

EXTERNAL DISTRIBUTION

177. D. H. Groelsema, AEC, Washington
178. F. P. Self, AEC, ORO
179. M. E. Wadsworth, University of Utah
180. Division of Research and Development, AEC, ORO
181-790. Given distribution as shown in TID-4500 (16th ed.) under Reactor Technology (75 copies - OTS)

Reports previously issued in this series are as follows:

ORNL-527	Date Issued, December 28, 1949
ORNL-630	Period Ending February 28, 1950
ORNL-730	Feasibility Report - Date Issued, July 6, 1950
ORNL-826	Period Ending August 31, 1950
ORNL-925	Period Ending November 30, 1950
ORNL-990	Period Ending February 28, 1951
ORNL-1057	Period Ending May 15, 1951
ORNL-1121	Period Ending August 15, 1951
ORNL-1221	Period Ending November 15, 1951
ORNL-1280	Period Ending March 15, 1952
ORNL-1318	Period Ending July 1, 1952
ORNL-1424	Period Ending October 1, 1952
ORNL-1478	Period Ending January 1, 1953
ORNL-1554	Period Ending March 31, 1953
ORNL-1605	Period Ending July 31, 1953
ORNL-1658	Period Ending October 31, 1953
ORNL-1678	Period Ending January 31, 1954
ORNL-1753	Period Ending April 30, 1954
ORNL-1772	Period Ending July 31, 1954
ORNL-1813	Period Ending October 31, 1954
ORNL-1853	Period Ending January 31, 1955
ORNL-1895	Period Ending April 30, 1955
ORNL-1943	Period Ending July 31, 1955
ORNL-2004	Period Ending October 31, 1955
ORNL-2057	Period Ending January 31, 1956
ORNL-2096	Period Ending April 30, 1956
ORNL-2148	Period Ending July 31, 1956
ORNL-2222	Period Ending October 31, 1956
ORNL-2272	Period Ending January 31, 1957
ORNL-2331	Period Ending April 30, 1957
ORNL-2379	Period Ending July 31, 1957
ORNL-2432	Period Ending October 31, 1957
ORNL-2493	Period Ending January 31, 1958
ORNL-2561	Periods Ending April 30 and July 31, 1958
ORNL-2654	Period Ending October 31, 1958
ORNL-2696	Period Ending January 31, 1959
ORNL-2743	Period Ending April 30, 1959
ORNL-2879	Period May 1 Through October 31, 1959
ORNL-2920	Period Ending January 31, 1960
ORNL-2947	Period Ending April 30, 1960
ORNL-3004	Period Ending July 31, 1960

OAK RIDGE NATIONAL LABORATORY
HOMOGENEOUS REACTOR PROGRAM

NOVEMBER 1, 1960

PROGRAM DIRECTOR
R. B. BRIGGS — D
A. L. GUNNELS — RD

PROGRAM EDITOR
W. D. REEL — TI

DESIGN AND ENGINEERING
R. N. LYON — RD
P. A. HICKEY* — RC

REACTOR ANALYSIS
P. R. KASTEN** — RD

REACTOR PHYSICS
M. TOBIAS — RD
T. B. FOWLER — RD
D. R. VONDY — RD

INSTRUMENTATION AND CONTROLS
R. L. MOORE** — I&C

REACTOR I&C SYSTEM DESIGN
J. R. BROWN** — I&C
R. W. BORGERS** — I&C

HRP SUPPORTING SERVICES
H. D. WILLS** — I&C
P. G. HERNDON** — I&C
R. M. BURNETT** — I&C

ENGINEERING DEVELOPMENT
I. SPIEWAK** — RD

HRE-2 DESIGN AND DEVELOPMENT ASSISTANCE
R. H. CHAPMAN — RD
J. E. JONES — RD
W. TERRY — RD
R. E. CARNES — RD

SLURRY ENGINEERING
D. M. EISSENBERG — RD
C. A. GIFFORD — RD
H. G. MOORE — RD

REACTOR MAINTENANCE
E. C. HISE** — RD
R. BLUMBERG** — RD
P. P. HOLZ** — RD
J. P. HURST — RD

CORE HYDRODYNAMICS
C. G. LAWSON** — RD
W. R. MIXON — RD
G. M. WINN — RD
B. J. YOUNG — RD

REACTOR MATERIALS RESEARCH
E. G. BOHLMANN — RC
P. A. HICKEY* — RC

SOLUTIONS
J. C. GRIESS** — RC
J. L. ENGLISH** — RC
L. L. FAIRCHILD** — RC
P. D. NEUMANN** — RC
H. L. BARKER** — RC
W. H. HINDS** — RC
B. L. JOHNSON** — RC

BLANKET MATERIALS
E. L. COMPERE — RC

OUT-OF-PILE STUDIES
S. A. REED — RC
J. L. RUTHERFORD* — RC
G. G. WARNER — RC

IN-PILE EXPERIMENTS
A. J. SHOR — RC
L. F. WOO — RC
J. L. RUTHERFORD* — RC

MATERIALS EXPERIMENT ENGINEERING
H. C. SAVAGE — RC

OUT-OF-PILE OPERATIONS
J. M. BAKER — RC
J. F. WINESETTE** — RC
C. R. BENSON — RC
C. M. BURCHELL — RC
J. R. HART — RC
R. W. RAY** — RC

IN-PILE EXPERIMENTS
V. A. DECARLO — RD
E. H. GUINN — RC
J. W. MYERS — RC
D. G. PEACH* — RC
C. E. ROBERTS — RC
R. G. ROSS — RC
A. L. SUTTON — RC
W. E. TEICHERT — RC
R. M. WALLER* — RC

SOLUTION MATERIALS RADIATION
G. H. JENKS — RC

IN-PILE STUDIES
J. E. BAKER — RC

SUPPORTING RESEARCH
A. L. BACARELLA — RC
R. J. DAVIS — RC
S. H. WHEELER — RC

METALLURGY
A. TABOADA** — M
F. W. COOKE — M
W. O. HARMS** — M
W. J. LEONARD — M
R. E. MCDONALD** — M
R. A. MCNEES — M
M. L. PICKLESIMER** — M
P. L. RITTENHOUSE** — M
C. H. WODTKE** — M
J. W. TACKETT** — M
A. J. TAYLOR** — M
P. J. JONES** — M
G. C. NELSON** — M
C. M. SMITH — M

METALLOGRAPHY
T. M. KEGLEY** — M
B. F. DAY** — M
T. J. HENSON** — M
H. R. TINCH** — M

CHEMICAL TECHNOLOGY
D. E. FERGUSON** — CT
J. MAYES — CT

CHEMICAL DEVELOPMENT
D. E. FERGUSON** — CT

OXIDE PREPARATION
O. C. DEAN** — CT
A. T. KLEINSTEUBER** — CT
C. E. SCHILLING** — CT
C. W. GREENE** — CT

THORIUM OXIDE STUDIES
J. P. MCBRIDE — CT
L. E. MORSE — CT
W. L. PATTISON — CT
P. F. HAYDON — CT

DESIGN
W. E. UNGER** — CT

ThO_2 DEVELOPMENT AND HRT-CP DESIGN SUPPORT
H. O. WEEREN** — CT

INSTRUMENTATION
C. S. LISSER** — CT

UNIT OPERATIONS
P. A. HAAS** — CT

IRRADIATION ENGINEERING
S. D. CLINTON** — CT

SLURRY PREPARATION DEVELOPMENT
C. C. HAWS, JR. — CT
V. L. FOWLER — CT

CHEMICAL RESEARCH
H. F. MCDUFFIE** — RC
M. M. PAYNE — RC

HETEROGENEOUS EQUILIBRIA IN AQUEOUS SYSTEMS
W. L. MARSHALL** — RC
J. S. GILL — RC
E. V. JONES — CONSULTANT
J. E. SAVOLAINEN — RC
R. SLUSHER — RC

SURFACE CHEMISTRY
C. H. SECOY — RC
H. F. HOLMES — RC
F. H. SWEETON — RC
H. F. SOARD — CT

REACTIONS IN AQUEOUS SOLUTIONS
M. J. KELLY** — RC
D. R. CUNEO** — RC
L. O. GILPATRICK** — RC
M. D. SILVERMAN** — RC
H. H. STONE** — RC

ANALYTICAL CHEMISTRY
MYRON T. KELLEY** — AC
C. D. SUSANO** — AC
K. A. ODOM** — AC

CORROSION ANALYTICAL LABORATORY
H. E. ZITTEL* — AC

RESEARCH
H. E. ZITTEL* — AC
C. M. BOYD — AC
D. L. MANNING — AC
G. GOLDSTEIN — AC

DEVELOPMENT AND SPECIAL ANALYSES
T. C. RAINS — AC
N. M. FERGUSON — AC

SERVICE
C. K. TALBOTT — AC
T. P. BACON — AC
C. A. CLARK — AC
P. S. GOODWIN — AC
E. ONKST — AC

SPECTROCHEMICAL SERVICES
C. FELDMAN** — AC
W. R. MUSICK** — AC
A. H. MARSHALL** — AC
J. A. NORRIS — AC

HRT AND IN-PILE LOOP ANALYSES
U. KOSKELA — AC
C. P. BAKER — AC
S. R. DINSMORE — AC
J. S. WIKE — AC
G. M. CAMPBELL — AC
F. E. HAGA — AC
F. K. HEACKER — AC
M. S. MCCORQUODALE — AC
J. L. SHARP — AC
H. L. WEBB — AC
A. D. WILSON — AC

RADIOCHEMICAL ANALYSIS
E. I. WYATT** — AC

HRT DEVELOPMENT
P. F. THOMASON** — AC
F. J. MILLER** — AC
S. A. REYNOLDS** — AC

HIGH RADIATION LABORATORY
L. G. FARRAR** — AC

NUCEAR ANALYSIS LABORATORY
G. W. LEDDICOTTE** — AC

OPTICAL AND ELECTRON MICROSCOPY
T. E. WILMARTH** — AC

HOMOGENEOUS REACTOR TEST
S. E. BEALL — RD
B. EUBANK — RD

HRT OPERATIONS
J. W. HILL, JR.* — RD
J. R. BUCHANAN — CT
R. H. GUYMON — CT
H. F. BAUMAN — CT
W. T. BOSTIC — CT
R. J. HUNTER — RD
W. A. LINDSEY — CT
H. C. ROLLER — RD
R. SMITH, JR. — RD
D. T. GODWIN — RD
T. G. HILL — RD
A. L. JOHNSON — RD
R. J. HARVEY — RD
E. W. BROWN — CT
E. D. BOLLING — RD
H. O. CURTIS — RD
J. W. MOSER — RD
D. F. FRECH — RD
R. J. SHANNON — CT
J. E. EVE — RD
J. D. JONES — RD
J. E. WOLFE — RD
P. N. HARLEY — RD
J. L. STEPP — RD
J. D. BARNES — RD
T. W. HODGE — RD
L. J. SHERSKY — CT

MAINTENANCE PLANNING
G. H. JOHNSTONE — RD
L. P. PUGH — RD
F. L. ROUSER — RD

INSTRUMENTATION
J. L. REDFORD — I&C

REACTOR ANALYSIS
P. N. HAUSENREICH — RD
S. R. BUXTON — RD
J. R. ENGEL — CT
J. O. KOLB — RD
H. B. PIPER — RD
J. A. WATTS — RD

REACTOR CHEMISTRY
D. M. RICHARDSON — RC
D. G. PEACH* — RC
R. M. WALLER* — RC

CHEMICAL PLANT
W. D. BURCH — CT
O. O. YARBRO — CT

PERSONNEL SUMMARY

	FULL TIME	PART TIME	TOTAL
ADMINISTRATION	5	4	9
ANALYTICAL CHEMISTRY	23	10	33
CHEMICAL RESEARCH	7	6	13
CHEMICAL TECHNOLOGY	6	10	16
DESIGN AND ENGINEERING	15	12	27
HOMOGENEOUS REACTOR TEST	40	0	40
REACTOR MATERIALS RESEARCH	29	23	52
TOTAL	125	65	190

AC ANALYTICAL CHEMISTRY DIVISION
CT CHEMICAL TECHNOLOGY DIVISION
D DIRECTOR'S DIVISION
I&C INSTRUMENTATION AND CONTROLS DIVISION
M METALLURGY DIVISION
RC REACTOR CHEMISTRY DIVISON
RD REACTOR DIVISION
TI TECHNICAL INFORMATION DIVISION
* DUAL CAPACITY
** PART TIME ON PROGRAM